Ciprofloxacin Conjugates as Potential Novel Antibiotics

Peter Hardwidge

MSc by Research

University of York

Chemistry

December 2017

Abstract

Antibiotic resistant bacteria have become a serious threat to modern medicine, as bacteria evolve new ways to counter existing treatments. Fluoroquinolones are an area of great interest for modifications and have been used as a framework for a range of conjugates, however fluoroquinolones can induce phototoxic effects in the patient by the generation of reactive oxygen species (ROS). Phenyl thiourea moieties are known to react with these ROS, thereby alleviating their toxic effect. In this work, the conjugation of ciprofloxacin a selection of substituted phenyl thioureas was investigated with the aim to of determining whether such conjugates could be viable as novel antibiotics whilst protecting against the phototoxic effects of fluoroquinolones. Four of these conjugates were successfully synthesised and screened against the BW25113 strain of *E. coli*. However, the conjugates were observed to have a higher MIC, i.e. lower antimicrobial activity, than ciprofloxacin. To probe if the drop in antimicrobial activity correlates with a decrease in the affinity of the conjugate for the drug target, DNA gyrase, a DNA gyrase binding assay was carried out. It was observed that the binding affinity of the conjugate had decreased. It was therefore concluded that the attachment of a thiourea moiety to ciprofloxacin decreases the DNA gyrase inhibitory activity of the parent drug, ciprofloxacin.

As an extension a study was undertaken into the use of a biolabile disulfide linker between the two moieties to investigate whether it would be suitable as a delivery mechanism for a ciprofloxacin thiourea conjugate. The initial synthetic target was a dimer of ciprofloxacin linked with a disulfide bridge, to allow the assessment of the disulfide. Screening of this molecule showed that the disulfide link was increasing the MIC compared to the monomer of ciprofloxacin.

Table of Contents

List of Tables

List of Figures

List of Schemes

Acknowledgements

I would first and foremost like to thank Professor Anne Duhme-Klair and Doctor Anne Routledge for their supervision of this project and continued support during the write up period. I would also like to thank Dr Gavin Thomas for his assistance with the biological sections of work.

Additional thanks go to Ms Heather Fish, Dr Karl Heaton, Dr Graeme McAllister and Ms Amanda Dixon for their assistance with the NMR, Mass Spectrometry, Elemental analysis and HPLC work respectively. I would also like to thank my lab colleagues Dr Daniel Raines, Dr Tom Sanderson, Dr Ellis Wilde, Ben Coulson and Sophie Rugg for all their help and advice.

Declaration

I declare that this thesis is a presentation of original work and I am the sole author. This work has not previously been presented for an award at this, or any other, University. All sources are acknowledged as references.

1.0 Introduction

1.1 Antibiotics

The term “antibiotic” was coined in 1941 to mean a class of molecules that kills or inhibits bacterial growth.[1] The discovery of penicillins **1** (1929), streptomycin **2** (1943), tetracycline **3** (1944) and chloramphenicol **4** (1946)[2] provided the starting point for the Golden Age of Antibiotics from 1950-1960. During the 1950s, around 50% of modern antibiotics used today were developed. [3]

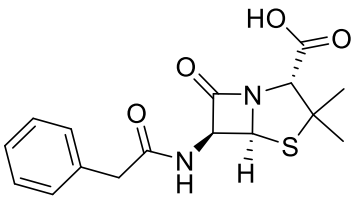

1
Penicillin G

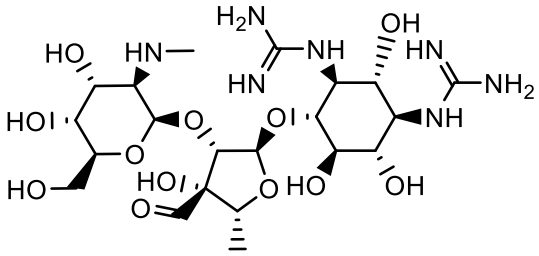

2
Streptomycin

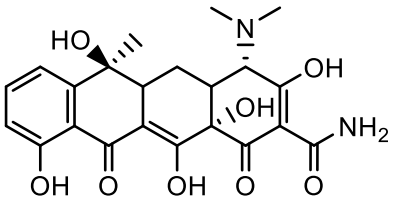

3
Tetracycline

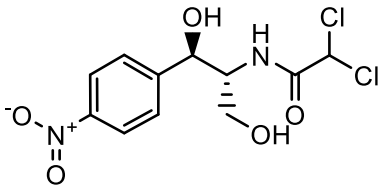

4
Chloramphenicol

Despite the initial successes, in the last fifty years only two new classes of synthetic antibiotics have been developed. These were the quinolones in

1962 and oxazolidinones in 2000, examples of which include ciprofloxacin **5** and linezolid **6**.[2] The lack of investment into new antibiotics, combined with overuse has led to the appearance of new multi-drug resistant (MDR) strains of pathogens.[4]

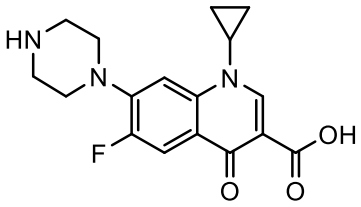

5
Ciprofloxacin

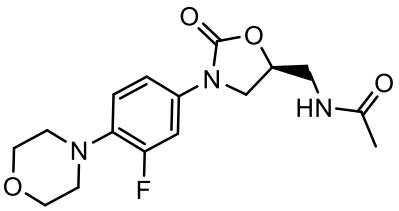

6
Linezolid

1.1.1 Antibiotic Resistance

Antibiotic resistance is now a threat to modern medicine. Not only are infections becoming harder to treat but routine operations are at risk of untreatable infection. In September of 2016, speaking at a UN general assembly, the Secretary General Ban Ki-moon called it a "fundamental, long-term threat to human health, sustainable food production and development." [5]

Antibiotic resistance can arise through different mechanisms: modification of target site, enzymatic deactivation, active efflux, a change in metabolic pathways or a decreased permeability at the cell membrane.[4] Once resistance has arisen, it will spread rapidly throughout a population vertically, through natural selection, and horizontally through plasmid transfer.[1] These are shown in **Figure 1**.

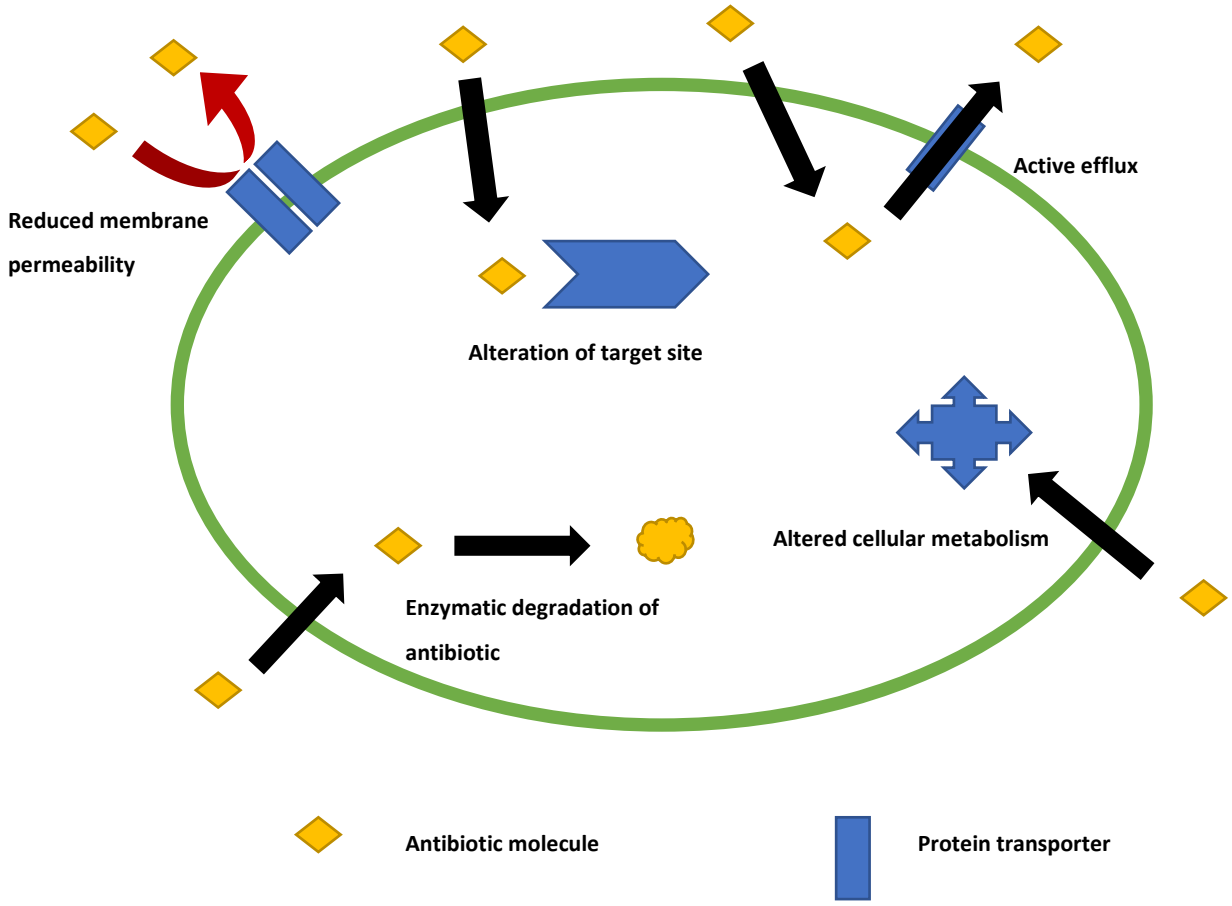

Figure 1 Schematic showing differing mechanisms of bacterial antibiotic resistance [6]

1.1.2 Intracellular Target Site Modification

To function as an antibiotic, the molecule must be able to bind to a specific target within the bacterial cell, therefore they are highly affected by a change in their target binding site. For example, the growing cell wall of Gram-positive bacteria is dependent on the extension of peptidoglycan chains. Without them, the bacterium can no longer contain its inner osmotic pressure and will rupture its cell membrane.[7] Vancomycin, **7**, inhibits the extension of these chains by hydrogen bonding to the growing tip and capping it as shown in **Figure 2**. In the case of the Vancomycin-resistant strains of *E. faecium*, two gene clusters, VanA and VanB, have been identified to encode enzymes that alter the peptidoglycan

precursors from D-Ala-D-Ala to D-Ala-D Lac. This change of terminal amino acid residue to lactate severely inhibits Vancomycin binding.[8] The change in structure changes the bonding pattern from five hydrogen bonds to four which results in a thousand-fold decrease in binding affinity.[9]

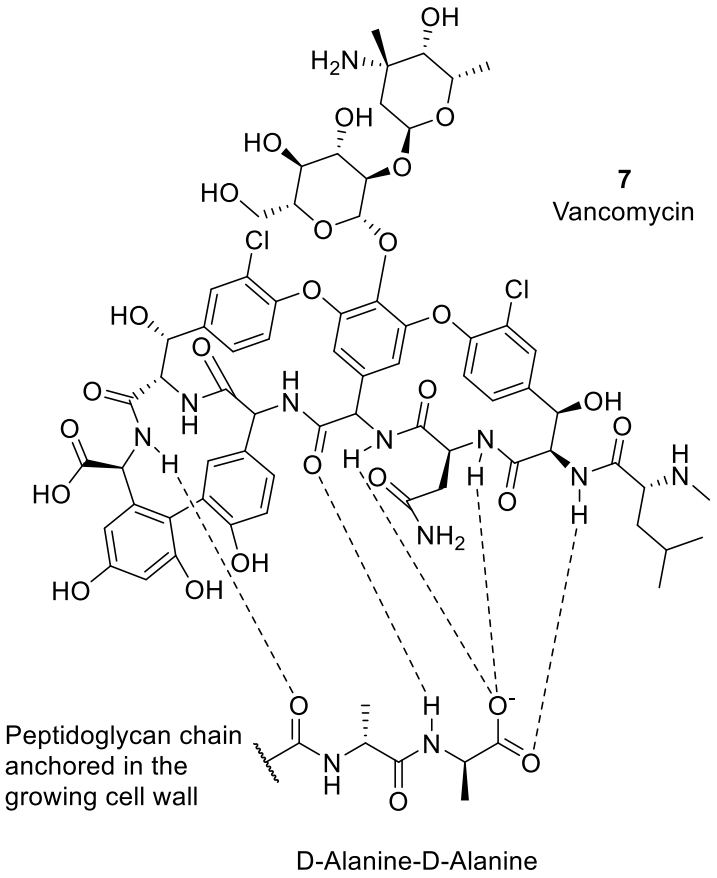

Figure 2 Vancomycin binding interactions with a growing peptidoglycan chain [10]

1.1.3 Antibiotic deactivation

When challenged with an antibiotic, bacteria can evolve enzymes that deactivate an antibiotic via covalent modification. An example of chemical modification is the degradation of β-lactam antibiotics by the β-lactamases. This enzyme hydrolyses the essential ring structure in β-lactam antibiotics, converting the drug to an inactive form as shown in **Scheme 1**. These enzymes were initially discovered in 1940,[11] one year

before the first clinical use of penicillins. Since then this family of enzymes has had over 1,300 distinct members identified.[12]

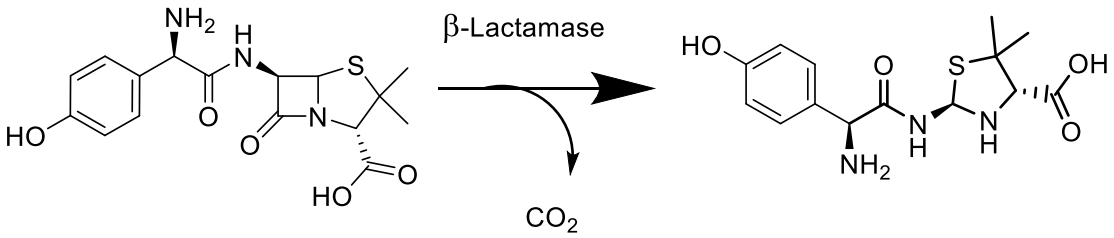

8
Amoxicillin

Scheme 1 The effect of β-lactamases on amoxicillin [13]

The β-lactamase class of enzymes binds and open the β-lactam four membered ring. During its action the penicillin binds to a target, a member of the penicillin binding protein (PBP) family and irreversibly acylates it. [13] The β-lactam ring is essential for this process. A β-lactamase will react with, and open this ring in such a way that the β-lactamase can be recycled. [13]

1.1.4 Antibiotic efflux

There are many bacterial membrane-bound efflux pumps. Normally these proteins are responsible for removing toxic compounds. For example, the *E.coli* AcrAB efflux system normally removes excess fatty and bile acids, however it has also been found to be the major pumping system responsible for resistance to tetracyclines, penicillins and fluoroquinolones in *E. coli*.[14] Due to this broad spectrum of activity, one efflux system can result in resistance to a wide variety of antibiotics.[15] The upregulation or development of a new transporter that can effectively transport the antibiotic away from its target site leads to the bacterium

becoming resistant.[6,15] Coldham *et al.* report that fluoroquinolone exposure increases the expression of 43 separate proteins in *E. coli*, including the AcrAB family of pumps. There is a great deal of research investigating whether chemical modifications can inhibit this efflux.

1.1.5 Altered Cellular Metabolism

The overexpression of targets can result in resistance to an antibiotic. The more of a target there is present in the cell, the higher the local concentration of antibiotic that is necessary to disrupt its function. For example incubation with low levels of Vancomycin will result in bacteria developing a much thicker cell wall, to increase the number of peptidoglycan chains and hence the number of targets.[6]

1.1.6 Reduced Cell Permeability of Antibiotics

Due to the hydrophobic nature of the inner cell membrane, many polar antibiotics find it difficult to penetrate the bacterial cell by diffusion alone.[16] The outer membrane of Gram-negative bacteria also contains a high proportion of lipopolysaccharides. These are highly anionic and coordinate divalent Mg^{2+} and Ca^{2+} cations from the surrounding environment. This network of charged ions provides a significant barrier to hydrophobic or detergent-like antibiotics such as the fluoroquinolones.[17] Fluoroquinolones are known to bind to Mg^{2+} ions and can be held in place at the membrane.[18] Instead of diffusion, a large proportion of antibiotics use porins to gain access to the intracellular target.[16] Porins are large, hollow β-barrel structured proteins that sit in the bacterial membranes and allow ions and small molecules to diffuse across.[19] OmpF is a major porin involved in fluoroquinolone uptake.[20] As such, the bacteria can gain at least partial resistance to an antibiotic by downregulating or otherwise modifying these uptake pathways.[21] It is

possible that modifications that remove the zwitterionic nature of ciprofloxacin and make it more lipophilic would increase the rate of passive diffusion through the bacterial cell membrane.

1.1.7 Preventing Antibiotic Resistance

The fight to stop bacteria evolving resistance to antibiotics has always been a losing fight.[3] The arms race between microorganisms developing new ways of attack and defence is driven by natural selection.[22] However there are several ways that humankind can reduce the rate of resistance development: reducing the over prescription of antibiotics and the prescription for minor illnesses, reducing the use of antibiotics in livestock and agriculture and ensuring the proper disposal of antibiotics to prevent contamination of groundwater.[3] As well as this it is important that new antibiotics are developed in response to new resistance that arises. These can be new modifications of existing antibiotics or even entirely new antibiotics designed for newly discovered intracellular targets.[6]

1.1.8 Combination Therapy

To overcome resistance, many antibiotics are used together with another molecule aimed to protect it, or to act synergistically at either the same target site or another in the bacterium.[23] The aim is to completely wipe out a population of bacteria so that there are no survivors to develop resistance. The principle was first demonstrated with β-lactamase inhibitors prescribed in conjunction with β-lactam antibiotics. Amoxicillin, **8**, and clavulanic acid, **9**, was the first therapeutically used combination, first employed in 1981.[23] Clavulanic acid is a β-lactamase inhibitor and prevents the hydrolysis of amoxicillin by these enzymes. The addition of clavulanic acid was found to greatly increase the susceptibility of β-lactamase producing pathogens to amoxicillin.[23]

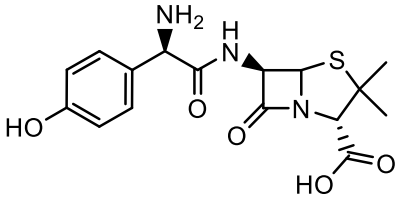

8
Amoxicillin

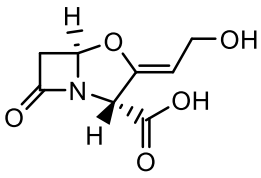

9
Clavulanate

From this first combination therapy, more clinical examples have been developed, including examples involving the fluoroquinolones. A combination therapy containing the antibiotic ciprofloxacin, **6**, and probenecid, **10**, an inhibitor of the renal organic anion transport system. Inhibiting these transport systems slows the rate of renal excretion of ciprofloxacin.[24] This has been shown to increase the plasma concentration and biological half-life of ciprofloxacin, increasing its efficacy.[25]

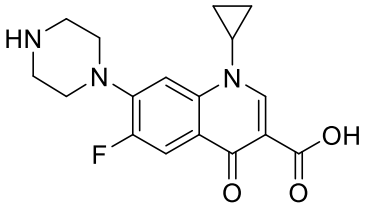

6
Ciprofloxacin

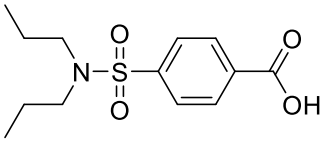

10
Probenecid

The recognition of the importance of combination therapy and the opportunities it presents has led to the creation of the field of perturbation biology. This involves the prediction of how cells will act once 'perturbed' by an outside action and uses computational modelling of cellular metabolic pathways pioneered by Molinelli *et al.* in 2013. Initially developed for studying cancer cells, it has been expanded to

model the impact of antibiotics, including fluoroquinolones such as ciprofloxacin, on gut flora. [26]

1.2 Fluoroquinolones

Fluoroquinolones are an essential part of the arsenal of modern medicine. Initially targeted against Gram-negative urinary tract infections, later generations can also target Gram-positive bacteria. However, resistance is rising. In 2009, in British Columbia, more than 20% of *E. coli* and *K. pneumoniae* infections were found to be resistant to fluoroquinolones. This is up from around 2% of resistant cases found in 1996.[27]

1.2.1 Development of the Fluoroquinolone Class of Antibiotic

The first precursor of this class of antibiotics was nalidixic acid, **11**. This is regarded as the first generation of quinolones.[28] It was first introduced in 1962 as an agent against Gram-negative bacterial infections of the urinary tract.[24] However nalidixic acid only acted on a very narrow spectrum of bacteria which led to the development of the second generation, the fluoroquinolones. These can be further classified into Class 1 and Class 2. Class 1 fluoroquinolones, for example norfloxacin, **12**, had an improved Gram-negative coverage and a small spectrum of Gram-positive activity.[24] Class 2 fluoroquinolones such as ciprofloxacin **6** had a wider bioavailability and were used to treat a wider variety of infections.[28]

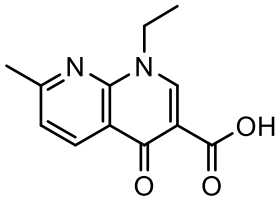

11
Nalidixic Acid

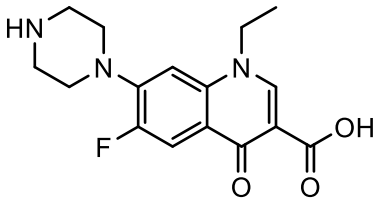

12
Norfloxacin

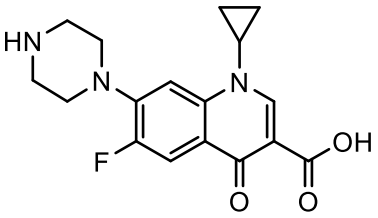

6
Ciprofloxacin

Further development of the third and fourth generations of fluoroquinolones widened the spectrum of susceptible bacteria.[28] The third generation, such as moxifloxacin **13**, were developed and found to have modest streptococcal coverage.[24] The fourth generation, such as trovafloxacin **14**, in particular was found to have action on Methicillin-resistant Staphylococcus aureus (MRSA)[24]

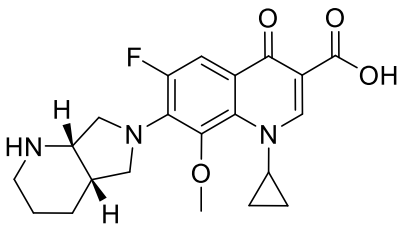

13
Moxifloxacin

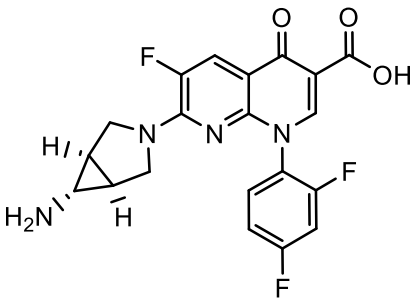

14
Trovafloxacin

1.2.2 Fluoroquinolone Toxicity

Fluoroquinolones as a class are generally considered to be mild antibiotics. Most adverse side effects are gastrointestinal upset (>7%) with very rare cases of central nervous system events (>5%), blood disorders (approximately 5%), renal disturbances (approximately 4.5%) and skin photosensitivity (approximately 2%).[29]

Fluoroquinolones are known for their photosensitising properties causing phototoxicity in human and animal models.[30] Both photoallergic reactions, an immune response based on previous exposure to fluoroquinolone antibiotics, and phototoxic responses have been documented.[29] Once excited by ultraviolet light, fluoroquinolones generate ROS. These include the singlet oxygen species $^1O_2$ which then decomposes to hydrogen peroxide, H_2O_2. These ROS can attack lipid membranes and cause DNA damage.[29] This lead to the development of tumours in mice treated with lomefloxacin.[29] M. Peacock *et al.* also report that the nucleotide excision repair (NER) pathway of DNA repair was heavily damaged by these ROS, increasing the chances of cells becoming cancerous.[31] Increased toxicity is linked with the C-8 halogenated position in fluoroquinolones.[30] There is scope for conjugates therapies that will counteract this toxicity by reacting with and removing the ROS. However, this would have to be balanced against the reduced potency of the fluoroquinolones.

Hayashi *et al.* report that modifications at position 1 of 7-(3-aminopyrrolidinyl) quinolones such as an aminodifluorophenyl, **15**, or an isoxazolyl group, **16**, decrease the phototoxicity. However, these modifications also resulted in a decrease in antibacterial activity. There is potential for modifications elsewhere on the fluoroquinolone could have similar effect without the loss of efficacy, and indeed this is what lead to the design of the thiourea conjugation on to the piperazine.[32]

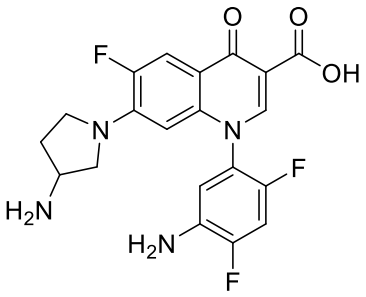

15

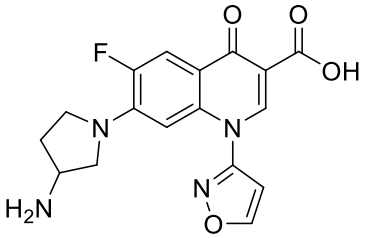

16

1.2.3 Fluoroquinolone Structure-Function

Since the initial discovery of nalidixic acid, there has been extensive research into how modifications on the bicyclic structure, **17**, affects the activity.

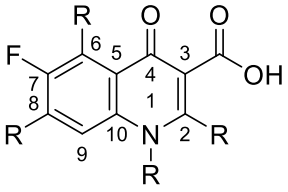

17

Figure 3 The pharmacophore of the fluoroquinolone class of antibiotics

The potency of the pharmacophore is increased by a cyclopropyl group at N1, exemplified by ciprofloxacin and found in third and fourth generations of fluoroquinolones.[33] One of the earliest additions to the quinolone pharmacophore was the fluorine at position 7. With this addition there was a 10-fold increase in DNA gyrase inhibition.[33] Attaching a five or six membered nitrogen heterocycle at the C8 position influences the pharmacokinetics of the antibiotics.[34] A piperazine will increase activity

against Gram-negative bacteria. An amino pyrrolidine group extends the spectrum of activity to Gram-positive bacteria.[34] It is thought that these groups inhibit efflux and so improve potency.[33]

The carboxylic acid at position C3 and the carbonyl at C4 are known to be essential for the formation of the bound gyrase complex.[35] These groups are involved in the formation of the Mg^{2+} water bridge for tight complex binding. If these groups are chemically modified or removed, the activity is reduced.[36] This factor was a major influence in the decision to conjugate the phenyl thiourea to the piperazine as discussed in later chapters.

1.2.4 Fluoroquinolone Uptake

Ciprofloxacin has two protonation sites. In water, the carboxylic acid has a pK_a of 6.5 and the terminal nitrogen on the piperazine has a pK_{aH} of 7.5.[17] Fluoroquinolones are also known to coordinate Mg^{2+} ions, which confers a positive charge to the complex. Once the molecule is charged, it is excluded from the lipid bilayer,[18] however it is known that porins in the bacterial outer membrane have a preference for transporting cations.[37] The porin OmpF is widely acknowledged as the primary fluoroquinolone transporter in the *E. coli* bacterial membrane.[16–18,37] As the modifications would mask the ionisable groups, it was theorised that they would improve the rate of diffusion across the bacterial plasma membrane.

1.2.5 DNA Gyrase and Topoisomerase IV

DNA gyrase is an enzyme responsible for the supercoiling of bacterial DNA in an series of reactions involving adenylate triphosphate (ATP) hydrolysis.[38] Gyrase is classed a Type II Topoisomerase, as it catalyses the breaking and reforming of both strands of DNA. The enzyme passes the

cut sections of duplex DNA through each other to remove or induce supercoils and knots as shown in **Figure 4**. It is active primarily during DNA replication to remove topological tension in the double helix caused by the replisome unwinding the double strands. Other roles include the folding and coiling of the bacterial chromosome, the knotting of plasmids and protecting the DNA from high temperatures.[35] DNA Gyrase binds as a tetramer around DNA as a dimer of dimers, containing two of each subunits denoted as GyrA and GyrB.[35] In the presence of ATP, DNA Gyrase introduces negative supercoiling into DNA. In the absence of ATP, DNA Gyrase removes supercoils. In this way, it is sensitive to the currently energy levels of the cell, which is in turn affected by the extracellular environment.[35]

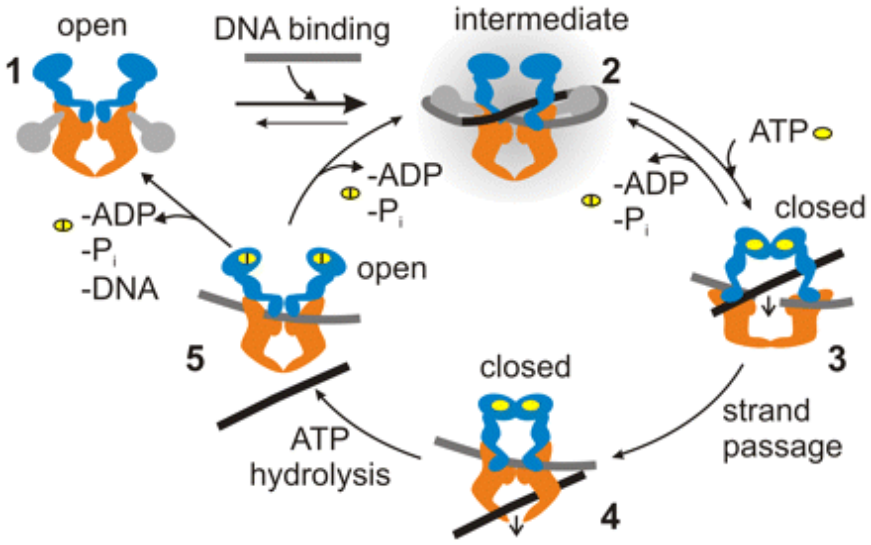

Figure 4 Sequential steps of DNA Gyrase passing one strand of DNA through another, using ATP. Figure numbering corresponds to the order of the steps in the cycle. Figure used with permission.[39]

Topoisomerase IV is another Type II topoisomerase. It is responsible for decatenating replicated circular DNA, as the semi-conservative method of DNA replication leaves the strands intertwined.[35] There is also evidence for it being involved in anchoring the newly replicated DNA to the

membrane, to aid in separation in much the same way spindle fibres do in eukaryotic cells.[40]

1.2.6 Fluoroquinolones Binding to DNA Gyrase

Fluoroquinolone antibiotics bind to DNA gyrase in the midst of the catalytic cycle, when the duplex DNA has been cut.[35] The stoichiometry is two fluoroquinolones per tetrad of gyrase subunit. Antibiotic binding in this way is DNA dependent and the molecules have a low affinity for free gyrase.[41] Gyrase itself forms a binding pocket for the fluoroquinolone in relaxed DNA substrate in the presence of ATP.[42] The drug intercalates into nicks in the DNA created by the enzyme.[43] The binding complex involves the carboxylic acids and carbonyl of the quinolone form a Mg^{2+} - water bridge to an aspartic/glutamic acid residue and a serine in helix IV of a GyrA subunit, as seen in **Figure 5**.[43] In *E. coli* the residues are Ser366 and Asp370 of GyrA and these are the residues most commonly associated with target-site modification resistance.[44,45]

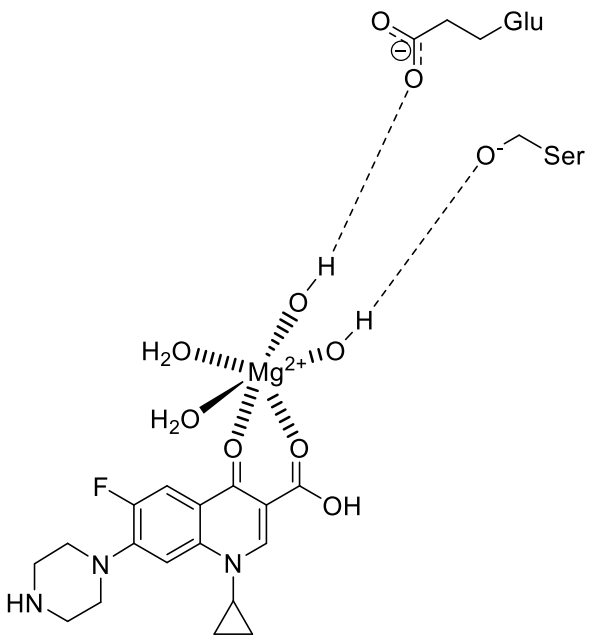

Figure 5 Ciprofloxacin – Mg^{2+} - water – enzyme bridge binding interactions adapted from Mustaev et al. [43] **The dashed lines indicate hydrogen bonds**

There is also substantial evidence for a second binding mode, however this has yet to be fully elucidated. It has been observed that the C-7 ring of fluoroquinolones interact with both GyrA and GyrB subunits. When point cysteine mutations were introduced and a modified chloroacetyl derivative of Ciprofloxacin bound, there was an unexpected cross link formation, correlated with exceptional bacteriostatic activity. The residues in question, GyrA-Gly81 and GyrB-Glu466 are around 17 Å apart, which suggests there are two separate binding interactions occurring.[43] These binding modes indicate that the pharmacophore is integral to the binding complex, and modifying these groups is likely to adversely affect the efficacy of any conjugate.

1.2.7 Protein Synthesis Dependent and Independent Modes of Action

Fluoroquinolones have two bactericidal mechanisms of action, one is protein synthesis dependent and the other is protein synthesis independent. These situations relate to whether or not a bacterium is

currently growing and reproducing.[46] This classification arises from the observation that the action of nalidixic acid being blocked by inhibiting protein synthesis with a prior incubation with chloramphenicol, however the action of ciprofloxacin is left unaffected.[46] Both of these processes follow on from the formation of double stranded DNA breaks capped with protein.[46] Both processes result in chromosome fragmentation, however even a single DNA double strand break can be lethal.[47] Previously it was thought that lethal DNA breaks occurred when the replication fork collided with the Gyrase-DNA complex, however recent evidence has shown that this is not the case.[46] The 'capping' of the broken DNA with Gyrase allows the DNA to reform intact. Therefore in order to be lethal, the complex must dissociate and the fragments be released.[46]

Fluoroquinolone lethality has also been found to involve reactive oxygen species (ROS).[48] It has been observed that a hydroxyl radical scavenger will completely inhibit the activity of oxolinic acid, **18**, but only partially inhibit moxifloxacin, **13**.[48] In fact, the same amount of inhibition occurs with both a pre-incubation of chloramphenicol as with a radical scavenger, and used together causes no additional effect. It can therefore be concluded that the protein synthesis dependent pathway depends upon these hydroxyl radicals, and that the protein synthesis independent pathway does not.

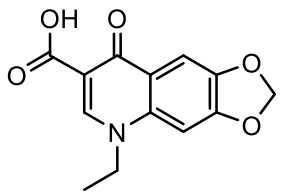

18
Oxolinic Acid

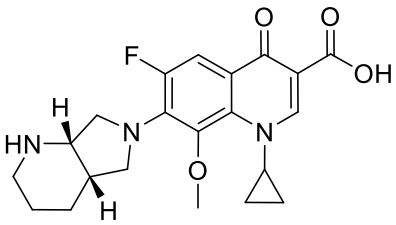

13
Moxifloxacin

The normal route of reactive oxygen species is shown in **Scheme 2**. It has been found that a double deficiency in the *sodA* and *sodB* superoxide dismutase enzymes in *E. coli* will decrease the lethality of norfloxacin, whereas a single knockout mutation in either one has no effect.[49] Further studies showed that a knockout mutation of catalase enzymes will drastically increase the lethality of norfloxacin. An iron chelator and a hydroxyl radical scavenging thiourea both reduced the activity of norfloxacin. The same experiments had no effect on the activity of chloramphenicol. Taken together, these findings suggest that the norfloxacin was generating the superoxide species, that was then converted to damaging hydroxyl radicals via hydrogen peroxide.[49]

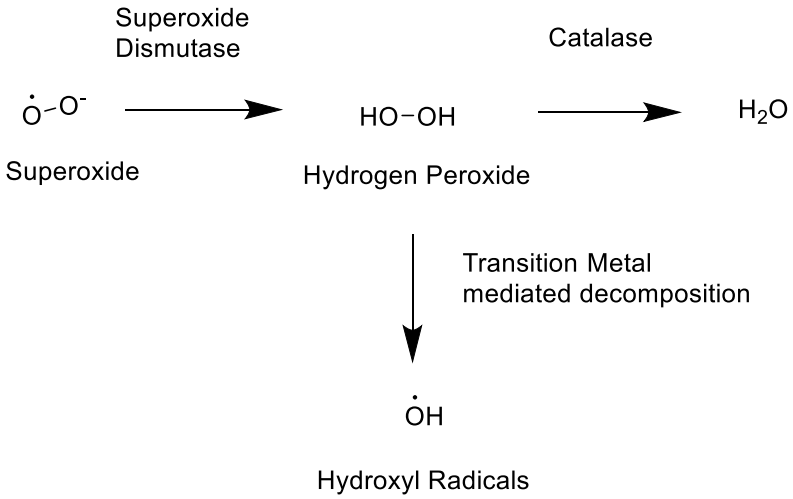

Scheme 2 Superoxide decomposition pathways[48]

Other studies performed on Mycobacteria proteasome accessory factor C (pafC) have found similar results. PafC is a factor in how mycobacteria break down proteins using superoxide species up in the process.[50] Knockout mutations were found to potentiate hypersensitivity to fluoroquinolones but no other classes of antibiotic. Exposure to thiourea or iron chelators was found to remove this hypersensitivity.[50] This

evidence points to the importance of reactive oxygen species in fluoroquinolone lethality.

The thiourea group was chosen as a conjugate to try and limit the damaging effect of ROS, which account for the phototoxicity of the fluoroquinolones.

1.2.8 Resistance to Fluoroquinolones

Specific target alteration of the DNA Gyrase GyrA subunit and Topoisomerase IV ParC subunit is a common mechanism of resistance, and possibly the most clinically important one.[51] The mutation most notably involved in *E. coli* Gyrase target modification is Ser82.[21] Other mutations are usually found amongst residues 67-106 in what is known as the quinolone resistance determining region (QRDR)[52] This region is the binding pocket for DNA Gyrase onto DNA and as fluoroquinolones bind on to the DNA Gyrase-DNA complex any alterations here can reduce the binding affinity.[51] Overcoming this kind of resistance is extremely difficult and no such examples have reached clinical use.[21]

Other chromosome-based methods of resistance exist. Fluoroquinolones cross the bacterial membrane mainly making use of porins, though they can diffuse across.[17] It has been shown that quinolone activity can decrease the synthesis of OmpF, one of two major porins in *E. coli*.[53] Under ideal growth conditions, this can lead to increased fluoroquinolone resistance, however due to the porin being an important ion channel too, taking steps to abolish the proton motive force will result in it being synthesised again.[53] Therefore, this is not an absolute mechanism resistance for bacteria and other mechanisms must exist. Since the design

of the conjugates was aimed to increase lipophilicity it was theorised that the OmpF porin uptake pathway could be circumvented.

Three main types of plasmid-based resistance occur. Qnr proteins are part of a family of pentapeptide repeat proteins and share homology with DNA mimics. These bind to DNA Gyrase and topoisomerase IV both in the cytoplasm and while complexed to DNA to reduce the number of enzyme target sites for fluoroquinolones and hence their efficacy.[21,54] The second type is an aac(6')-Ib-cr mutant protein belonging to the aminoglycoside transferase family. The enzyme acetylates the piperazine ring found in Ciprofloxacin and Norfloxacin, reducing the activity.[21] The third is a family of Multidrug Resistance (MDR) transporters which are a classification of membrane based efflux proteins.[53] A significant mechanism of resistance is the evolution and overexpression of these transports.[55] Three members have been identified to be involved in fluoroquinolone resistance, OqxAB, QepA1, and QepA2.[21]

1.2.9 Fluoroquinolone Conjugate Therapies

The development of the different generations of fluoroquinolones has shown that they are an excellent target for further modifications. Having two intracellular targets can be beneficial, especially if a modification decreasing binding affinity at one could be offset by increased inhibition of the other.[56]

As discussed above, the C-3 carboxyl and the C4 carbonyl are essential for fluoroquinolone function. As a result, non-immolative attachments at this point can have a detrimental effect on the efficacy. Replacing the carboxylic acid with a hydrazide, **19**, decreases the zone of inhibition (ZI) when tested against *S. aureus* in well-diffusion assays.[57]

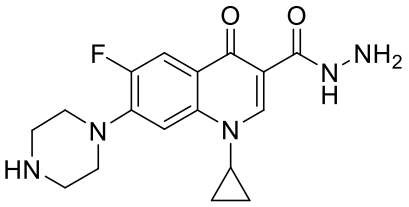

19

Due to the downsides mentioned above, extensive work has been carried out investigating the effects of modifying the piperazine ring of ciprofloxacin. In 2012 S. Wang *et al.* found that modifying ciprofloxacin with a N-terminal 4-methoxybenzene, **20**, was up to eight times more potent than ciprofloxacin against Gram-positive bacteria.[58] Their reasoning being that, in general, fluoroquinolone activity increases with lipophilicity.[59]

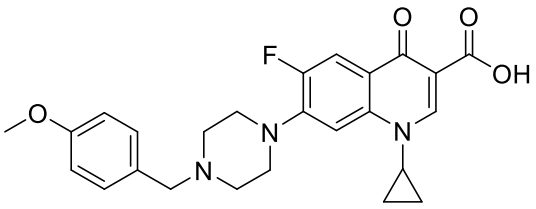

20

This is very much an area of active research. Leading on from simple chemical modifications, investigations into linking two antibiotic moieties together were performed. In 2016 S. Panda *et al.* published a study on a conjugate between fluoroquinolones and the antituberculotic drug pyrazinamide. Pyrazinamide derivatives have been shown to have increased effect on drug resistant tuberculosis. The ciprofloxacin-alanine-pyrazinamide conjugate, **21**, had a drastically reduced MIC against *S. aureus* but an increased MIC against *S. typhi*.

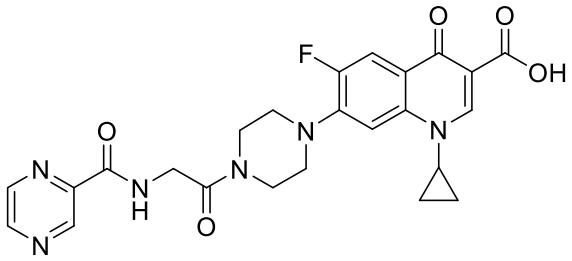

21

Some of the most successful hybrid antimicrobials involve the conjugation of fluoroquinolones to oxazolidinones, **22**.[56] Oxazolidinones inhibit protein synthesis by binding the P-site of the ribosomal protein synthesis complex.[60] It has been reported that conjugates with structures based on this have shown to have a lower MIC than Moxifloxacin and activity against several MDR strains of pathogens.[56]

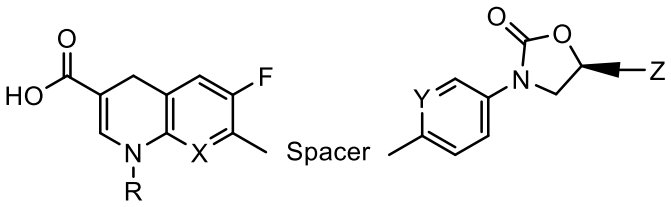

22

Figure 6 General structure of fluoroquinolone-oxazolidinone conjugate hybrids. **R = cPr**, **Et**, **X = N**, **CH**, **Y = CF**, **N**, **Z =NHAc**, **NH(CS)OMe**[56]

Another example is the rifampin-fluoroquinolone conjugate, **23**. This is rifampicin conjugated to a fluoroquinolone *via* a hydrazide. Rifampicin is a potent inhibitor of bacterial RNA polymerase in a wide variety of Gram-positive bacteria, however resistance quickly and easily arise *via* point mutations. Combining it with fluoroquinolones helped prevent this resistance arising as it was discovered at affect three separate targets, RNA polymerase, DNA gyrase and topoisomerase IV.[56]

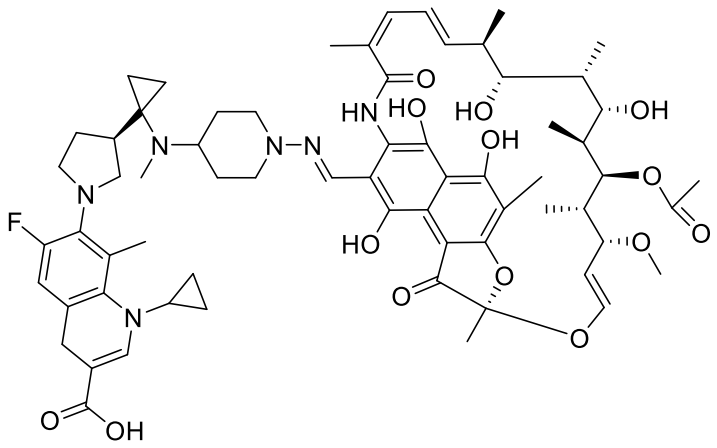

23

Some of the most recent conjugate therapies are antibiotic-antibody conjugates (AACs). These AACs are combine the target site specificity, superior absorbance and distribution of antibiotics with the favourable pharmacokinetics of antibodies, namely long half-life and slow clearance.[61] The conjugate system binds to the antigens via the antibody section and the bound AAC-bacterium is recognised by the immune system of the host and taken up. Inside the cell the bacterium is destroyed, in part by the immune cell and in part by the conjugated antibiotic.[61] While still a very novel area of research, fluoroquinolone based AACs could hold great potential.

1.2.10 Fluoroquinolone Dimers

Fluoroquinolone dimers have been a topic of in depth research, as the structure of the gyrase binding site and the stoichiometry of binding have led to the possibility of bisintercalation into the two binding sites.[62] Previous examples have used permanent linkers between the two fluoroquinolone moieties. In 2006 Kerns *et al.* developed the fluoroquinolone dimers, **24**. These dimers were found to be equipotent or

±2-fold MIC against ciprofloxacin susceptible strains of *S. pneumoniae.* However, the dimers had reduced MIC compared to ciprofloxacin when tested on ciprofloxacin resistant strains of *S. pneumoniae* possessing efflux-mediated or topoisomerase IV mutation-mediated resistance mechanisms. However they were also found to have a raised MIC against Gram-negative bacteria.[63]

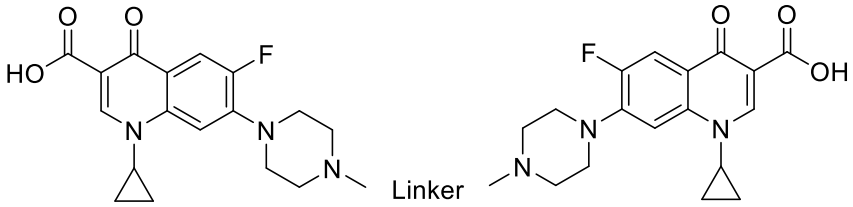

24

Linkers:

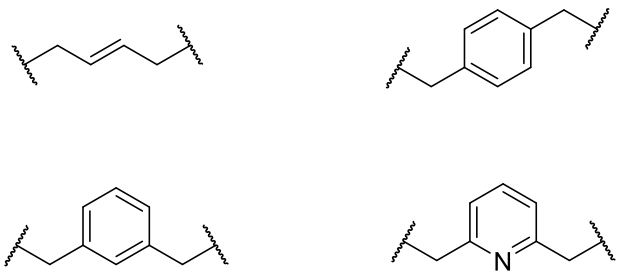

Figure 7 Ciprofloxacin dimers synthesised with a range of linkers, adapted from Kerns et al.[63]

In 2015, A. Ross *et al.* undertook further analysis of ciprofloxacin dimers. Amide linked dimers, **25** and **26**, were synthesised with the aim of improving interactions with DNA and the solubility profile.[62] However the dimerisation resulted in a drastically increased MIC (32 µM) against *E. coli* compared to ciprofloxacin (<0.03 µM). The MIC was decreased when tested against an *imp*-4213 outer membrane permeability mutant, suggesting that part of the problem was with diffusion past the membrane, however direct DNA Gyrase assays indicated a three-fold decrease in IC_{50}, leading them to conclude that it was a combination of these two effects.[62]

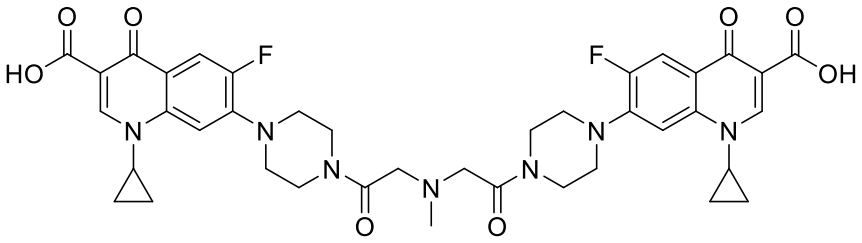

25

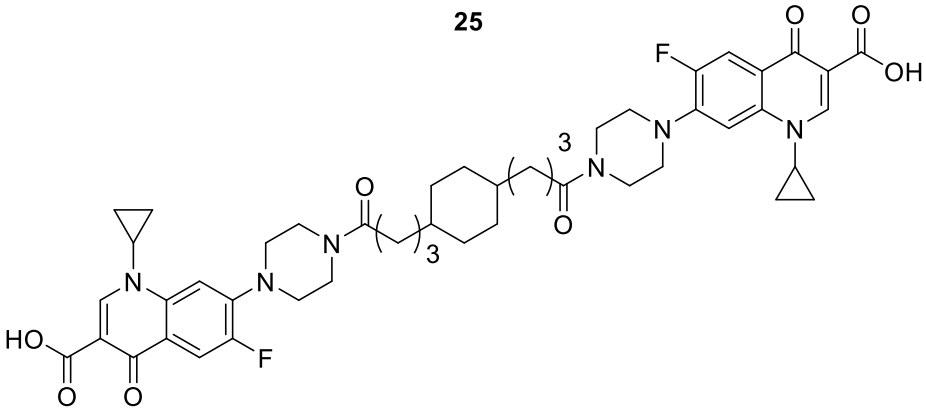

26

Ross *et al.* also investigated PEG dimers of ciprofloxacin. The most efficacious one of these, **27**, had a much lower MIC than the amide linked dimers, however still much higher than ciprofloxacin. Interestingly, the IC_{50} of DNA Gyrase was much higher for **27** than **25** and **26**, and the MIC for the *imp*-4213 mutant was lower for **27**. This suggest that the PEGylation is reducing Gyrase binding but increasing the membrane permeability of **27**.[62] It is hypothesised that the PEG linker can stretch across the phospholipid bilayer without concomitant membrane disruption.[62] It was thought that this could also apply to the disulfide link based dimer investigated in the later chapters.

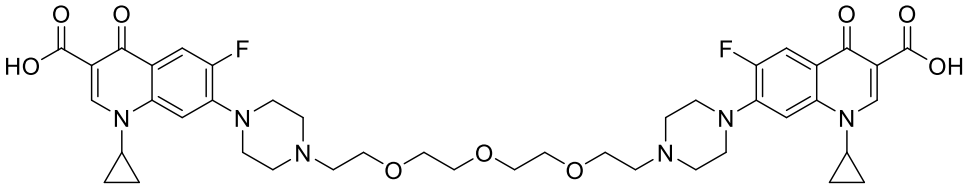

27

These results indicate that the correct linker design can improve upon the rate of cellular uptake for the antibiotic to offset the decrease binding affinity for DNA Gyrase. This led to us considering the effect of biolabile linkers eliminate the problems of permanent linkers while retaining the benefits.

1.3 Biolabile Linkers

All the above examples use a permanent linker between the two drug moieties. It has been observed that permanently modifying fluoroquinolones can decrease their efficacy *in vitro*.[33,36,64–66] Co-drugs can be designed with a biolabile linker and are known as mutual prodrugs, as they act as a mutual pro-moiety for each other.[67] The criteria for a mutual prodrug are (a) the prodrug itself is not pharmacologically active, (b) the release of the two drugs is fast and does not produce toxic side products, (c) the linker should be bio-cleavable by enzymes or other cellular agents.[67]

In 2014, Sinha, S *et al.* filed a patent for a variety of covalently linked conjugates, for example the gatifloxacin-prednisolone conjugate, **28**.[68] Prednisolone, as a corticosteroid, is highly lipophilic so it was thought that conjugation could improve the ability of the drug to permeate lipid bilayers.[69] Once inside the cell, the molecule is theorised to be hydrolysed

and the two drug moieties released, though whether this is an enzyme-mediated process or not is unknown. Once released, the antibiotic gatifloxacin and the anti-inflammatory prednisolone would act independently from each other.

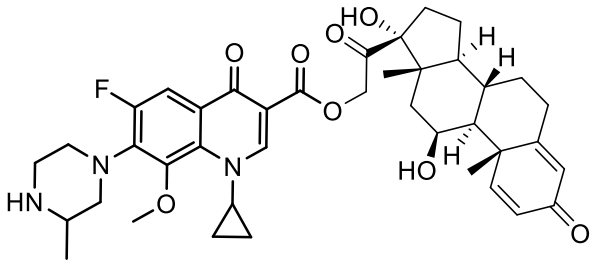

28

1.3.1 Disulfide Bridges

The dimer designed in this work would incorporate a biolabile link designed to break down in the bacterial cytoplasm, specifically a disulfide bridge between two ciprofloxacin molecules. The structure, **29**, is the general structure for the disulfide bridge.

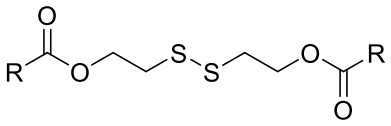

29

The S-S connection is seen extensively in proteins where it assists in the folding of the protein.[70] It is also commonly associated with cellular reducing agents, such as glutathione **30** or free cysteine.[67,71] Glutathione acts as an antioxidant in the cell via conversion to the Glutathione

Disulfide, **31**. It can be converted back to Glutathione by the NADP-H dependent enzyme Glutathione Reductase **(Scheme 3)**.[72]

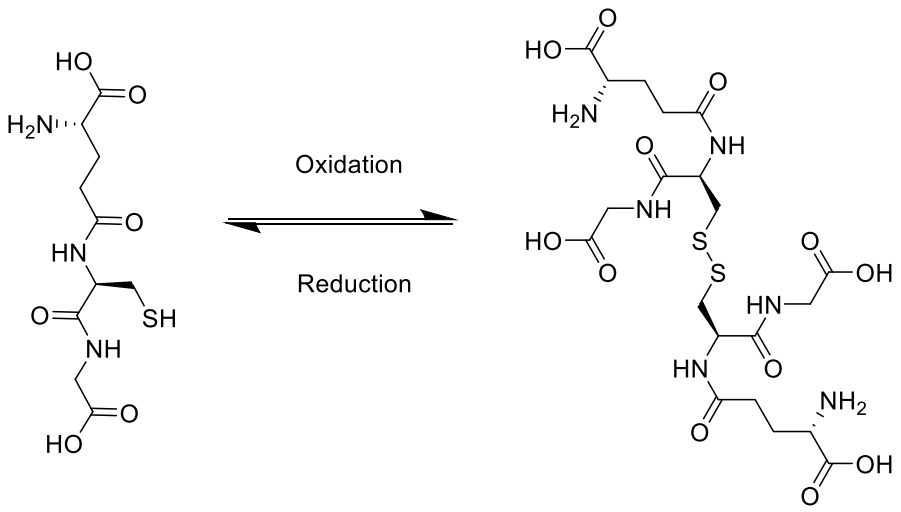

30 **31**

Scheme 3 Interconversion of Glutathione and Glutathione Disulfide in a redox process

1.3.2 Disulfide linker Reductive Cleavage

Jain et al. synthesised several prodrugs and conducted mechanistic studies into how the disulfide bridge cleaves.[67] They detected the by-products monothiolcarbonate, **32**, ethylene sulphide, **33**, and CO_2, as well as the released terminal drug moieties shown in **Scheme 4**. It was proposed that the bridge cleaves due to cellular thiol groups on glutathione and cysteine residues. This would only release the drug once in the cytoplasm of the bacterial cell.

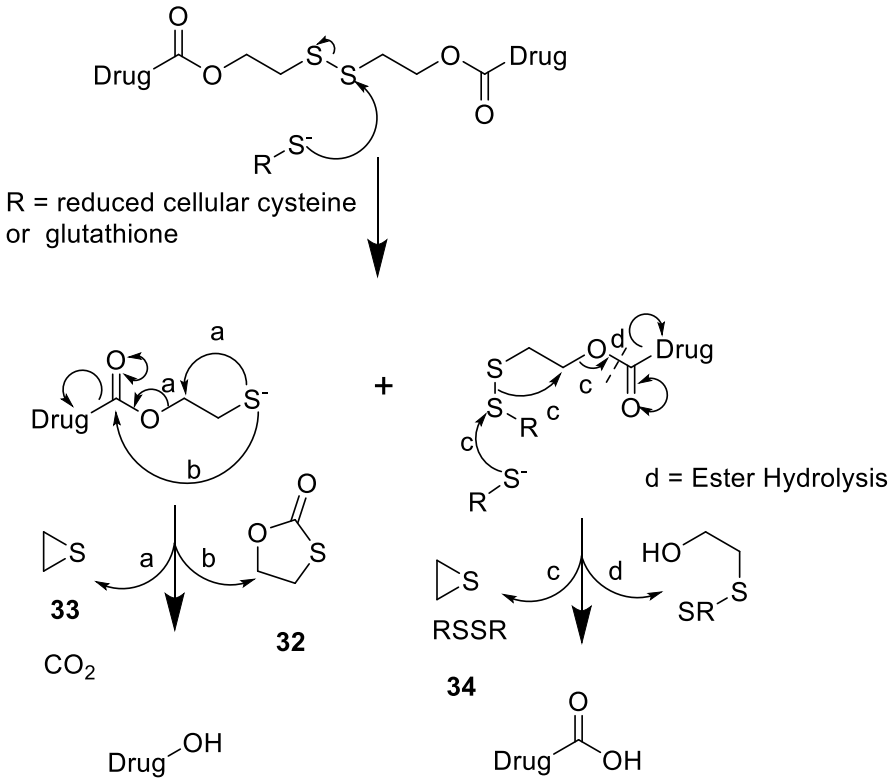

Scheme 4 Disulfide bridge breakdown in the presence of cellular reducing agents. **Scheme adapted from Jain et al**. [67]

1.3.3 Disulfide Linkers can be Tuned

The structure of the disulfide can be 'tuned' to affect the rates of breakdown. Using luciferin as a releasable fluorophore, Jones *et al.* found that increasing the length of the carbon chain slowed the rate of Luciferin release, as the longer chained monothiol intermediate took longer to decompose extracellularly.[73] However when incubated with a 1 mM concentration of the redox agent dithiothreitol (DTT) for thirty minutes it was seen that the disulfide decomposed fully for both examples, **35A** and **35B**. From this Jones *et al.* concluded that intracellular release was still very quick, no matter the length of the chain.

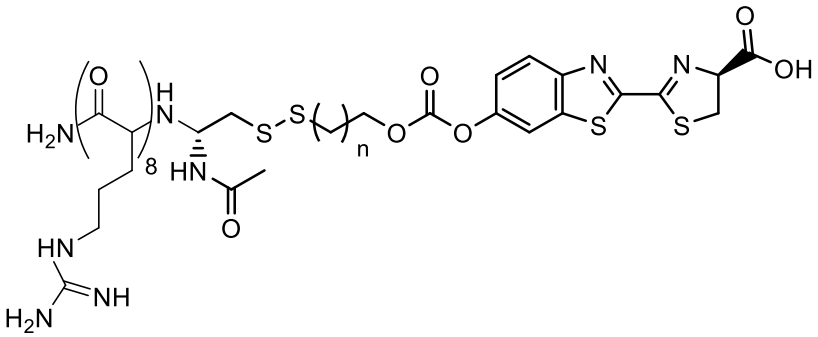

35

Figure 8 Luciferin-disulfide-polypeptide conjugate with variable chain length. **33A n=2**, **33B n=3**

It has also been reported that sterically hindering the disulfide chain can decrease the rate of release.[74] Initially, disulfides were considered to cleave in the extracellular medium and release the drug at non-target sites. However molecules with sterically-hindered linkers were found to have much larger half lives *in vivo.*[75] Phillips *et al.* report that increasingly hindering the linker with methyl groups as shown by **36A-D** gives increasing biological half-life and slower clearance *in vivo* in antibody conjugated molecules.[76] This would allow further tuning of future ciprofloxacin conjugates made using the disulfide to increase its activity *in vivo*.

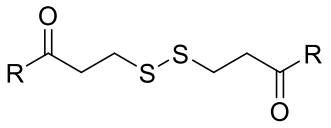

36A

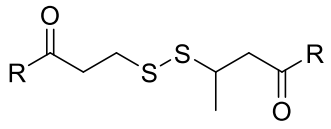

36B

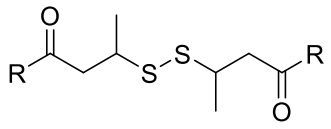

36C

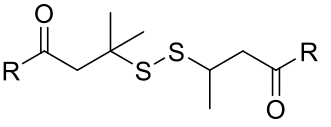

36D

1.3.4 Disulfide Based Drug Uptake

Whilst it is thought that small molecule-based conjugates can diffuse through the cell membrane, it is increasingly clear that there is an endocytotic mechanism of uptake for the larger polypeptide-drug and antibody-drug conjugates in eukaryotes.[77] Once taken up in this manner, the disulfide linkage remains intact until the lysozyme is dissipated, as the interior is oxidising and acidic.[77] There is also clear evidence that the disulfide can trigger the uptake of previously membrane-impermeable polypeptides via conjugation to an actively transported moiety.[73]

Evidence exists for a disulfide containing protein shuttling mechanism in the *E. coli* periplasm. The disulfide bond forming (Dsb) proteins are active in the periplasm to form disulfide bonds in the oxidising extracellular environment. It has been reported that DsbD can transport intact disulfide bonds across the cell membrane.[78]

1.3.5 Disulfide Based Prodrugs

The advantage of the disulfide bridge is that it is resistant to the oxidising environment of the extracellular fluid whilst being vulnerable to break down in the reducing environment of the cell. This property allows drugs to be very narrowly targeted, resulting in an increased local concentration at the target site.[79] It also allows precise delivery of cytotoxic components, such as nitric oxide-diclofenac prodrugs, **37**.[80] Containing the breakdown to the cytoplasm avoids the highly toxic effects that diclofenac, **38**, has on the gastrointestinal tract.[81]

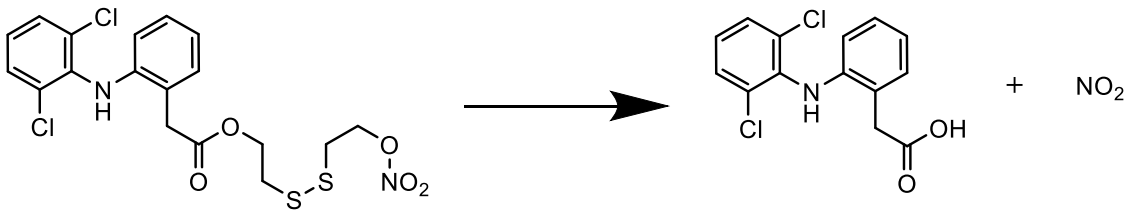

37
Diclofenac-disulfide-NO_2 conjugate

38
Diclofenac

Scheme 5 Cleavage of the diclofenac-disulfide-NO_2 conjugate

Another use is as diagnostic probes for the redox state of cells, as indicated by the level of free reactive Glutathione. Molecular probes incorporating fluorescent naphthalimide, **39**, have been developed using the disulfide bridge.[82] Once the disulfide cleaves, the fluorescence of the

naphthalimide, **40**, moiety changes, indicated an area of redox stress. This can help identify cancerous tissue.[83] The fluorescence-changing would also allow investigations into the rate of cleavage of the ciprofloxacin dimers discussed in later chapters.

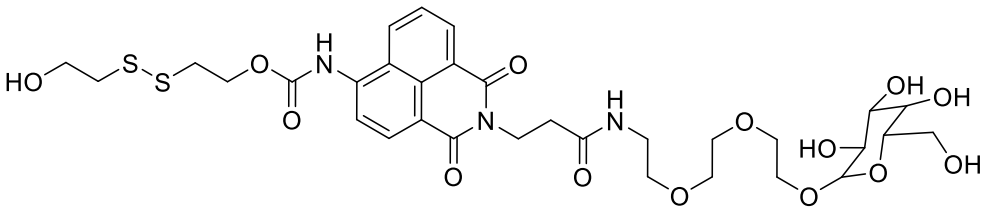

39

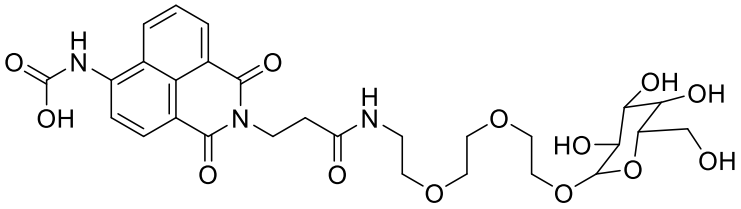

40

Scheme 6 Cleavage of a naphthalimide based fluorescent probe

Disulfide bridges have started to be used as linkers between antibodies and antibiotics.[84] Small molecules can be conjugated to free cysteine residues on a mutant antibody to take advantage of the antibody's superior biostability. Target cell internalisation and degradation of the antibody via lysozyme leads to release of the antibiotic inside.[84] The disulfide linker is thought to break down inside the cytoplasm of the cell, having escaped the strongly oxidising environment of the lysozyme.[85] There were initially problems with this design. The linker would break down through thiol exchange leading to a very fast clearance of the

attached drug. More recently advances have been made to improve the stability of the linker with hindered disulfide linkers, however there is little data available on the longer term activity and half-life within *in vivo* models.[86]

1.4 Thioureas

41

Figure 9 General thiourea functional group

Thioureas, **41**, are known to have antimicrobial, antiviral and anticancer properties.[87] Thioureas have a broad spectrum of antibacterial activity,[88] especially when conjugated to adjacent aromatic systems. Examples include thiacetazone **42**, mathisazone, **43**, and thiocarlide, **44**, that are known to have antibiotic properties.[89]

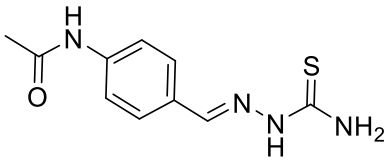

42
Thiacetazone

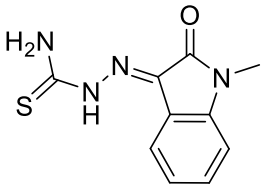

43
Methisazone

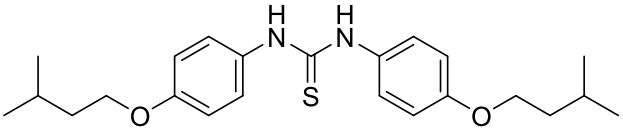

44
Thiocarlide

1.4.1 Interactions with DNA Gyrase

Phenyl thiourea based compounds containing a 3-trifluoromethylphenyl group have been shown to inhibit the action of DNA Gyrase and topoisomerase IV, similar to the fluoroquinolones.[90] The most active of these compounds, **45**, provided a starting point for the design of the library of thiourea conjugates chosen as synthetic targets.

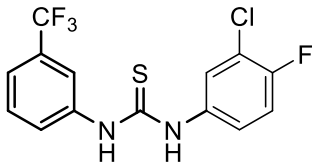

45

It was found that halogenated, especially fluorinated, phenyl rings are the best substituents for the R group, a factor that influenced the choice of target molecules discussed in later chapters.[90]

Docking studies involving quinolones conjugated to thioureas have begun to elucidate how those compounds bind. In 2015 Medapi *et al.* performed docking studies on a series of quinolone-thiourea hybrids. They report multiple binding modes to the GyrB subunit of *Mycobacterium tuberculosis*, shown in **Figure 10**.[91] These multiple binding modes are very dependent on the modifications made to the adjacent phenyl ring to the thiourea. This prompted the investigation into synthesising a library of halogenated phenyl thioureas, to determine whether this would affect the potency of the conjugates.

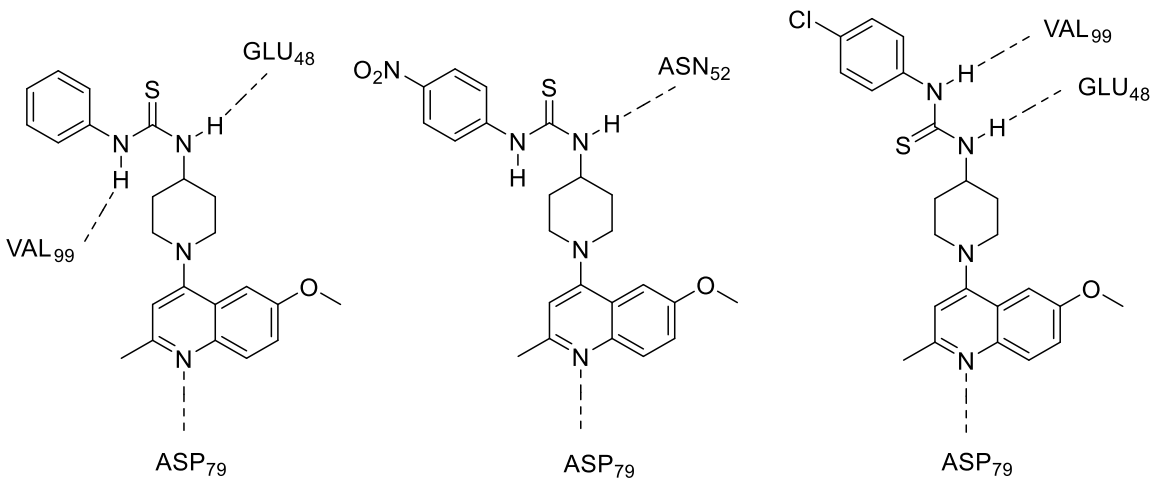

Figure 10 The binding modes of three thiourea quinolone conjugates in GyrB subunit of DNA gyrase in *Mycobacterium tuburculosis*. The strongest binding mode (lowest IC_{50}) if shown on the right.[91]

1.4.2 Thioureas as Radical Scavengers

Thioureas will readily react with hydroxyl radicals and hydrogen peroxide.[92] Superoxide radicals can abstract a single hydrogen from either nitrogen of a thiourea group in aqueous media which can then rearrange to form a sulfhydryl.[93,94] The ROS then reacts with water to form hydroxide ions. Thiourea will also react with hydrogen peroxide to generate formamidinesulfinic acid, **46**.[95]

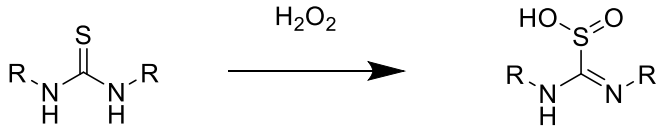

46

Scheme 7 Reaction of the thiourea group with hydrogen peroxide

Thiourea has been used as an experimental tool to investigate fluoroquinolone mechanisms of action.[48] The thiourea fluoroquinolone conjugates were designed with this in mind, to try to prevent the ROS from causing phototoxicity *in vivo*.

1.4.3 Fluoroquinolone-Thiourea Conjugates

Previously, ciprofloxacin-thiourea conjugates **47**, **48**, **49**, have been synthesised by esterifying the carboxylic acid group and functionalising the piperazine ring.[36] When tested against *E. coli*, most of these molecules did not retain the efficacy of ciprofloxacin, they had a reduced zone of inhibition (ZI). It was thought that the altering of the carboxylic acid could interfere with the formation of the ciprofloxacin-Mg^{2+}-enzyme water bridge and decrease the binding affinity.[36]

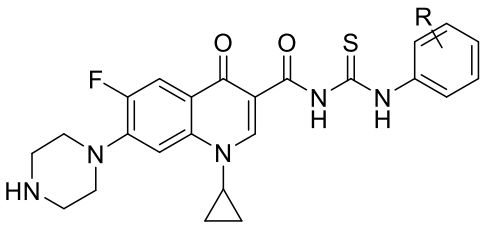

47

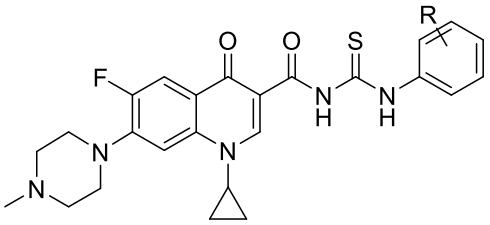

48

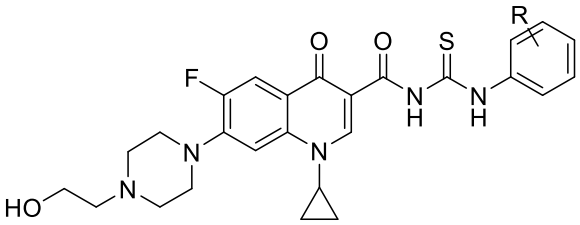

49

Figure 11 Previously synthesised Ciprofloxacin-thiourea conjugates. **R = H**, **2-CH_3**, **3-CH_3**, **4-CH_3**, **2-NO_2**, **3-NO_2**, **4-NO_2**, **2-OCH_3**, **4-OCH_3**, **3-Cl**, **4-Cl**, **4-COOH**[36]

However, one molecule, **50**, increased the ZI against the Gram-negative *E. coli* and decreased the ZI against the Gram-positive *S. aureus* compared to ciprofloxacin. In fact, all molecules **47-49** had this effect, though not to the same extent.[36] This suggests that some feature of Gram-negative bacteria increases the efficiency of uptake of the thiourea group in Gram-negative bacteria.

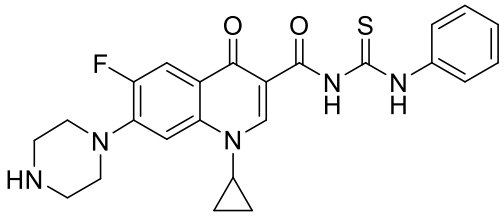

50

Investigations have also been carried out on forming dimers of Ciprofloxacin, **51**, and Norfloxacin, **52**, using thioureas. Polyethylene Glycol (PEG) linkers have been shown to increase lipophilicity and hence bioavailability of antibiotics, without decreasing the efficacy too much *in vitro*.[64] PEG has also been used to form ciprofloxacin slow release liposomes that would circulate the blood stream and diffuse ciprofloxacin out into the surrounding tissue.[96]

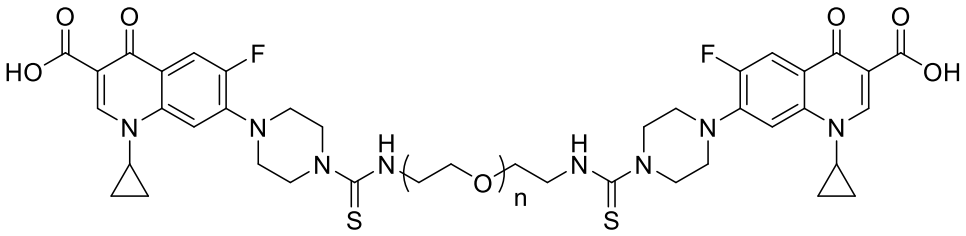

51

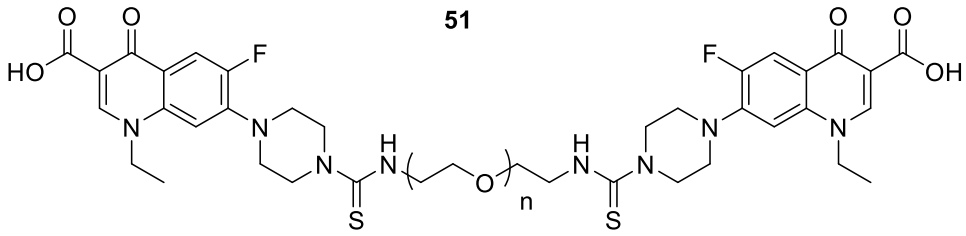

52

These type of ciprofloxacin dimers appear to have an upper limit to the molecular weight as larger dimers appeared to be generally less effective. The OmpF porin that ciprofloxacin diffuses through has a molecular weight limit of around 600 daltons.[20]

1.5 Project Overview

The initial aim of the project was to synthesise a small library of N-thioureido phenyl ciprofloxacin conjugate compounds. Fluoroquinolone conjugates have been shown to be a very effective class of antibiotics.[97–99] The phenyl thiourea group was chosen as a target due to the evidence for the binding to DNA Gyrase at a separate site to the fluoroquinolones.[91] We hoped that the two groups would act synergistically, and each help localise the other to the respective target binding site of the protein. There is proven track record of thiourea modifications at the C3 carboxyl group[36] affecting the activity of Ciprofloxacin so we felt there was merit in investigating similar conjugations at the piperazine.[97]

Before synthesising and screening the thiourea conjugates, it was realised that their activity was reduced in comparison to the parent antibiotic, ciprofloxacin. As biolabile linkers, the disulfide bridge in particular, is a well-studied area, hence it was decided to investigate a system that could release the antibiotic in the cytoplasm of the bacterial cell.[67] Initially, the target molecule was chosen as the ciprofloxacin dimer due to the previous promising examples discussed above. It was believed that this would be a suitable first target due to the simplicity in the design and it would allow investigation into the cleavage of the disulfide before proceeding with the ultimate aim of combining thioureas and ciprofloxacin linked by a disulfide biolabile link.

2.0 Results and Discussion of Synthesis and Biological Screening of the Thiourea Linked Ciprofloxacin Conjugates

2.1 Synthesis of Thiourea Linked Ciprofloxacin Conjugates

Phenyl thioureas have been noted to inhibit one of the same intracellular targets as ciprofloxacin, DNA Gyrase, by binding at a separate site.[43,91] The thiourea groups could react with the ROS produced by the ciprofloxacin,[92] which would decrease its efficacy. It was thought that the thiourea groups could also remove the phototoxic effects of ciprofloxacin and produce a safer antibiotic.

Conjugation of a thiourea to the terminal carboxylic acid has been shown to decrease efficacy relative to ciprofloxacin.[36] Attaching the group to the nitrogen of the piperidine ring was decided to be the best approach as this position is not part of the pharmacophore.[24] A variety of such conjugates have been synthesised with nitrogen as an attachment point and although activity was reduced, it was still present.[66,65] As thiourea is a DNA gyrase binding moiety itself it was theorised that it could counteract the loss of efficacy seen in other modifications of this type.[91]

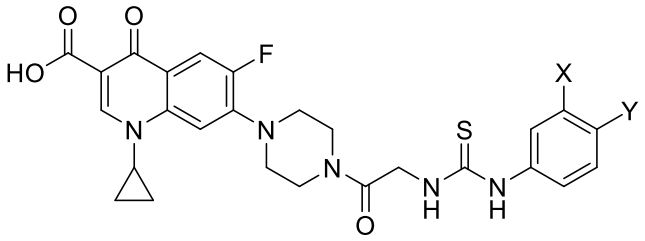

53

Figure 12 Structure of ciprofloxacin-thiourea conjugates. **X = H**, **Cl Y = H**, **Cl**, **F**

The designed conjugates have a phenyl thiourea group linked to ciprofloxacin via a glycine spacer, **53**, as shown in **Figure 12**. These spacers have been shown to be most effective against Gram-negative strains when used in ciprofloxacin-citrate conjugate systems, though overall efficacy was reduced.[45] The intended synthesis is shown in **Scheme 8**.

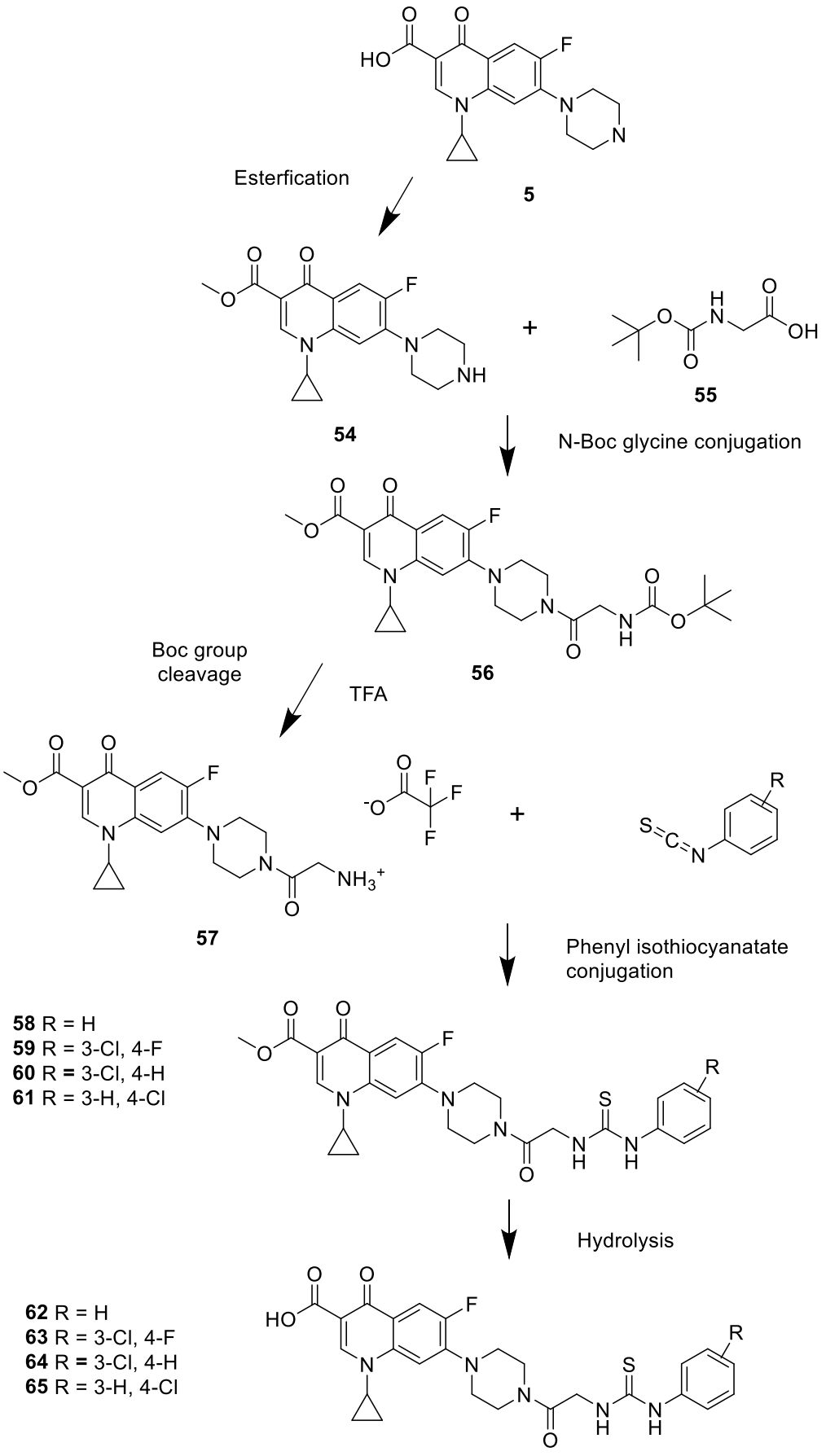

Scheme 8 Proposed synthesis for a ciprofloxacin-thiourea conjugate

As a point of variety, the antimicrobial effects of halogen substituents on the phenyl ring were explored. These combinations were selected based on the observations of A. Bielenica *et al.* on a 3-trifluoromethylphenyl thiourea conjugate. The conjugate with the lowest MIC was the 3-chloro-4-fluorophenyl species, **45**.[90]

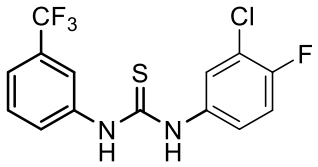

45

This prompted us to investigate the effects of varying the positions of halogens on the ring as this has been shown to affect the activities of phenyl thiourea conjugates. In order to do this, compounds **62-65** were made. The synthesis of each is discussed in later paragraphs. [36,90,100]

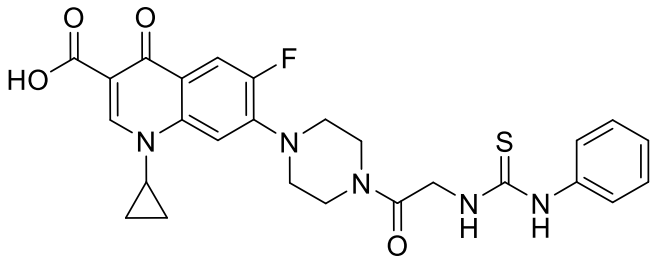

62

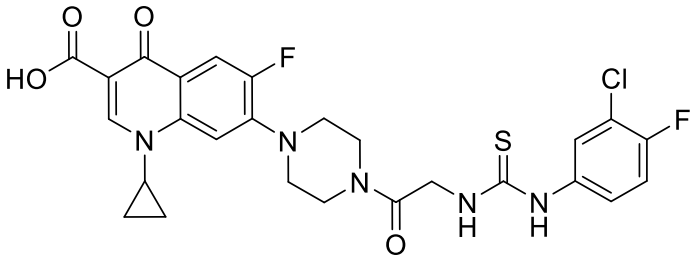

63

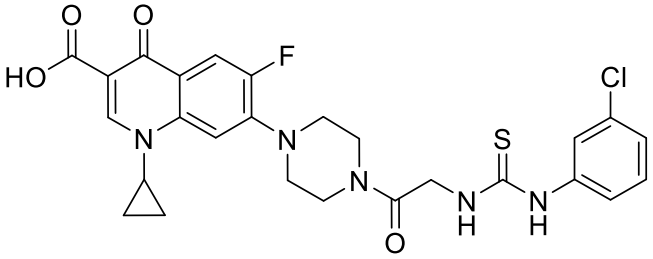

64

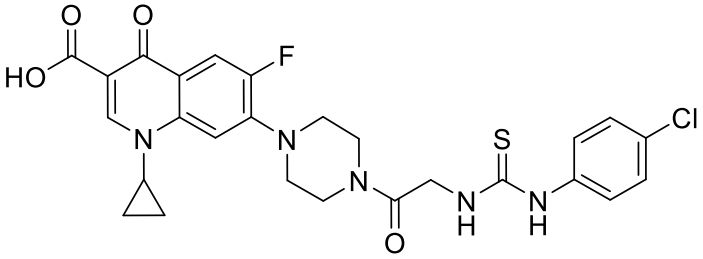

65

2.1.1 Methylation of Ciprofloxacin

The first step in the synthesis requires the protection of the carboxylic acid group of ciprofloxacin. This is done for two reasons, first removing the zwitterionic nature of ciprofloxacin making it easier to dissolve in organic solvents.[101] It also prevents any competing coupling reactions when amidation is undertaken.[102] The methyl protecting group was chosen as it is base labile[103], so orthogonal to the Boc protecting group on the nitrogen of the glycine spacer. Methylation was performed as shown in **Scheme 9**.

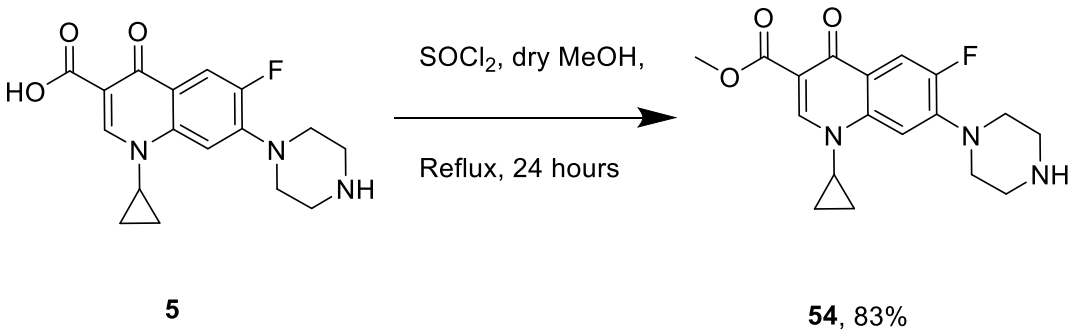

5 **54**, 83%

Scheme 9 Methylation of ciprofloxacin

Ciprofloxacin methanoate, **54**, was isolated in 83 % yield. The successful synthesis of **54** was supported by ^{1}H NMR analysis with a signal at 3.91 ppm of relative integration of 3 present in the spectrum. In addition, a signal at 51.95 ppm was observed in the ^{13}C NMR spectrum, both signals can be attributed to the methyl group of the ester formed. IR spectrometric analysis showed a new peak at 1720 cm^{-1}. Additionally, mass spectrometric analysis showed a peak at 346.1568 corresponding to ($[C_{18}H_{20}FN_3O_3+H]^+$

2.1.2 Conjugation of Me-Ciprofloxacin with N-Boc protected Glycine

With the protected ciprofloxacin in hand, conjugation to the spacer was explored. EDC-mediated coupling to commercially available N-Boc glycine, **55**, was performed as shown in **Scheme 10**.

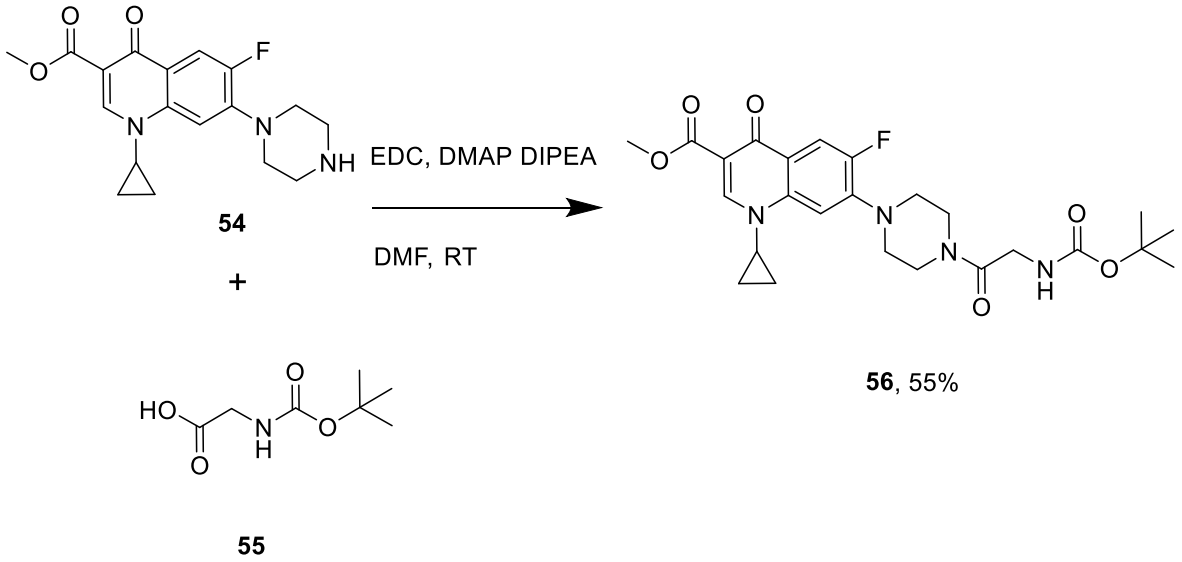

Scheme 10 EDC-mediated coupling of Me-ciprofloxacin to N-Boc glycine

Ciprofloxacin methanoate was reacted with N-Boc glycine using EDC as a coupling agent, with DMAP and DIPEA conjugate. **56** was isolated by column chromatography in 55% yield. Successful synthesis of **56** was supported by the observation of a peak at 1.46 ppm with a relative integration of 9 and a peak at 4.04 ppm of relative integration of 2 in the ^{1}H NMR trace. These signals correspond to the t-butyl protons of the Boc group and the alpha protons of the glycine respectively. Signals observed in the ^{13}C spectrum at 41.72 ppm and 169.18 ppm correspond to the alpha carbon and the amide carbonyl of the glycine respectively. Signals corresponding to the Boc group were also observed at 169.18 ppm, 79.80 ppm and 28.30 ppm. Mass spectrometric analysis revealed a signal at 503.2306 corresponding to ($[C_{25}H_{31}FN_4O_6+H]^+$

2.1.3 Boc Cleavage

The terminal Boc group was removed with 20% trifluoroacetic acid (TFA) in dichloromethane, as seen in **Scheme 11**.

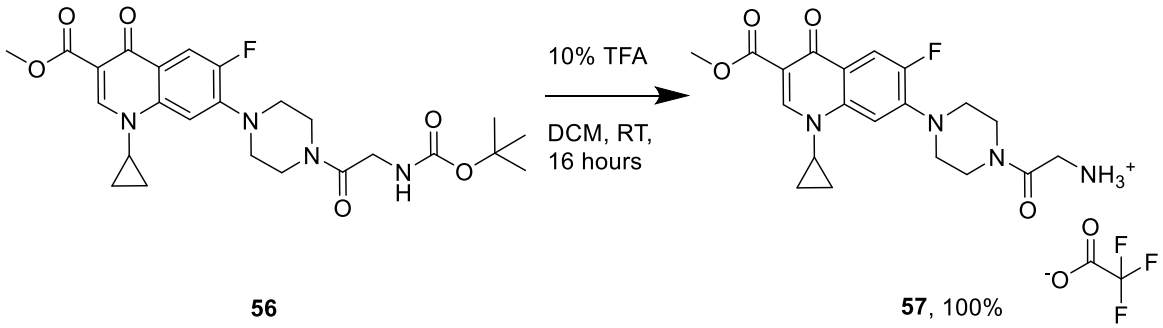

Scheme 11 Boc cleavage of 56

The deprotected product, **57**, was isolated in quantitative yields and the ^{1}H NMR spectrum showed the expected loss of peaks at 1.46ppm, and the peaks at 169.18ppm, 79.80ppm and 28.30ppm in the ^{13}C NMR were also absent. The TFA counterion is observed in the ^{19}F NMR at -73.46ppm. No residual free TFA was present as the other signals in the ^{19}F NMR trace were due to the fluorine present on ciprofloxacin at -124.43 – -124.49 ppm. Mass spectrometric analysis revealed a peak at 403.1776 corresponding to ($[C_{20}H_{24}F_1N_4O_4+H]^+$

2.1.4 Synthesis of Ciprofloxacin-Thiourea Conjugates

The next step was the construction of the thiourea moiety **Scheme 12**.

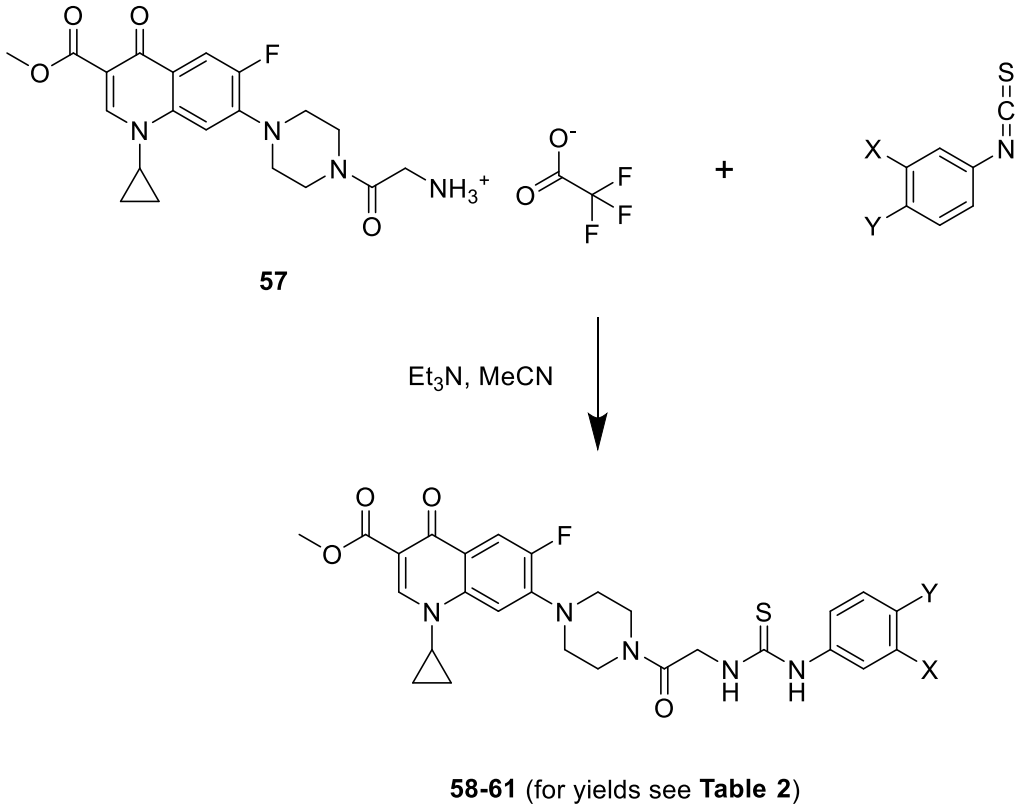

Scheme 12 Reaction of 57 with isothiocyanate. Conjugates 58 X = H, Y = H 59 X = Cl, Y = F 60 X = Cl, Y = H 61 X = H, Y = Cl

The reaction was carried out with Et_3N in MeCN. MeCN was chosen as a solvent due to the solubility of the isothiocyanates used and the corresponding insolubility of the resultant product, allowing isolation by simple filtration. The relevant data is shown in **Table 1** and **Table 2**.

Compound	Isolated Yield / %	IR Spectrometry values for the thiourea / cm^{-1}	ESI-MS m/z observed	Molecular ion
58	96	3409	538.1910	$[C_{27}H_{28}FN_5O_4S +H]^+$
59	85	3293	590.1442	$[C_{27}H_{26}ClF_2N_5O_4S +H]^+$
60	87	3281	572.1538	$[C_{27}H_{27}ClFN_5O_4S +H]^+$
61	81	3279	572.1538	$[C_{27}H_{27}ClFN_5O_4S+H]^+$

Table 1 Yields, IR wavenumbers and mass spectrometric analysis of Compounds 58-61

Compound	Key ^{1}H NMR signals observed / ppm	Assignment	Key ^{13}C NMR signals observed / ppm	Assignment
58	10.02	NH thiourea	171.58	Thiourea carbonyl
	7.83	NH thiourea	139.18	Phenyl
	7.51	CH phenyl	128.69	Phenyl
	7.34	CH phenyl	124.45	Phenyl
	7.12	CH phenyl	122.80	Phenyl
59	10.05	NH thiourea	171.54	Thiourea carbonyl
	8.01	NH thiourea	160.68	Phenyl
	7.93	CH phenyl	124.41	Phenyl
	7.37-7.39	CH phenyl	124.35	Phenyl
			124.29	Phenyl
			118.82	Phenyl
			116.65	Phenyl
60	10.20	NH thiourea	171.53	Thiourea carbonyl
	8.05	NH thiourea	141.06	Phenyl
	7.88	CH phenyl	132.70	Phenyl
	7.32-7.40	CH phenyl	130.00	Phenyl
	7.14	CH phenyl	123.52	Phenyl
			121.56	Phenyl
			120.59	Phenyl
61	10.13	NH thiourea	171.53	Thiourea carbonyl
	7.96	NH thiourea	138.43	Phenyl
	7.59	CH phenyl	128.44	Phenyl
	7.37	CH phenyl	127.76	Phenyl
			124.10	Phenyl

Table 2 Relevant spectroscopic data on the synthesis of Compounds 58-61

The successful synthesis of the thiourea conjugates **58-61** is supported by the information above in **Table 1** and **Table 2**.

2.1.5 Carboxylic Acid Deprotection

The final stage of the reaction scheme was base hydrolysis of the methyl ester on the C-terminal carboxylic acid. NaOH dissolved in dimethylformamide (DMF) was used, as shown in **Scheme 13**. After deprotection, subsequent acidification resulted in deprotected conjugate precipitating and it could be isolated without any further purification. The relevant NMR peaks lost in the analysis of the products are shown in **Table 3**. Elemental analysis was performed, and the results are shown in **Table 4**. Trace amounts of DMF were detected in the ^{1}H NMR spectra of some of the samples. The percentage level of DMF in each sample has been calculated from the integration of the peaks relative to the thiourea conjugate in the NMR spectrum and is shown in **Table 4**.

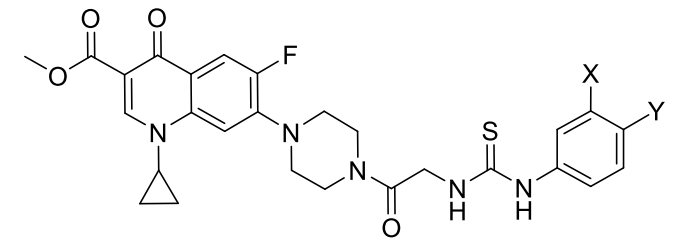

58-61

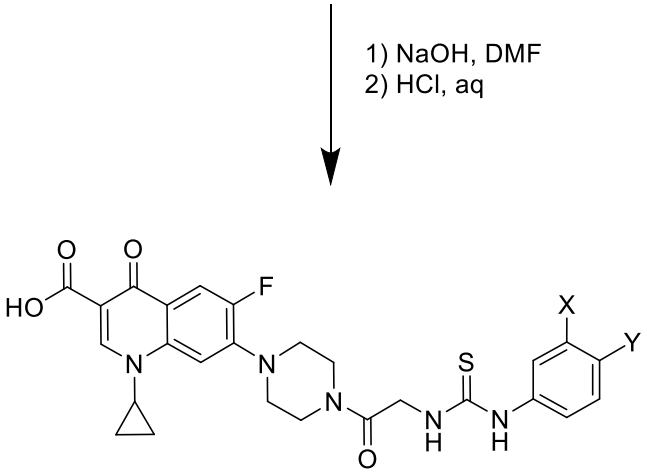

62-65 (for yields see Table 3)

Scheme 13 Deprotection of the C-terminal carboxylic acid. Conjugates 58 X = H, Y = H 59 X = Cl, Y = F 60 X = Cl, Y = H 61 X = H, Y = Cl. Deprotected conjugates 62 X = H, Y = H 63 X = Cl, Y = F 64 X = Cl, Y = H 65 X = H, Y = Cl

Compound	Isolated Yield / %	Key ^{1}H NMR signals absent / ppm	Key ^{13}C NMR signals absent / ppm	ESI-MS m/z observed
62	52	3.73	51.28	524.1772
63	49	3.73	51.28	576.1280
64	75	3.73	51.28	572.1538
65	40	3.73	51.30	572.1538

Table 3 Yields and spectrometric data for the synthesis of Compounds 62-65

Compound	Calculated Elemental Analysis / %	Observed Elemental analysis / %	Percentage of DMF contaminant / %
62	C 58.73 H 5.10 N 13.17	C 58.59 H 4.98 N 13.08	2
63	C 52.57 H 4.41 N 11.79	C 52.29 H 4.11 N 11.69	1
64	C 53.31 H 4.41 N 11.96	C 53.29 H 4.35 N 11.90	2
65	C 52.66 H 4.39 N 11.67	C 53.81 H 4.25 N 11.67	0

Table 4 Spectrometric and elemental analysis results for Compounds 62-65

The successful deprotection of each of **58-61** to generate **62-65** was supported by the disappearance of the peaks corresponding to the methyl groups from both ^{1}H and ^{13}C NMR spectra of the starting material. The deprotection reaction was shown to be complete by TLC. The loss of yield is due to the incomplete crystallisation when acid was added. The conjugates have multiple protonation sites on the ciprofloxacin and thiourea moieties and as a result could not be fully crystallised out of solution. The elemental analysis was calculated to be consistent with the adjusted formulae.

2.2 Biological Screening of Ciprofloxacin Thiourea Conjugates

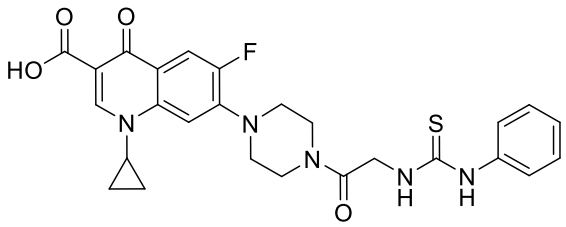

62

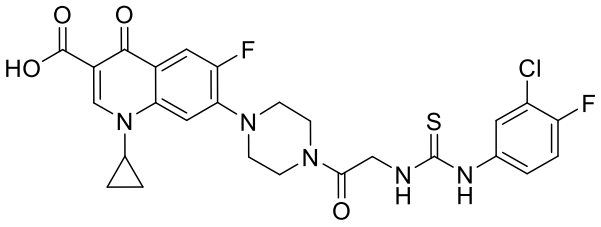

63

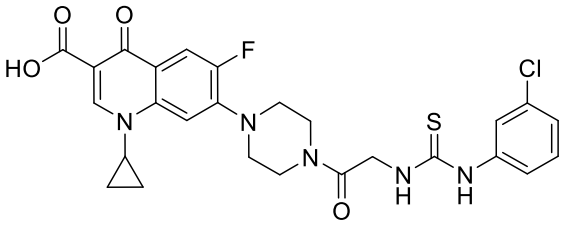

64

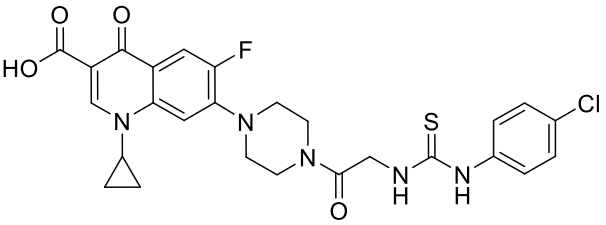

65

Conjugates **62-65**, were screened for antimicrobial activity against BW25113 wt *E.coli* in Lysogenic Broth (LB). Ciprofloxacin was also tested as a direct comparison as the parent antibiotic. Due to the synthesis leaving trace amounts of DMF, that was also run as a control.

Below is shown the general plate layout used for these experiments in **Table 5**, as well as the stock solutions used to fill the wells. Each stock solution was made up using the calculated mass from the elemental analysis and dissolved in DMSO. The triplicate repeats function as biological controls with each being grown from a different bacterial colony overnight in LB at 37°C. The three cultures were corrected to an OD_{650} of 2.0 before inoculation.

	1	2	3	4	5	6	7	8	9	10	11	12
A	H_2O	H_2O	H_2O	H_2O	H_2O	H_2O	H_2O	H_2O	H_2O	H_2O	H_2O	H_2O
B	H_2O	Drug 1	Drug 1	Drug 1	Drug 2	Drug 2	Drug 2	Drug 3	Drug 3	Drug 3	Blank	H_2O
C	H_2O	Drug 1	Drug 1	Drug 1	Drug 2	Drug 2	Drug 2	Drug 3	Drug 3	Drug 3	Blank	H_2O
D	H_2O	Drug 1	Drug 1	Drug 1	Drug 2	Drug 2	Drug 2	Drug 3	Drug 3	Drug 3	Blank	H_2O
E	H_2O	Drug 1	Drug 1	Drug 1	Drug 2	Drug 2	Drug 2	Drug 3	Drug 3	Drug 3	DMF	H_2O
F	H_2O	Drug 1	Drug 1	Drug 1	Drug 2	Drug 2	Drug 2	Drug 3	Drug 3	Drug 3	DMF	H_2O
G	H_2O	Drug 1	Drug 1	Drug 1	Drug 2	Drug 2	Drug 2	Drug 3	Drug 3	Drug 3	DMF	H_2O
H	H_2O	H_2O	H_2O	H_2O	H_2O	H_2O	H_2O	H_2O	H_2O	H_2O	H_2O	H_2O

Well Conc / µM	Stock Conc / µM
0	0
2	10
4	20
6	30
8	40
10	50

Table 5 Well lay out and stock solutions for the biological screening of Compounds 62-65

The outer wells of the plate were filled with 200µl of deionised water to minimise evaporation effects over the 20 hours. Into each blank well was placed 196µl of LB and 4µl of DMSO. Into each test well was placed 191µl of LB, 4µl of drug stock solution of the appropriate concentration and 5 µl of OD corrected bacterial culture. The blank wells were averaged and subtracted from the other values to control for any effect of DMSO or LB on the OD_{650} values.

Since the NMR spectra of the thiourea conjugates showed trace amounts of DMF in them, a control was run to evaluate the effect of DMF on bacterial growth. The stock concentration of DMF was calculated to equate to the amount of DMF in the most heavily contaminated conjugate when 10µM concentration of the conjugate is used in the screening. The results are shown in **Figure 13**.

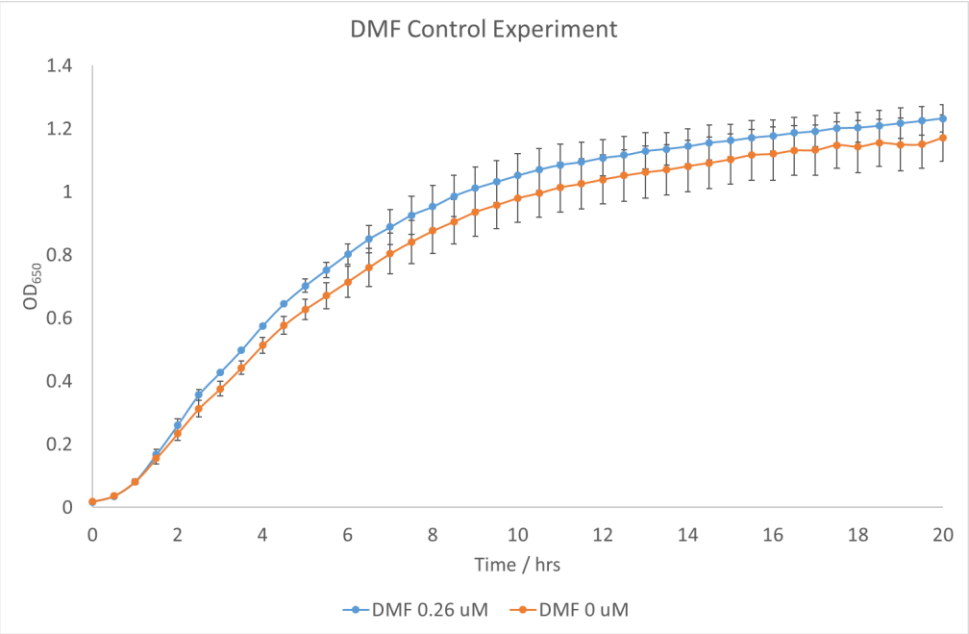

Figure 13 Bacterial growth curve of *E. coli* BW25113 with 0.26 µM DMF additive. Error bars are ± standard deviation of three biological replicates

As can be seen, DMF has no discernible effect on bacterial growth.

The results of the thiourea conjugate growth assays at increasing concentration are shown in **Figures 14-19**.

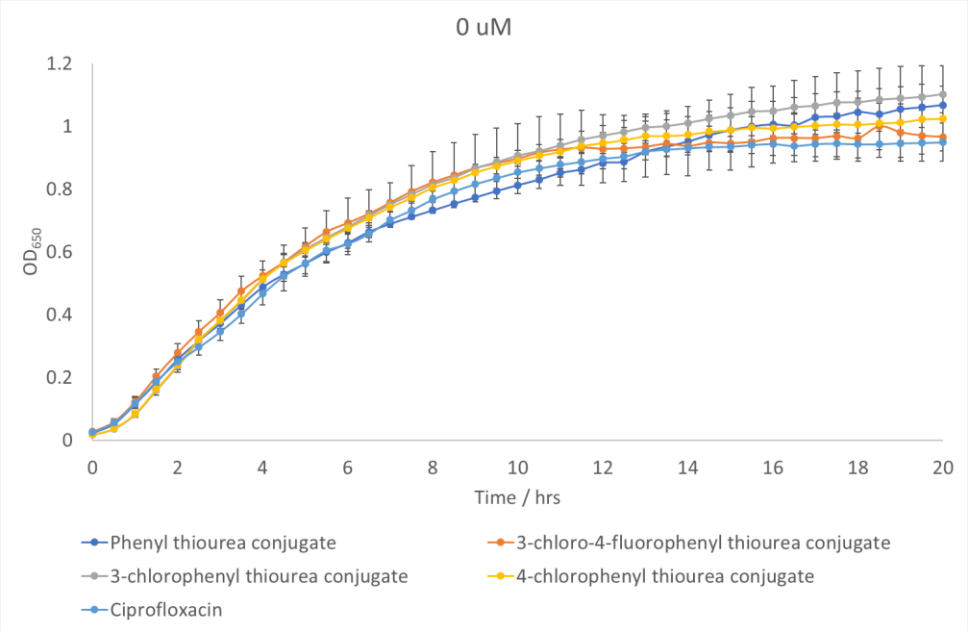

Figure 14 Control bacterial growth curve of BW25113 strain of E. coli. Error bars are ± standard deviation of three biological replicates

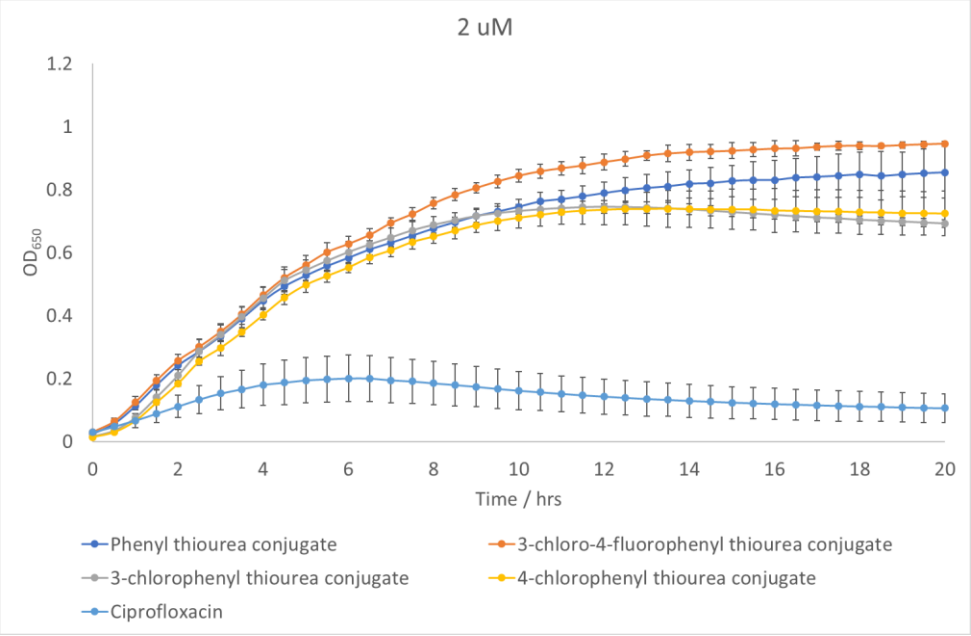

Figure 15 Bacterial growth curve of *E. coli* BW25113 with 2.0 µM additives. Error bars are ± standard deviation of three biological replicates

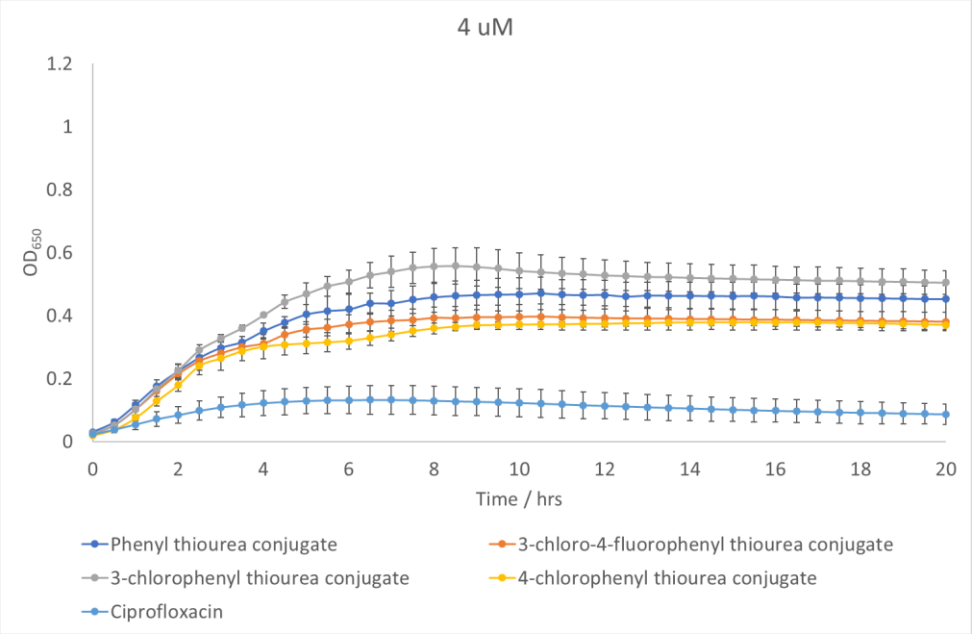

Figure 16 Bacterial growth curve of *E. coli* BW25113 with 4.0 µM additives. Error bars are ± standard deviation of three biological replicates

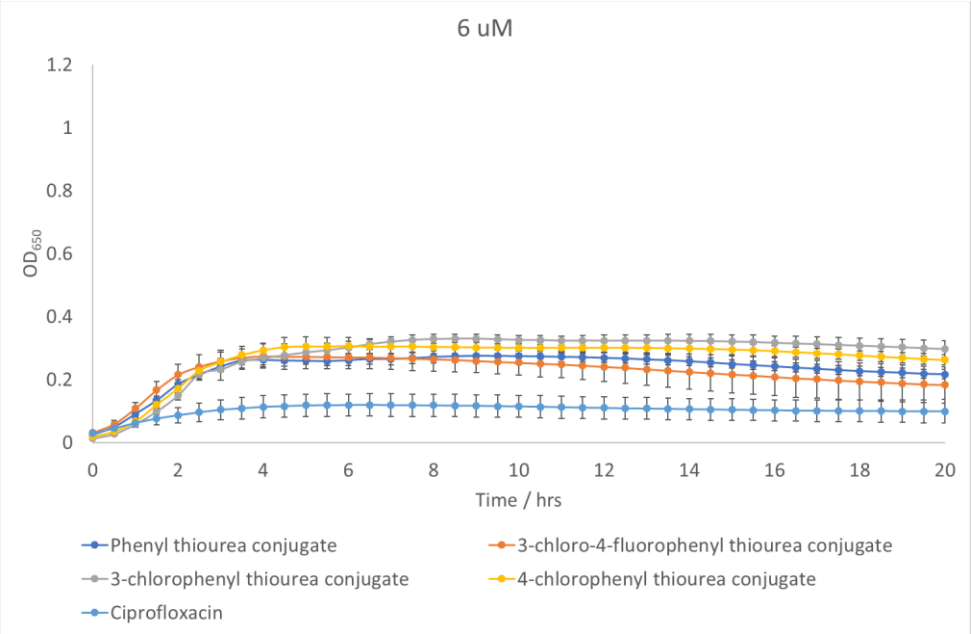

Figure 17 Bacterial growth curve of *E. coli* BW25113 with 6.0 µM additives. Error bars are ± standard deviation of three biological replicates

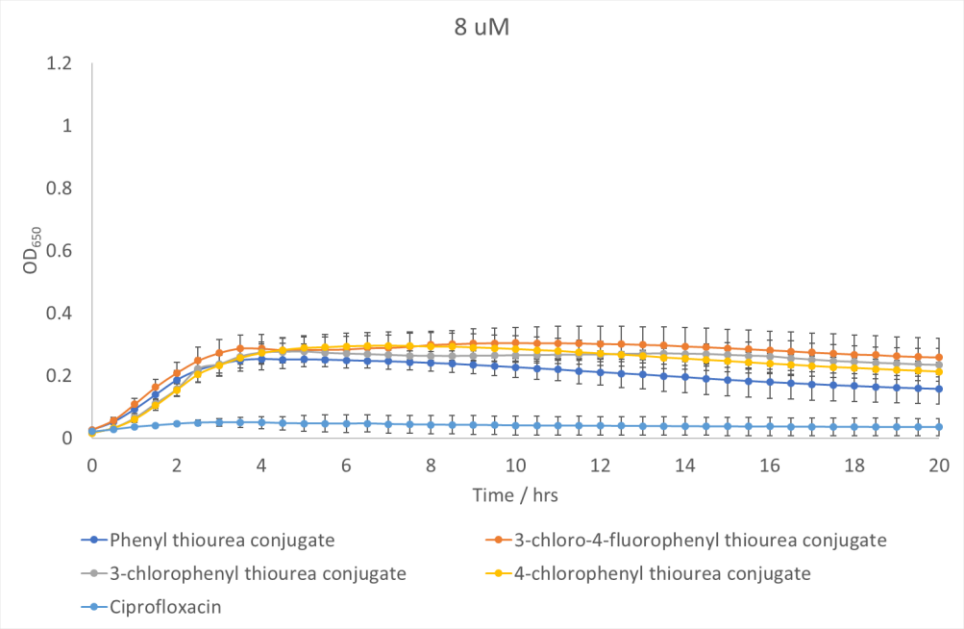

Figure 18 Bacterial growth curve of *E. coli* BW25113 with 8.0 µM additives. Error bars are ± standard deviation of three biological replicates

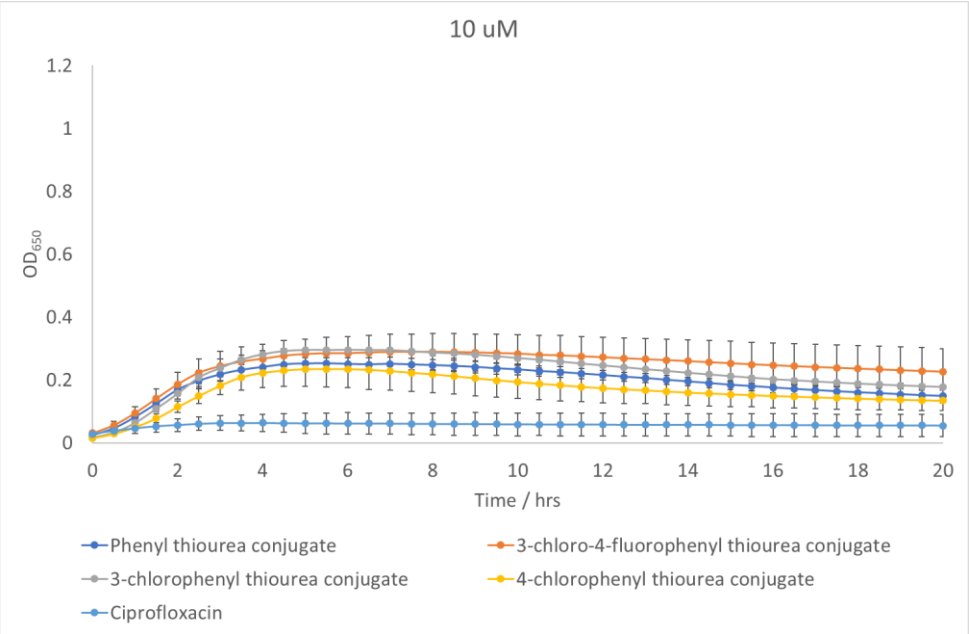

Figure 19 Bacterial growth curve of *E. coli* BW25113 with 10.0 µM additives. Error bars are ± standard deviation of three biological replicates

As can be seen, all four thiourea conjugates have a concentration dependent effect on bacterial growth. The maximum OD_{650} reached in the control experiment was around 1.1, however, the maximum OD_{650} reached decreases as concentration increases.

There is a significant drop in max OD_{650} when the concentration is increased to 6 µM and no significant further change with higher concentrations. The data suggests the MIC for these thiourea conjugates is between 4 µM and 6 µM. This is a large drop in efficacy from Ciprofloxacin which has a MIC of 0 µM to 2 µM in these studies. Since the activity of Ciprofloxacin is due to the formation of a tight, specific enzyme complex,[24] the additional steric bulk could be inhibiting the binding as observed in other studies.[56,68,85,99] In addition, the piperazine's function is to prevent the drug being effluxed. The thiourea modification could be blocking this function resulting in a lowered intracellular concentration of the conjugates.

At all concentrations, the thiourea conjugates appear to have a lag time of around three hours before beginning to influence the rate of growth of the bacteria. This lag time is much longer than the Ciprofloxacin experiments, suggesting that the thiourea modifications are slowing down the rate of uptake of the drug into the cell. The zwitterionic nature of ciprofloxacin has been removed by the modifications. Removal of the ionisable group increases the lipophilicity, and hence the ability to diffuse through the lipid bilayer.[17] However the porins in the bacterial outer membrane transport have a higher affinity for charged molecules so the rate of uptake through the OmpF porin could be slowed.[19] The molecular weight is still under the cut-off for OmpF, though the shape of the molecule may be incompatible with the porin.[18]

The four different thiourea conjugates show no significant difference in efficacy as can be seen in **Figure 20**. As all error bars overlap they can be assumed to be, within the margin of error of the experiment, the same. No difference can be seen by varying the halogens or substitution positions on the phenyl ring, albeit with a limited number of examples.

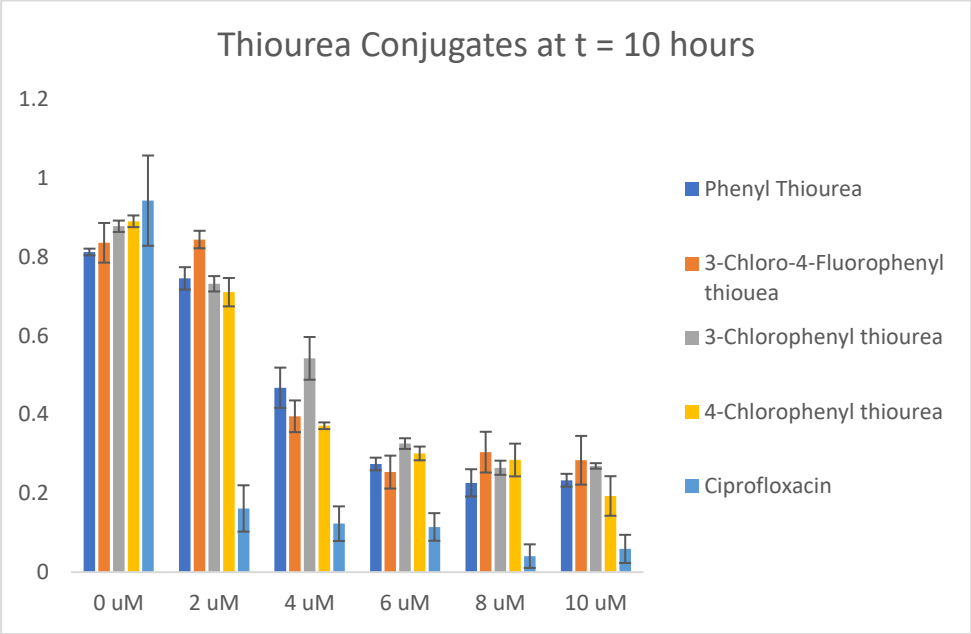

Figure 20 OD_{650} values for all thiourea conjugates at 10 hours. Error bars are ± standard deviation of three biological replicates

These experiments showed that the thiourea modification was decreasing the efficacy of the parent antibiotic, ciprofloxacin. To explore the interaction of the conjugates with the intracellular target, a DNA gyrase assay was performed on a representative conjugate **62**.

2.3 DNA Gyrase Assay of Conjugate 62

DNA Gyrase binding assays were used to explore whether the observed decrease in antimicrobial activity was, at least partly, due to decreased binding affinity to the target DNA gyrase. A negative control with no added DNA gyrase and a positive control with no added inhibitor were included.

Relaxed plasmid pBR322 DNA was incubated with *E. coli* DNA Gyrase in the presence of various concentrations of **62** to investigate its ability to inhibit the supercoiling activity of Gyrase. As DMSO, a known inhibitor of Gyrase,[104] was used to solubilise the compound, a DMSO control was included. The contents of each well are listed in **Table 6**.

	Positive	**Negative**	**Test Wells**	**DMSO control**
H_2O / µL	21.5	23.5	20.5	20.5
pBr322 / µL	0.5	0.5	0.5	0.5
Assay Buffer / µL	6	6	6	6
Drug Stock / µL	0	0	1	0
DMSO / µL	0	0	0	1
Gyrase Aliquot / µL	2	0	2	2

Stock Drug Conc / µM	**Assay Drug Conc / µM**
15	0.5
30	1
150	5
300	10
600	20

Table 6 Contents of each experiment in the DNA gyrase assay of Compound 62 and the stock solutions

After an incubation time of 30 minutes, the reaction was stopped with a 50:50 mix of isoamyl alcohol and chloroform. Each sample was loaded into a well in a 1 % w/v agarose gel and run at 75 V for 90 minutes. The gel was then stained using 10 µL SYBR SAFE in 100 mL TBE buffer for 60 minutes, destained in TBE buffer and imaged. The picture was enhanced and is presented in **Figure 21**.

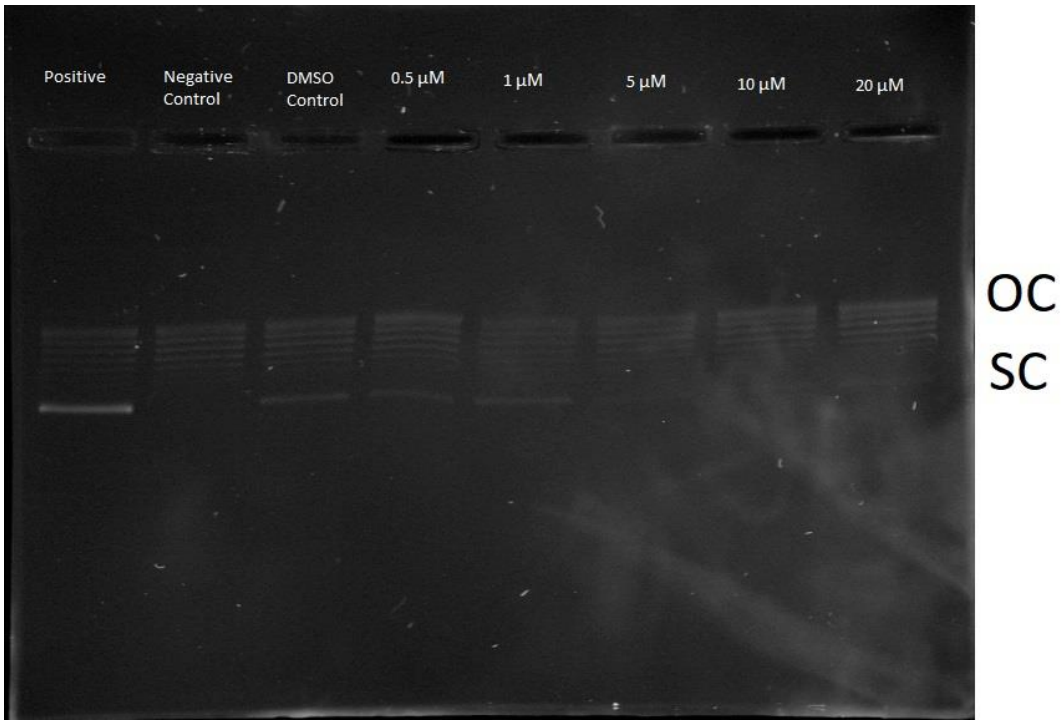

Figure 21 DNA gyrase assay of compound 62 at different concentrations with positive control (+ve) – 2 µL DNA gyrase and 0.0 µM of drug, negative control (-ve) – no DNA gyrase and 0.0 µM of drug and a DMSO control. OC- open circular and SC- supercoiled plasmid

The open circular (OC) plasmid moves more slowly through the agarose gel as it presents more surface area to the direction of movement. The supercoiled (SC) DNA moves more quickly as it is smaller. Incubating the OC plasmid with Gyrase will convert it into the SC form over time, and the inhibitor will prevent the SC band formed. More effective inhibitors and higher concentrations result in a fainter SC band.

The conjugate investigated has some DNA Gyrase binding affinity. The DMSO control indicates that the DMSO is having a small inhibitory effect. However, as the drug concentration increases, the supercoiled band is seen to fade. Ciprofloxacin shows complete inhibition of Gyrase activity with a concentration of 0.5 µM.[66] For **62** the supercoiled band fades at 10 µM. This data suggests that the binding affinity has been reduced with the thiourea modifications, possibly due to the increased steric bulk of the molecule. Previous work in the Duhme-Klair/ Routledge laboratory has found similar results when modifying ciprofloxacin with sterically bulky groups. [65,66]

2.4 Conclusions

Thiourea moieties has been attached via a non-biolabile linker to ciprofloxacin. It has been demonstrated that these modifications have slowed uptake into the cell, as seen by the lag in the growth assays before growth is being inhibited, and that the binding affinity for DNA gyrase has also been reduced, as seen in the gel assays.

The complex formed when ciprofloxacin binds to DNA gyrase is known to be tight and specific. The increased steric bulk of **62** could be interfering with the formation of this complex and there is no enhanced binding to gyrase with the thiourea present as proposed. Another possibility is that the thiourea may be binding at an alternate site on the enzyme and preventing the more effective ciprofloxacin from reaching its binding site.

3.0 Results and Discussion of The Synthesis and Biological Screening of a Biolabile Ciprofloxacin Dimer

As explored in the previous chapter, it was found that conjugating a thiourea moiety to ciprofloxacin with a non-biolabile linker resulted in reduced bactericidal activity and DNA gyrase inhibition. It was theorised that using the biolabile linker to link the two moieties could prevent these negative effects, as the linker would cleave to release the two active moieties to act independently.[67] The disulfide bridge was chosen as it is proven to be stable in the extracellular medium in humans and cleaves in the intracellular medium of bacteria.[84]

It was decided to explore the application of a biolabile linker by the synthesis of a ciprofloxacin dimer as the effect of linker would be easily comparable to the monomer, without the complication of the thiourea. The formation of ethylene sulphide[67] as the link cleaved would potentially be quite slow, so the rate of cleavage needed investigating.

3.1 Ciprofloxacin Dimer Synthesis

A dimer of Ciprofloxacin was chosen as an initial target molecule, with a disulfide bridge link **66**. The dimer was designed to be stable in the extracellular medium[84] and periplasm.[78] As the carboxylic acid is modified it would no longer be charged, meaning the molecule would be less hydrophilic and hence have the potential to cross the lipid bilayer more rapidly than the monomer.[16–18] Once the dimer entered the cytoplasm of the bacterium, it would be cleaved by the bacterium's endogenous reductive pathways, such as reacting with glutathione and free cysteine residues.[71,77] As Jain *et al.* also note, the carboxylic acid groups on

ciprofloxacin make it an excellent candidate for disulfide attachment via an ester link. [67] The cleavage of **66** is shown in **Scheme 14**.

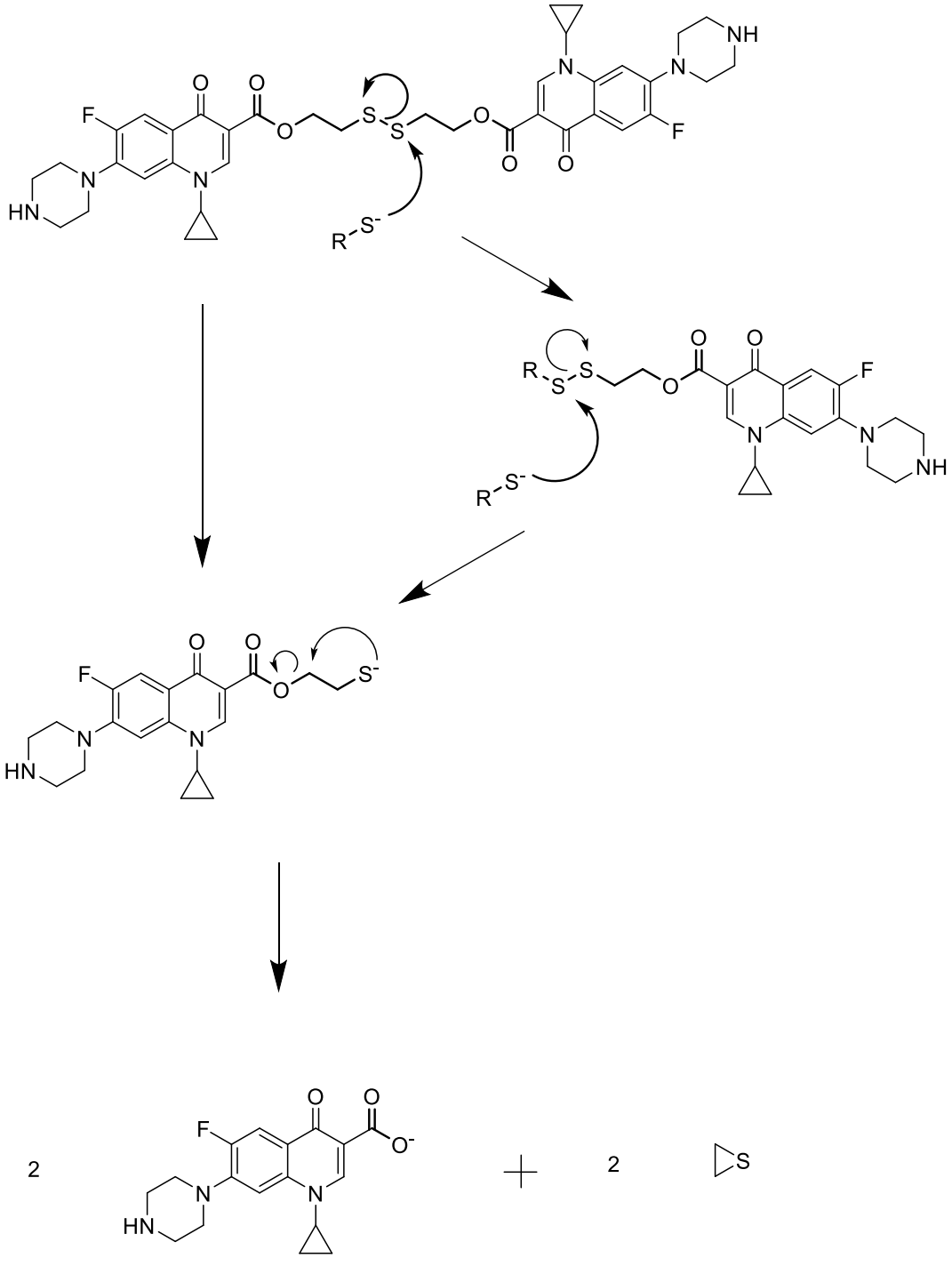

Scheme 14 Proposed mechanism of ciprofloxacin-disulfide dimer cleavage.[67] **R = glutathione or cysteine**

The N-terminal piperazine will be protected to prevent competing coupling reactions. An acid labile tert-butyloxycarbonyl (Boc) protecting group was chosen as the disulfide was prone to cleavage under basic conditions.[65] Attaching the linker to the free carboxylic acid group would allow the dimer to cleave in the cytoplasm, releasing ciprofloxacin as seen in **Scheme 14** above. The proposed synthesis of **66** is shown in **Scheme 15**.

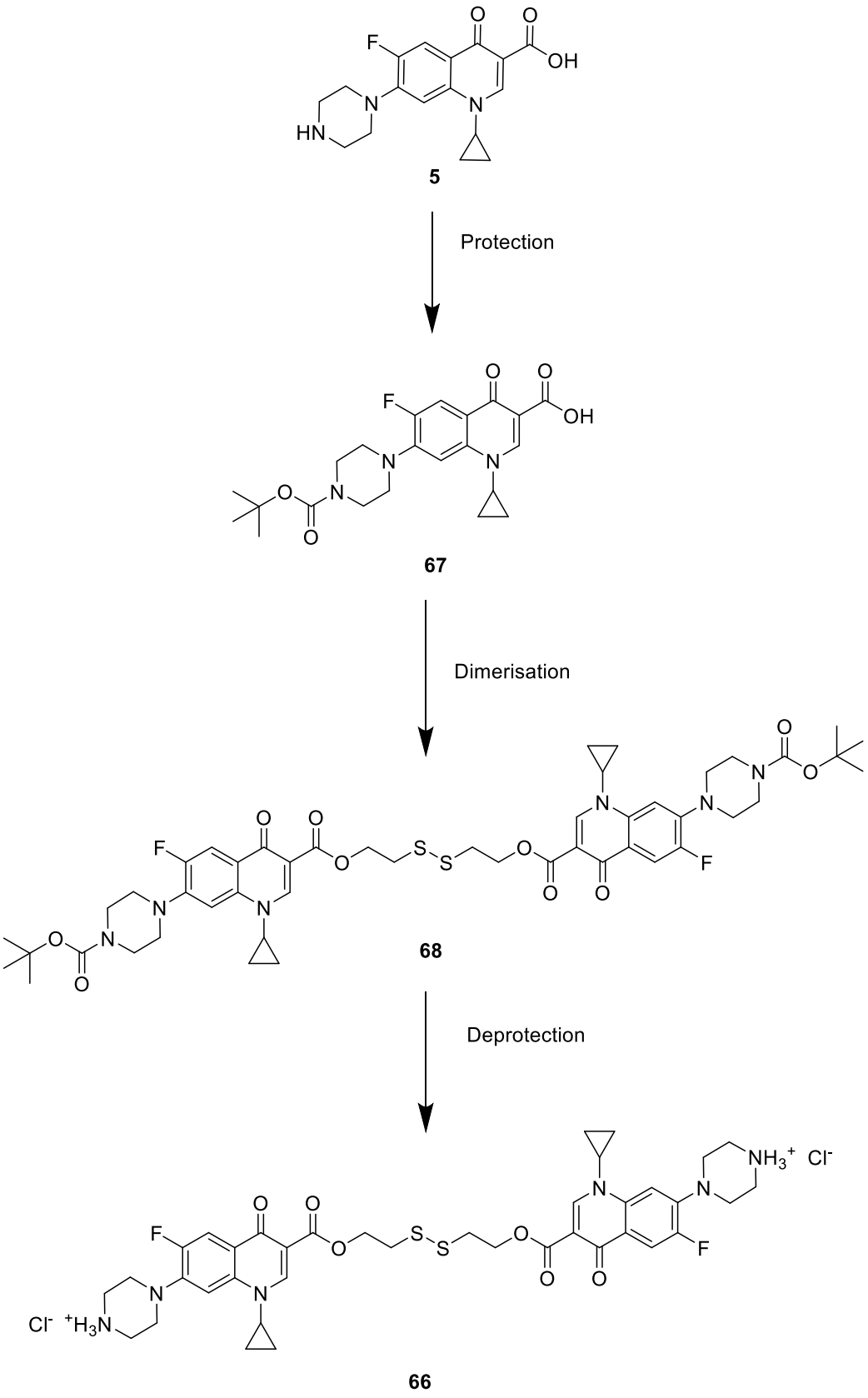

Scheme 15 Proposed synthesis of 66

3.1.1 N-Boc protection of Ciprofloxacin

The first step was the protection of the N-terminus of ciprofloxacin with a Boc group. The reaction is shown in **Scheme 16**.

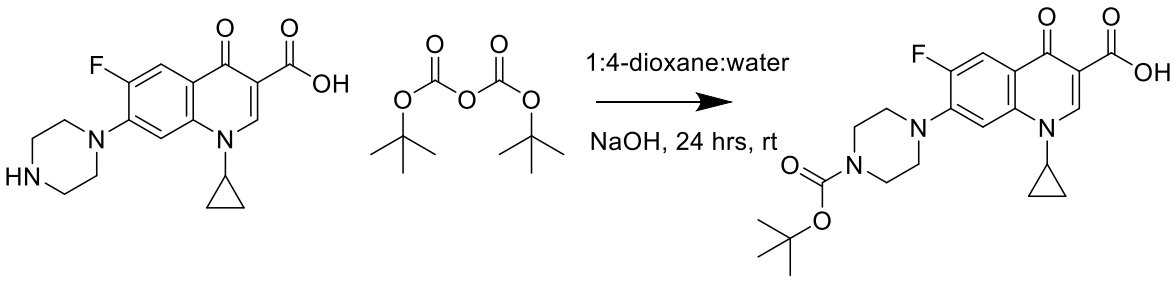

5 **67**, 99 %

Scheme 16 Boc protection of ciprofloxacin

The successful synthesis of **67** was supported by ^{1}H analysis with a peak at 1.50 ppm with relative integration of 9 observed in the spectrum. The presence of a Boc group was also supported by peaks at 166.87 ppm, 80.3 ppm and 28.36 ppm observed in the ^{13}C NMR spectrum. In addition, a peak at 432.1923 corresponding to $[C_{22}H_{26}FN_3O_5+H]^+$ was present in the mass spectrum.

3.1.2 HATU-coupled Dimerisation of N-Boc Ciprofloxacin via a Disulfide Linker

With the protected ciprofloxacin in hand, the construction of the disulfide link was investigated, **Scheme 17**.

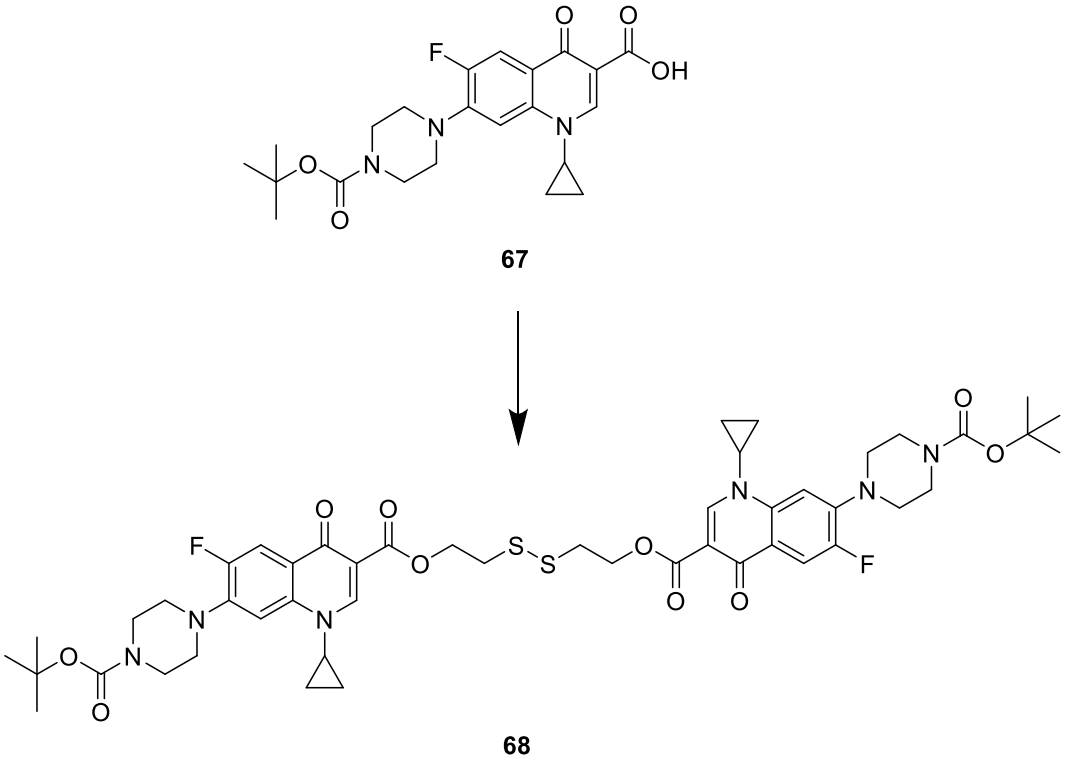

Scheme 17 Formation of the protected ciprofloxacin dimer, 68

A variety of coupling agents were investigated. Initially members of the carbodiimide family were tested. Both 1-ethyl-3-(3-dimethylaminopropyl) carbodiimide (EDC) and *N,N'*-dicyclohexylcarbodiimide (DCC) failed to give the desired disulfide. There were no triplet peaks that suggest the presence of the bridging carbon chains in the ^{1}H NMR, nor was the dimer seen in mass spectrometric analysis. Instead, in mass spectrometric analysis, a peak was seen at 587.3376 that matched the rearranged N-acylurea, **70**, often seen with carbodiimides[105] and shown in **Scheme 18**.

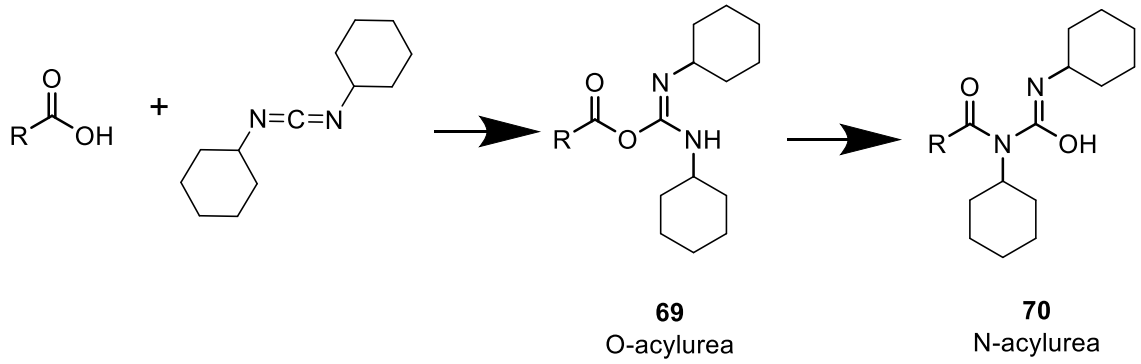

Scheme 18 Carbodiimide intermediate rearrangement from O-acylurea to unreactive N-acylurea using DCC as an example. **R = ciprofloxacin**

Propyl phosphonic anhydride (**T3P**) was the next coupling agent investigated and was also unsuccessful. T3P has come to prominence due to its ability to prevent the epimerisation seen with the carbodiimide coupling agents. Alongside this, it is known for a facile work up due to water soluble by-products, its solubility in a range of organic and polar solvents, and its reactivity in mild reaction conditions.[106]

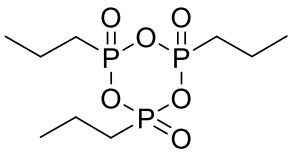

T3P

The proposed reaction is shown in **Scheme 19.** After a 3-day reflux and an aqueous wash, only signals corresponding to the starting material was observed in the ^{1}H spectrum of the crude material recovered after an aqueous wash to remove unreacted T3P.

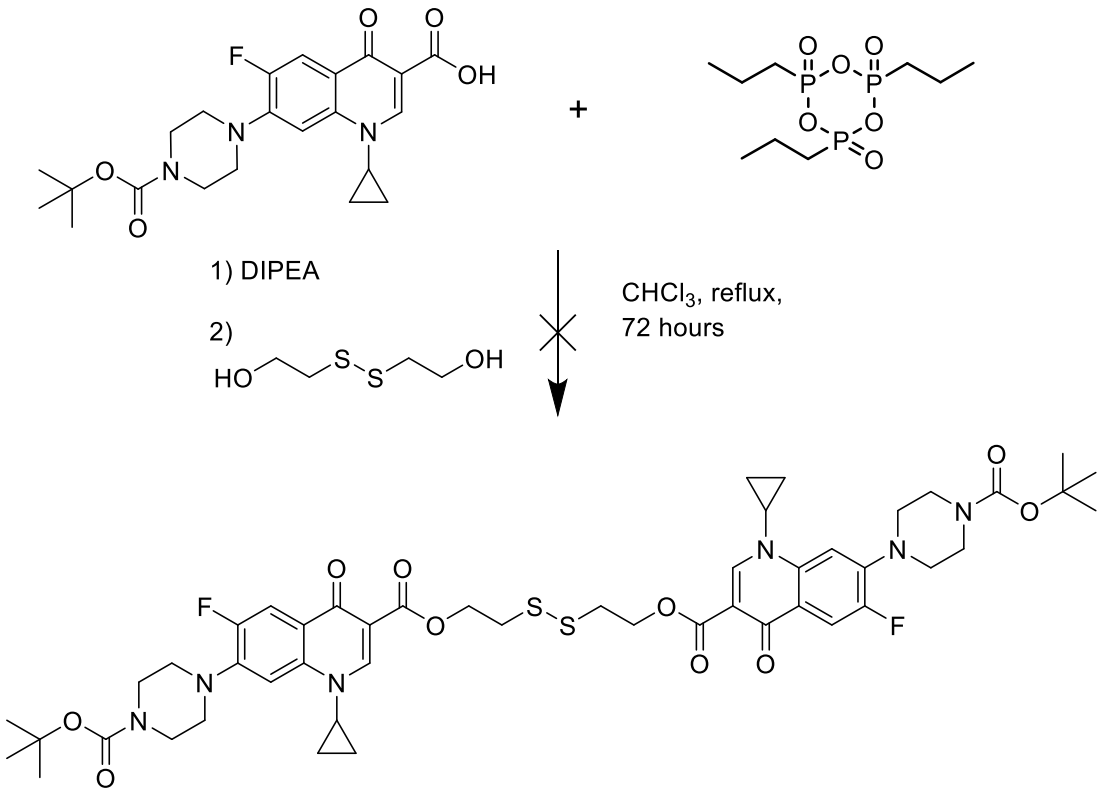

Scheme 19 The unsuccessful proposed synthesis of the protected dimer using T3P

Next, 1-[bis (dimethylamino) methylene]-1H-1,2,3-triazolo[4,5-b] pyridinium 3-oxid hexafluorophosphate (HATU) was investigated. The reaction can be seen in **Scheme 20**.

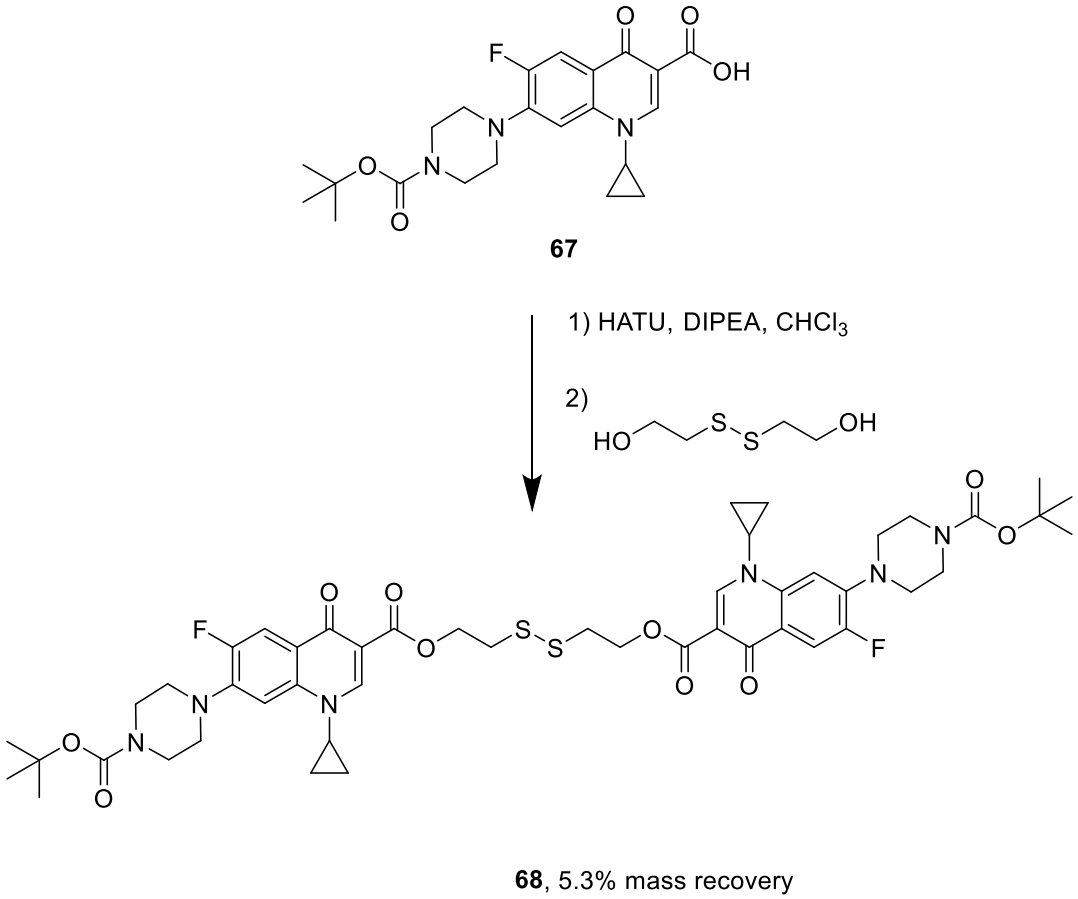

Scheme 20 Successful synthesis of 68

Analysis of the unpurified reaction mixture suggested the presence of three ciprofloxacin-containing compounds, judging from the singlet peaks at 8.45 ppm, 8.55 ppm and 8.59 ppm with relative integrations of 1.00, 0.36 and 0.14 respectively. Several sets of triplet peaks were observed to overlap that correspond to the CH_2 groups in the disulfide bridge. The disulfide bridge peaks of 2-hydroxyethyl disulfide appear at 3.88 ppm and 2.87 ppm, which are absent from the crude spectrum. It was decided to try to isolate these separate species but attempts using column chromatography failed. In all cases it was seen that the multiple ciprofloxacin species co-eluted in the solvent mixtures. The stationary and mobile phases that were investigated are noted in **Table 7**.

Attempt	Stationary Phase	Solvent 1	Solvent 2	Additives
1	Silica	100 % EtOAc	-	-
2	Silica	90 % $CHCl_3$	10 % MeOH	-
5	Silica	95 % EtOAc	5 % MeOH	-
6	Silica	97 % $CHCl_3$	3 % MeOH	-
7	Alumina	50 % MeCN	50 % $CHCl_3$	-
8	Alumina	80 % MeCN	20 % $CHCl_3$	0.1% NH_3
9	Silica	100% MeCN	-	-

TABLE 7 Unsuccessful solvent systems investigated to purify Compound 68

With the lack of success with column chromatography the next technique investigated was preparatory High-Performance Liquid Chromatography (**HPLC**) as described in the Experimental Chapter. The HPLC method successfully managed to purify the desired product **68** although at extremely low yield. The HPLC trace is shown in **Figure 22**.

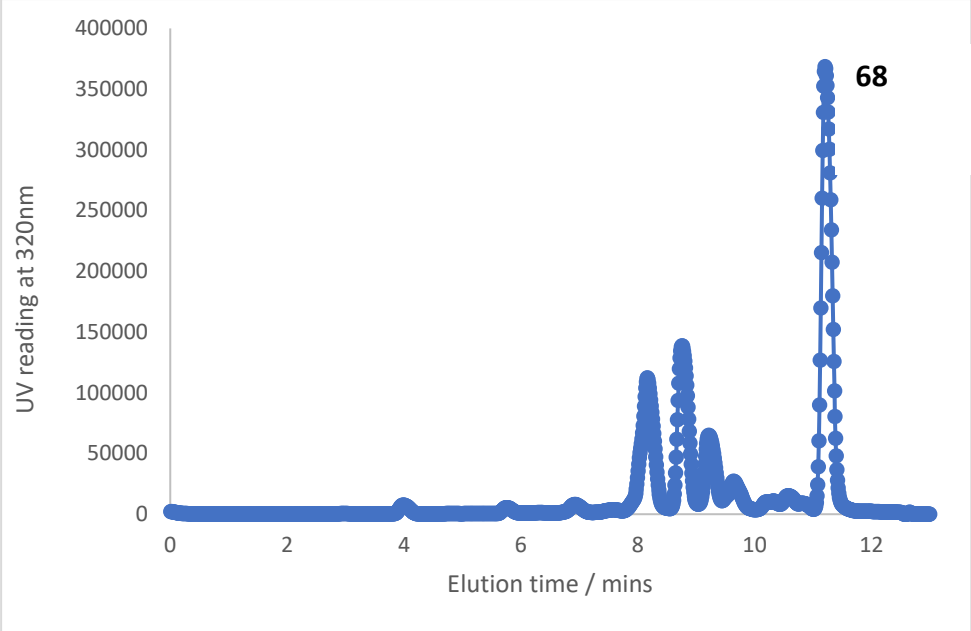

Figure 22 HPLC trace for the isolation and purification of compound 68, which eluted at 11 minutes

The successful synthesis of **68** was supported by ^{1}H NMR spectroscopy. The appearance in the spectrum of triplets at 4.55 ppm and 3.09 ppm each with a relative integration of 4H corresponding to the CH_2 groups in the disulfide bridge. The ^{13}C NMR also showed peaks at 62.35 ppm and 37.37 ppm corresponding to these CH_2 groups too. Mass spectrometric analysis also showed a peak at m/z = 1003.3514 which corresponds to the presence of $[C_{48}H_{58}F_2N_6O_{10}S_2+Na]^+$ The target molecule was synthesised with a 5.3 % mass recovery after HPLC purification.

As mentioned above the overlapping sections of the ^{1}H NMR made it impossible to determine the relative integrations of the different ciprofloxacin-disulfide species in the reaction mixture before HPLC. The low mass recovery could be due to an incomplete reaction, with the dimer being a minor species hidden under the other side products in the ^{1}H NMR spectrum. It is also possible that the product was lost during the filtration process or on the HPLC column itself.

3.1.3 HCl deprotection of the Dimer

As shown in **Scheme 21**, protected dimer **68** was initially deprotected with TFA and isolated as the TFA salt. However TFA ions are known to perturb screening results[107] so ion exchange to the chloride salt was undertaken. To exchange ions the solid was dissolved in aqueous HCl (10 mM) and then freeze dried. Unfortunately, this ion exchange resulted in disulphide cleavage, as seen by the disappearance of the triplets at 4.55 ppm and 3.09 ppm in the ^{1}H NMR spectrum.

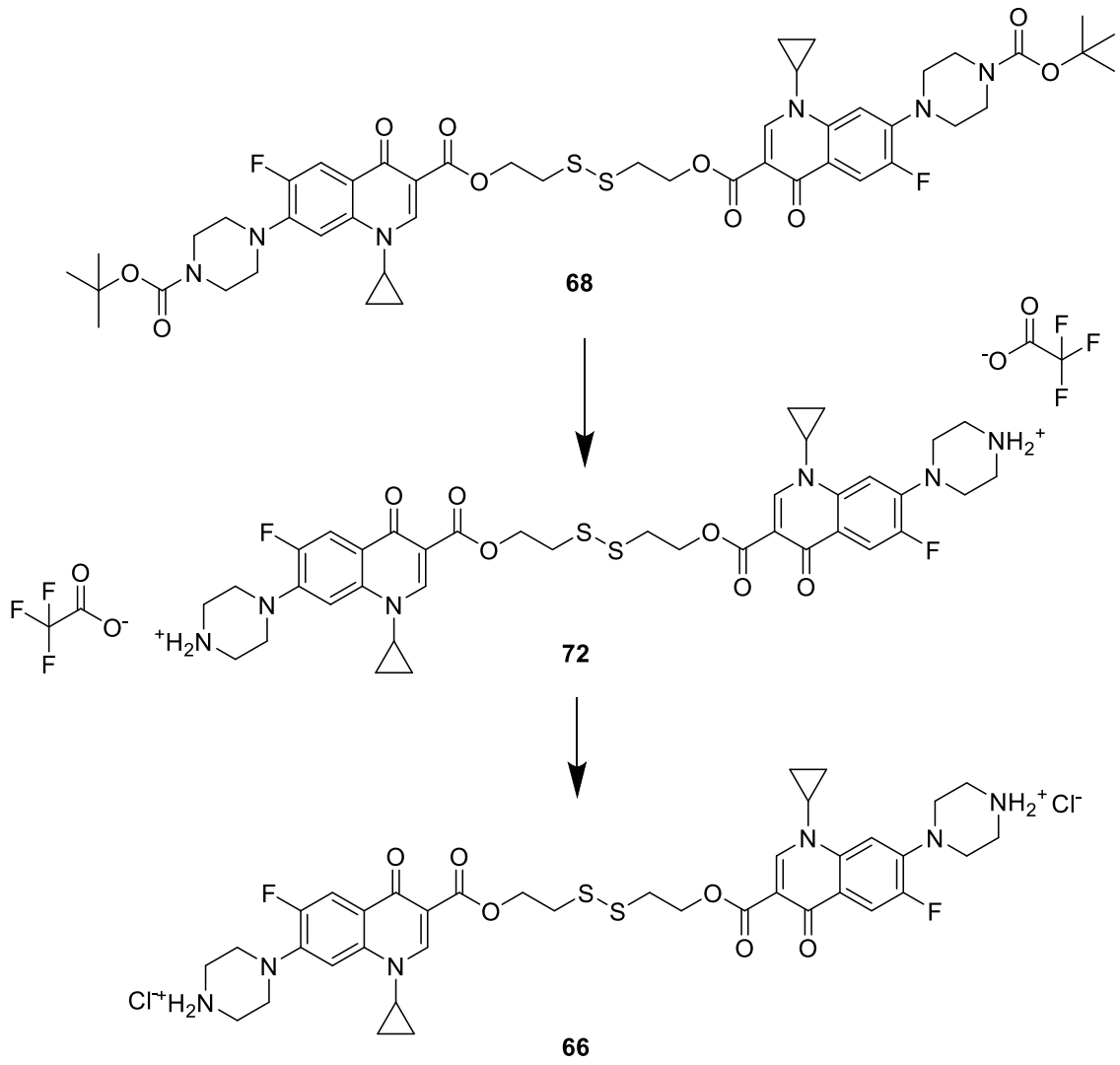

Scheme 21 Deprotection with TFA and ion exchange of compound 72

What proved more successful was using HCl mediated deprotection. The reaction was found to be complete in under 10 minutes as judged by TLC analysis. This process can be seen in **Scheme 22**.

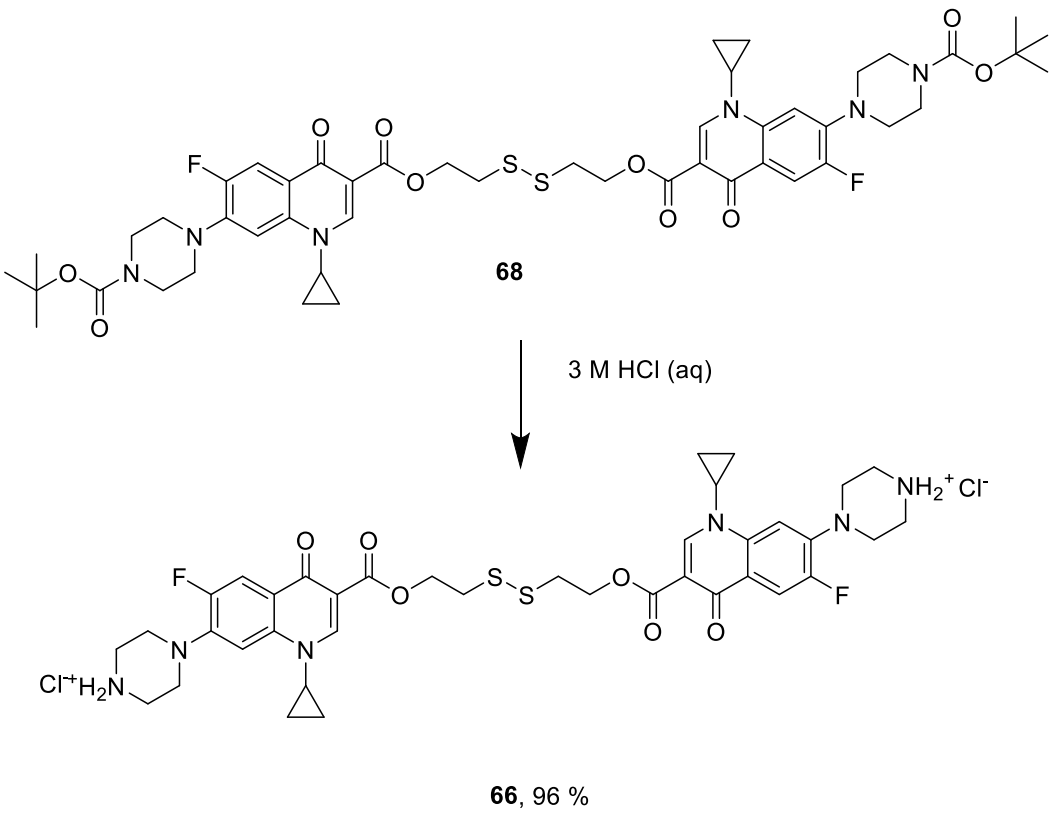

Scheme 22 HCl mediated deprotection of 68

The success of the deprotection was supported by the disappearance of the peaks at 1.50 ppm, relative integration 18, in the ^{1}H NMR spectrum. The presence of the triplets at 4.41 ppm and 3.09 ppm in the ^{1}H NMR spectrum and the corresponding peaks at 61.82 ppm and 36.68 ppm in the ^{13}C NMR spectrum indicate that the disulphide bridge remained intact. The mass spectrometric analysis also showed a peak at m/z 781.2662 corresponding to $[C_{38}H_{46}Cl_2F_2N_6O_6S_2+H]^+$, the intact dimer.

3.2 Biological Screening of Ciprofloxacin Dimer

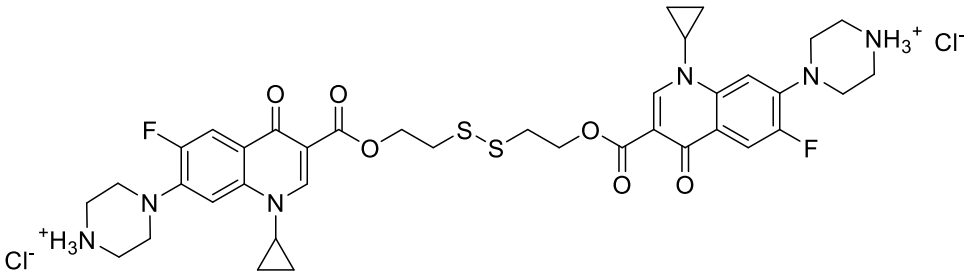

66

The deprotected dimer, **66**, was screened against wt B25113 *E. coli* to evaluate its potential as an antimicrobial agent. Ciprofloxacin was also tested as a positive control. The concentrations were calculated assuming 100% purity.

The plate layout is shown in **Table 8**. **Compound 66** was loaded in deuterated DMSO and the Ciprofloxacin was loaded in DMSO, so blanks were included for both DMSO and d_6-DMSO.

	1	2	3	4	5	6	7	8	9	10	11	12
A	H_2O	H_2O	H_2O	H_2O	H_2O	H_2O	H_2O	H_2O	H_2O	H_2O	H_2O	H_2O
B	H_2O	Dimer	Dimer	Dimer				Ciprofloxacin	Ciprofloxacin	Ciprofloxacin	Blank DMSO	H_2O
C	H_2O	Dimer	Dimer	Dimer				Ciprofloxacin	Ciprofloxacin	Ciprofloxacin	Blank DMSO	H_2O
D	H_2O	Dimer	Dimer	Dimer				Ciprofloxacin	Ciprofloxacin	Ciprofloxacin	Blank DMSO	H_2O
E	H_2O	Dimer	Dimer	Dimer				Ciprofloxacin	Ciprofloxacin	Ciprofloxacin	Blank d6-DMSO	H_2O
F	H_2O	Dimer	Dimer	Dimer				Ciprofloxacin	Ciprofloxacin	Ciprofloxacin	Blank d6-DMSO	H_2O
G	H_2O	Dimer	Dimer	Dimer				Ciprofloxacin	Ciprofloxacin	Ciprofloxacin	Blank d6-DMSO	H_2O
H	H_2O	H_2O	H_2O	H_2O	H_2O	H_2O	H_2O	H_2O	H_2O	H_2O	H_2O	H_2O

Well Conc / µM	Stock Conc / µM
0	0
2	10
4	20
6	30
8	40
10	50

Table 8 Plate layout and stock solutions used in the biological screening of Compound 66

The outer wells of the plate were filled with 200 µL of deionised water to try and minimise evaporation effects over the 20 hours. Into each blank well was placed 196 µL of LB and 4 µL of DMSO or d_6-DMSO as appropriate. Into each test well was placed 191 µL of LB, 4 µL of drug stock solution of the appropriate concentration and 5 µL of OD corrected bacterial culture.

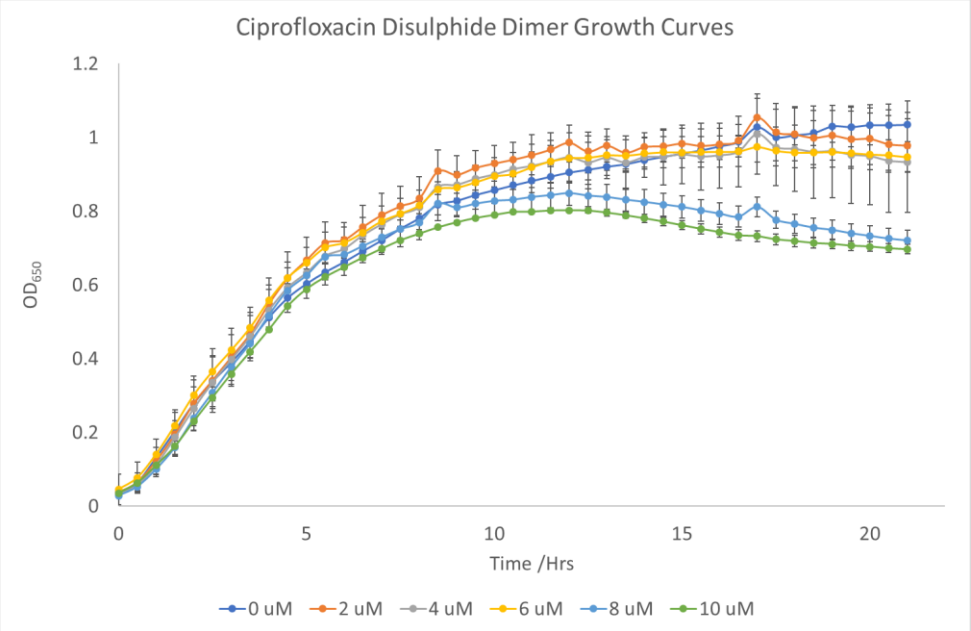

Figure 23 Bacterial growth curve of *E. coli* BW25113 with varying concentrations of additive. Error bars are ± standard deviation of three biological replicates

The data shows there is no significant concentration dependence for the first 10 hours of the experiment. It is only in the latter half of the experiment, and at higher concentrations that we see any significant changes in bacterial growth. The large lag phase, much longer than that of ciprofloxacin, suggests that the rate of target delivery has been drastically reduced. It is unknown at this point whether the lag phase represents slow uptake of the prodrug before activation. The molecular weight (781 Daltons) is above the nominated maximum of the OmpF porin (around 600 Daltons)[19] so this uptake pathway is likely to be inhibited. It could be the slow breakdown of the disulfide linker once inside the cell, but it is generally believed that this process is rapid.[74,84] It is unlikely to be the slow breakdown of the disulphide outside of the cell and release of free ciprofloxacin into the extracellular media as there are no reducing components in LB buffer.

3.3 Conclusions

The successful synthesis of **66** was completed, albeit at low yield. Preparative HPLC was needed for the purification as the protected dimer **68** could not be separated from other contaminants by standard silica chromatography. Due to the crude ^{1}H NMR spectrum showing overlapping triplet peaks, it was impossible to determine whether the low yield was due to a low reaction yield or whether the mass was being lost in the HPLC process.

The biological screening showed the molecule has some antimicrobial activity at very high concentrations and in the later stages of the experiment. These limited biological screening experiments did not show conclusively whether the disulphide is breaking down extracellularly in the media or in the cytoplasm.

3.4 Future Work

The screening of **66** suggested that it was not inhibiting bacterial growth as quickly as the parent monomer, ciprofloxacin. However, in the later stages of the screening and at the higher drug concentrations, **66** was starting to have a bactericidal effect. Therefore, it would be prudent to run the experiment over a longer period, to investigate this lag phase in more detail. The rate of cleavage of the bridge could also be studied *in vitro* by monitoring the cleavage of the disulfide by glutathione.

Once the ciprofloxacin dimer had been investigated, the next stage would be conjugating the phenyl thiourea groups discussed in the first section of the project to ciprofloxacin using the either the disulfide linker or other examples in the literature. These include but are not limited to the para-aminobenzyl alcohol spacer[108] and the tetrazine self-immolative linker.[109] As fluoroquinolones have a UV light-dependent ability to produce damaging ROS, these experiments could be performed in both the light and the dark to determine whether the released thiourea was having an inhibitory effect on this pathway.

4.0 Experimental

4.1 General Chemistry Procedure

4.1.1 Mass Spectrometry

High resolution positive and negative ESI mass spectrometry was performed on a Thermo-Finnigan LCQ Spectrometer by Karl Heaton.

4.1.2 NMR

^{1}H NMR (400 MHz), ^{13}C NMR (100.6 MHz) and ^{19}F NMR (376 MHz) spectra were acquired on a Jeol ECX400 spectrometer in the stated deuterated solvents. ^{13}C NMR (125 MHz), ^{1}H NMR (500 MHz) and ^{19}F NMR (376 MHz) were acquired on a Bruker AV500 NMR spectrometer by Ben Coulson. Variable temperature NMR was performed on either a Jeol ECX400 spectrometer. All chemical shifts (δ) are reported in parts per million (ppm) and referenced to the residual solvent. All *J* values are reported in Hertz to one decimal place. All ^{13}C NMR spectra are proton de-coupled. The reference signals used were: 7.26 ppm and 77.16 ppm ($CDCl_3$), 3.31ppm ,2.50 ppm and 39.52 ppm (d6-DMSO). Chemical shifts for multiplets are reported from the middle of the multiplet. Multiplicity abbreviations are as follows: s = singlet; d = doublet; t = triplet; q = quartet; m = multiplet; dd = double doublet; dt = double triplet. All NMR assignments were aided by HMQC, COSY and HMBC experiments when required. All spectra were processed using ACD/NMR Processor Academic Edition software.

4.1.3 IR

IR were recorded on a Perkin Elmer FT-IR Spectrum Two spectrometer (ATIR) in the region 4000-400 cm^{-1}.

4.1.4 HPLC

Analytical HPLC was performed on a Shimadzu HPLC system (Prominence) with a LC-20AD pump, SIL-20A autosampler, DGU-20AS degasser, CTO-20AC column oven, CBM-20A communication bus module and SPD-M20A diode array detector, using a SunFire C_{18} column (5 µm, 4.6 x 150 mm) with the specified eluent gradient.

Preparative HPLC was performed on a Varian ProStar HPLC system with two 210 series pumps (25 mL), a 325 series UV detector, a model 701 fraction collector and model 410 autosampler, using a SunFire Prep C_{18} column (10 µm, 19 x 250 mm), with a SunFire C_{18} Prep Guard Cartridge (10 µm, 19 mm X 10 mm) with the specified eluent gradient. The compound was dissolved in 2 mL of DCM and filtered through nylon filters with a 0.45µm pore size before injection. Each injection was 200 µL.

HPLC Analytical Method A

Starting ratio is 65 : 35 MeCN + 0.1% Formic Acid (FA) : H_2O + 0.1% FA. The gradient was raised over 12 minutes to 90 : 10 MeCN + 0.1% FA : H_2O + 0.1% FA and stayed constant for 30 seconds. The ratio was reduced to 65 : 35 MeCN + 0.1% FA : H_2O + 0.1% FA over 2.5 minutes. Total run time 15 minutes. Flow rate 1 mL/min

HPLC Analytical Method B

Starting ratio is 65 : 35 MeOH + 0.1% FA : H_2O + 0.1% FA. The gradient was raised over 12 minutes to 90 : 10 MeOH + 0.1% FA : H_2O + 0.1% FA and stayed constant for 30 seconds. The ratio was reduced to 65 : 35 MeOH + 0.1% FA : H_2O + 0.1% FA over 2.5 minutes. Total run time 15 minutes. Flow rate 1 mL/min

HPLC Preparative Method A

Injection volume of 200µl. Starting ratio is 65 : 35 MeCN + 0.1% Formic Acid (FA) : H_2O + 0.1% FA. The gradient was raised over 12 minutes to 90 : 10 MeCN + 0.1% FA : H_2O + 0.1% FA and stayed constant for 30 seconds. The ratio was reduced to 65 : 35 MeCN + 0.1% FA : H_2O + 0.1% FA over 2.5 minutes. Total run time 15 minutes. Flow rate 1 mL/min

4.1.5 Melting Points

Uncorrected melting points were recorded using a Stuart Scientific SMP3 instrument and are accurate to ± 0.05 °C.

4.1.6 Elemental Analysis

Elemental analysis was collected on an Exeter CE-440 elemental analyser by Dr Graeme McAllister.

4.1.7 Solvents

Solvents were supplied by Aldrich, Fischer Scientific and VWR. Where required solvents were dried over 3 or 4 Å molecular sieves prior to use. Deionised water was used for all synthetic procedures. Dry solvents were obtained from departmental solvent stills (Prosolv MD 7 solvent purification system where solvents are passed through two columns of molecular sieves). For the EDC coupling reaction Acros Organics DMF AcroSeal® (99.8%, extra dry, over molecular sieves) was used.

4.1.8 Reagents

All chemical reagents were used as supplied unless otherwise stated and purchased from commercial suppliers: Acros, Alfa-Aesar, Fisher Scientific, Fluorochem, Sigma Aldrich. Chemicals were handled with appropriately according to their toxicity.

4.1.9 Moisture-Sensitive Reactions

Moisture-sensitive reactions were carried out under an atmosphere of N_2.

4.1.10 Chromatography

Analytical TLC used Merck silica gel 60 F_{254} aluminium-backed plates, with the specified eluent. All plates were visualised through UV light using Chromato-vue Model CC-10 at 254 nm or 365 nm, or stained with potassium permanganate. Column chromatography was performed with the specified eluent using Sigma-Aldrich high-purity grade silica gel, pore size 60 Å, 220-440 mesh particle size, 35-75 μm.

4.2 Chemical Synthesis

4.2.1 Synthesis of Ciprofloxacin Phenyl Thiourea Conjugates

4.2.1.1 Methyl-1-cyclopropyl-6-fluoro-4-oxo-7-(piperzin-1-yl)-1,4-dihydroquinoline-3-carboxylate, 54

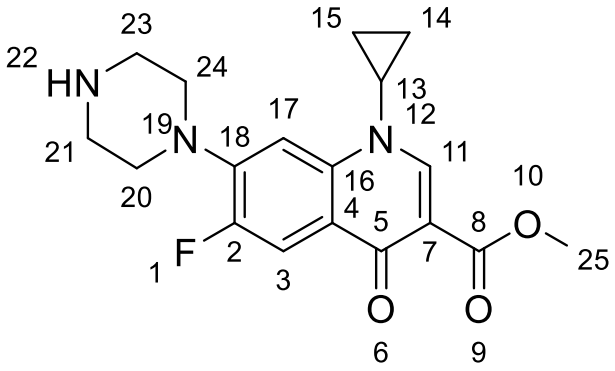

Chemical Formula: $C_{18}H_{20}FN_3O_3$

Molecular Weight: 345.3744 $gmol^{-1}$

Ciprofloxacin (1.91 g, 5.79 mmol) was dissolved in dry MeOH (100 mL) and cooled in ice. Thionyl chloride (8.38 mL g, 0.116 mol) was added dropwise with stirring, resulting in a yellow solution. This solution was heated under reflux for 17 hours. The solution was concentrated under reduced pressure giving a yellow oil. This was dissolved in sat. aq. K_2CO_3 (25 mL) and extracted with DCM (4 x 40 mL). The organic layers were combined and washed with water (40 mL) which was reextracted with DCM (3 x 40 mL). The organic layers were combined and dried over anhydrous $MgSO_4$. The solvent was removed under reduced pressure to give the title compound as a white crystalline solid.

Yield:

1.657 g, 83 %

m/z (ESI)

346.1568 ($[C_{18}H_{20}FN_3O_3+H]^+$ calculated mass 346.1561, 2.3 ppm mean error)

^{1}H NMR: (400 MHz, $CDCl_3$, δ_H (ppm)):

8.53 (s, 1H, **H-11**, **CH**), 8.01 (d, $^3J_{F-H}$ = 13.3 Hz, 1H, **H-3**, **CH**), 7.26 (d, $^4J_{F-H}$ = 7.8 Hz, **H-17**, **CH**), 3.91 (s, 3H, **H-25**, **CH_3**), 3.46-3.40 (m, 1H, **H-13**, **cyclopropane**, **CH**) 3.24-3.21 (m, 4H, **H-21**, **H-23 piperazine**, **CH_2**), 3.10-3.07 (m, 4H, **H-20**, **H-24 piperazine**, **CH_2**), 1.34-1.29 (m, 2H, **cyclopropane**, **CH_2**), 1.16-1.12 (m, 2H, **cyclopropane**, **CH_2**)

^{13}C NMR: (100 MHz, $CDCl_3$, δ_C (ppm)):

172.9 (d, $^4J_{C-F}$ = 1.9 Hz, **C-5**), 166.3 (s, **C-8**), 153.3 (d, $^1J_{C-F}$ = 248.3 Hz, **C-2**) 148.2 (s, **C-11**), 144.9 (d, $^2J_{C-F}$ = 10.5 Hz, **C-18**), 137.9 (s, **C-7**), 122.7 (d, $^3J_{C-F}$ = 7.7 Hz, **C-4**), 113.1 (d, $^2J_{C-F}$ = 22.0 Hz, **C-3**), 109.8 (s, **C-16**), 104.7 (d, $^3J_{C-F}$ = 2.9 Hz, **C-17**), 52.0 (s, **C-25**), 51.1 (s, **C-20**, **C-21**, **C-23**, **C-24**), 51.1 (s, **C-20**, **C-21**, **C-23**, **C-24**), 45.9 (s, **C-20**, **C-21**, **C-23**, **C-24**), 34.5 (s, **C-13**), 8.0 (s, **C-14**, **C-15**)

^{19}F NMR: (376 MHz, $CDCl_3$, δ_F (ppm)):

-123.4 (dd, $^3J_{H-F}$ = 13.3 Hz, $^4J_{F-H}$ = 7.8 Hz, **F-1**)

IR: (cm^{-1})

2950 (C-H), 2832 (C-H), 1720 (C=O, **C-8**, **O-9**), 1616 (C=O, **C-5**, **O-6**)

Melting Point: (°C)

Unable to be determined within the range of the instrument

4.2.1.2 Methyl 7-(4-((*tert*-butoxycarbonyl)glycyl)piperazin-1-yl)-1-cyclopropyl-6-fluoro-4-oxo-1,4-dihydroquinoline-3-carboxylate, 56

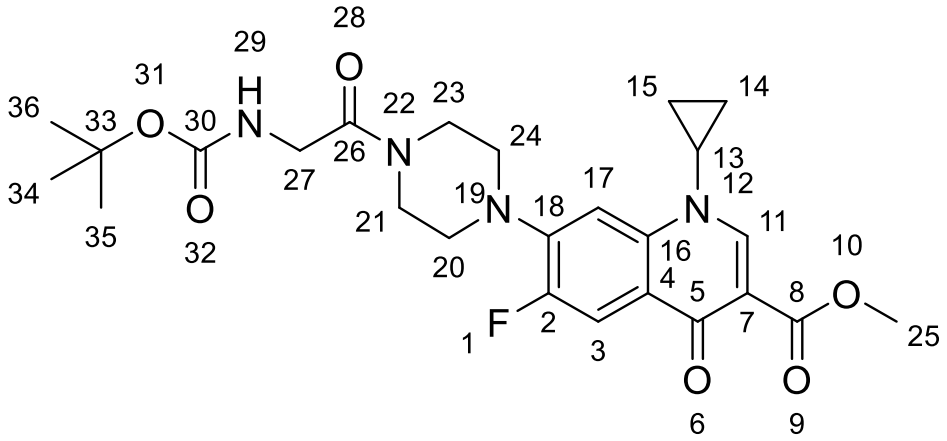

Chemical Formula: $C_{25}H_{31}FN_4O_6$

Molecular Weight: 502.5434 $gmol^{-1}$

Compound 54 (1.099 g, 3.19 mmol), N-Boc-glycine (0.836 g, 4.77 mmol), and 4-dimethyl amino pyridine (DMAP) (0.363 g, 2.971 mmol) were dissolved in dimethyl formamide (DMF) (25 mL) under a nitrogen atmosphere. 1-Ethyl-3-(3-dimethylaminopropyl) carbodiimide (EDC) (1.11 mL, 6.37 mmol) and diisopropylethylamine (DIPEA) (2.21 mL, 12.73 mmol)) were added and the reaction stirred at room temperature for 60 hours. The solvent was removed under reduced pressure and redissolved in $CHCl_3$ (30 mL). The organic layer was washed with water (10 mL), saturated brine (10 mL) and water (10 mL). The solution was dried over anhydrous $MgSO_4$ and the solvent removed under reduced pressure. The crude solid was purified by column chromatography (5 : 1 $CHCl_3$: isopropyl alcohol) to give the title compound as a white solid.

Yield:

0.877 g, 55 %

m/z (ESI)

503.2306 ($[C_{25}H_{31}FN_4O_6+H]^+$ calculated mass 503.2300, -1.0 ppm mean error)

^{1}H NMR: (400 MHz, $CDCl_3$, δ_H (ppm)):

8.56 (s, 1H, **H-11**, **CH**), 8.08 (d, $^{3}J_{F-H}$ = 13.3 Hz, 1H, **H-3**, **CH**), 7.27 (d, $^{4}J_{F-H}$ = 7.8 Hz, **H-17**, **CH**), 4.04 (d, $^{3}J_{H-H}$ = 4.6 Hz, **H-27**, **CH_2**), 3.92 (s, 3H, **H-25**, **CH_3**), 3.87 (t, $^{3}J_{H-H}$ = 4.6 Hz, 2H, **H-21**, **H-23**, **piperazine**, **CH_2**), 3.63 (t, $^{3}J_{H-H}$ = 4.6 Hz, 2H, **H-21**, **H-23**, **piperazine**, **CH_2**), 3.45-3.40 (m, 1H, **H-13**, **cyclopropane**, **CH**), 3.28-3.23 (m, 4H, **H-20**, **H-24**, **CH_2**), 1.46 (s, 9H, **H-34**, **H-35**, **H-36**, **Boc group**, **CH_3**), 1.36-1.31 (m, 2H, **cyclopropane**, **CH_2**), 1.17-1.13 (m, 2H, **cyclopropane**, **CH_2**)

^{13}C NMR: (100 MHz, $CDCl_3$, δ_C (ppm)):

172.9 (s, **C-5**), 169.2 (s, **C-30**), 167.0 (s, **C-26**), 166.3 (s, **C-8**), 153.3 (d, $^{1}J_{C-F}$ = 249.2 Hz, **C-2**) 148.5 (s, **C-11**), 143.8 (d, $^{2}J_{C-F}$ = 10.5 Hz, **C-18**), 137.9 (d, $^{5}J_{C-H}$ = 1.9 Hz, **C-7**), 123.6 (d, $^{3}J_{C-F}$ = 6.7 Hz, **C-4**), 113.5 (d, $^{2}J_{C-F}$ = 23.0 Hz, **C-3**), 110.1 (s, **C-16**), 105.2 (d, $^{3}J_{C-F}$ = 2.9 Hz, **C-17**), 79.8 (s, **C-33**), 52.1 (s, **C-25**), 50.0 (s, **C-20**, **C-21**, **C-23**, **C-24**), 49.63 (s, **C-20**, **C-21**, **C-23**, **C-24**), 44.3 (s, **C-20**, **C-21**, **C-23**, **C-24**), 42.2 (s, **C-20**, **C-21**, **C-23**, **C-24**), 41.7 (s, **C-27**), 34.5 (s, **C-13**), 28.3 (s, **C-34**, **C-35**, **C-36**), 8.1 (s, **C-14**, **C-15**)

^{19}F NMR: (376 MHz, $CDCl_3$, δ_F (ppm)):

-123.84 (dd, $^{3}J_{H-F}$ = 13.0 Hz, $^{4}J_{F-H}$ = 5.8 Hz, **F-1**)

IR: (cm^{-1})

3418 (C-H), 2978 (C-H), 1720 (C=O, **C-8**, **O-9**), 1617 (C=O, **C-5**, **O-6**),

Melting Point: (°C)

180.5-183.1

4.2.1.3 2-(4-(1-cyclopropyl-6-fluoro-3-(methoxycarbonyl)-4-oxo-1,4-dihydroquinolin-7-yl)piperazin-1-yl)-2-oxoethan-1-aminium 2,2,2-trifluoroacetate, 57

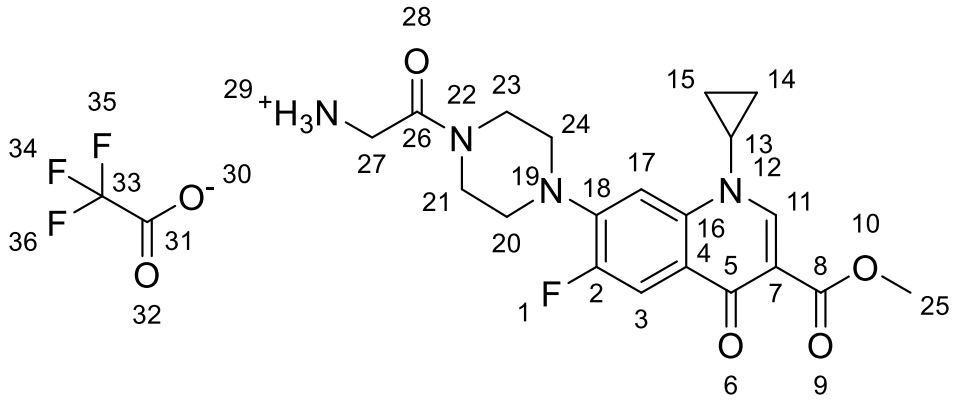

Chemical Formula: $C_{22}H_{24}F_4N_4O_6$

Molecular Weight: 516.4496 $gmol^{-1}$

Compound 56 (0.429 g, 0.854 mmol) was taken up in DCM (20 mL) and TFA (4 mL) was added. The solution was stirred overnight and concentrated under reduced pressure to give a yellow oil. This was suspended in EtOH (10 mL) and the solvent removed under reduced pressure. This was resuspended in EtOH (10ml) and solvent removed 8 times to give the title compound as an off-white solid.

Yield:

0.434 g, 98 %

m/z (ESI)

403.1776 ($[C_{20}H_{24}FN_4O_4+H]^+$ calculated mass 403.1776, -1.0 ppm mean error)

^{1}H NMR: (400 MHz, d6-DMSO, δ_H (ppm)):

8.45 (s, 1H, **H-11**, **CH**), 8.12 (s, broad, **N-29**), 7.77 (d, $^3J_{F-H}$ = 13.3 Hz, 1H, **H-3**, **CH**), 7.44 (d, $^4J_{F-H}$ = 7.3 Hz, **H-17**, **CH**), 3.97 (s, **H-27**, **CH_2**), 3.73 (s, 3H, **H-25**, **CH_3**) 3.61 (t, $^3J_{H-H}$ = 6.4 Hz, 2H, **H-21**, **H-23**, **piperazine**, **CH_2**), 3.64 (q, $^3J_{H-H}$ = 3.7, 1H, **H-13**, **cyclopropane**, **CH**) 3.29 (t, $^3J_{H-H}$ = 4.6 Hz, 2H, **H-20**, **H-**

24, **piperazine**, **CH_2**), 3.25 (t, $^3J_{H-H}$ = 5.0 Hz 2H, **H-20**, **H-24**, **piperazine**, **CH_2**) 1.27-1.11 (m, 4H, **cyclopropane**, **CH_2**),

^{13}C NMR: (100 MHz, d6-DMSO, δ_C (ppm)):

171.6 (d, $^4J_{F-C}$ = 1.9 Hz, **C-5**), 165.5 (s, **C-26**), 165.0 (s, **C-8**), 152.6 (d, $^1J_{F-C}$ = 152.7 Hz, **C-2**), 148.4 (s, **C-11**), 143.5 (d, $^2J_{F-C}$ = 10.5 Hz, **C-18**), 138.0 (s, **C-7**), 122.2 (d, $^3J_{F-C}$ = 6.7 Hz, **C-4**), 111.7 (d, $^2J_{F-C}$ = 23 Hz, **C-3**), 109.0 (s, **C-16**), 106.7 (d, $^3J_{F-C}$ = 2.9 Hz, **C-17**), 51.3 (s, **C-25**), 49.4 (q, $^1J_{F-C}$ = 13.4 Hz, **C-33**), 43.9 (s, **C-20**, **C-21**, **C-23**, **C-24**), 41.3(s, **C-20**, **C-21**, **C-23**, **C-24**), 36.0 (s, **C-20**, **C-21**, **C-23**, **C-24**), 34.8 (s, **C-13**), 33.6 (s, **C-20**, **C-21**, **C-23**, **C-24**), 7.6 (s, **C-14**, **C-15**)

^{19}F NMR: (376 MHz, d6-DMSO, δ_F (ppm)):

-73.46 (s, 3F, **F-34**, **F-35**, **F-36**, **TFA salt**, **CF_3**) -124.48 - -124.43 (m, 1F, **F-1**)

IR: (cm^{-1})

3096 (C-H), 1711 (C=O, **C-8**, **O-9**), 1651 (C=O, **C-5**, **O-6**),

Melting Point: (°C)

Unable to be determined within the range of the instrument

4.2.1.4 Methyl 1-cyclopropyl-6-fluoro-4-oxo-7-(4-((phenylcarbamothioyl)glycyl)piperazin-1-yl)-1,4-dihydroquinoline-3-carboxylate, 58

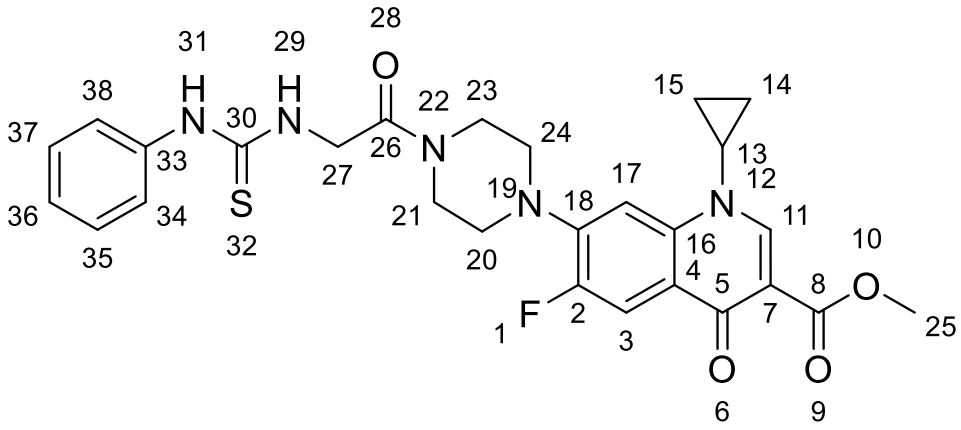

Chemical Formula: $C_{27}H_{28}FN_5O_4S$

Molecular Weight: 537.61 $gmol^{-1}$

Compound 57 (0.32 g, 0.619 mmol) was dissolved in MeCN (20 mL). Et_3N (0.13 mL, 0.931 mmol) was added followed by phenyl isothiocyanate (0.08mL g, 0.682 mmol). The solution was stirred under nitrogen at room temperature for 24 hours. The mixture was cooled in ice and filtered to give the title compound as white crystals.

Yield:

0.177g, 53%

m/z (ESI)

538.1910 ($[C_{27}H_{28}FN_5O_4S + H]^+$ calculated mass 538.1919, 2.5 ppm mean error)

^{1}H NMR: (400 MHz, d6-DMSO, δ_H (ppm)):

10.02 (s, 1H, broad, **H-31**, **NH**) 8.44 (s, 1H, **H-11**, **CH**), 7.83 (s, 1H, broad, **H-29**, **NH**), 7.77 (d, $^3J_{F-H}$ = 13.3 Hz, 1H, **H-3**, **CH**), 7.51 (d, $^3J_{H-H}$ = 7.3 Hz, 2H, **H-34**, **H-38**), 7.46 (d, $^4J_{F-H}$ = 7.3 Hz, 1H, **H-17**), 7.34 (t $^3J_{H-H}$ = 7.8 Hz, **H-35**, **H-37 CH**), 7.12 (t, $^3J_{H-H}$ = 7.3 Hz, 1H, **H-36**), 4.45 (d, $^3J_{H-H}$ = 3.7 Hz, 2H, **H-27**), 3.73 (s, 3H, **H-25**, **CH_3**) 3.62-3.70 (m, 4H, **H-21**, **H-23**, **piperazine**, **CH_2**), 3.35-3.30

(m, **H-20**, **H-24**, **piperazine**, **CH_2**, **H-13**, **cyclopropane**, **CH**, under water peak), 3.27-3.23 (m, 2H, **H-13**, **piperazine**, **H-20**, **H-24**, **CH2**) 3.29 (t, $^3H_{H-H}$ = 5 Hz, 2H, **H-20**, **H-24)** 3.23 (t, $^3H_{H-H}$ = 5 Hz, 2H, **H-20**, **H-24**) 1.23-1.28 (m, 2H, **H-14**, **H-15**, **cyclopropane**, **CH_2**), 1.10-1.11 (m, 2H, **H-14**, **H-15**, **cyclopropane**, **CH_2**)

^{13}C NMR: (100 MHz, d6-DMSO, δ_C (ppm)):

179.9 (s **C-5**), 171.6 (s, **C-30**), 166.6 (s, **C-8**), 165.0 (s, **C-26**), 153.3 (d, $^1J_{C-F}$ = 248.3 Hz, **C-2**) 148.4 (s, **C-11**), 143.6 (d, $^2J_{C-F}$ = 10.5 Hz, **C-18**), 139.2 (s, **C-33**) 138.0 (s, **C-7**), 128.7 (s, **C-35**, **C-37**), 124.3 (s, **C-36**), 122.8 (s, **C-38**, **C-34**), 122.1 (d, $^3J_{C-F}$ = 6.7 Hz, **C-4**), 111.5 (d, $^2J_{C-F}$ = 23.0 Hz, **C-3**), 109.0 (s, **C-16**), 106.6 (d, $^3J_{C-F}$ = 1.9 Hz, **C-17**), 51.3 (s, **C-25**), 49.6 (s, **C-20**, **C-21**, **C-23**, **C-24**), 49.5 (s, **C-20**, **C-21**, **C-23**, **C-24**), 45.8 (s, **C-27**), 43.8 (s, **C-20**, **C-21**, **C-23**, **C-24**), 43.8 (s, **C-20**, **C-21**, **C-23**, **C-24**), 34.8 (s, **C-13**), 8.0 (s, **C-14**, **C-15**)

^{19}F NMR: (376 MHz, d6-DMSO, δ_F (ppm)):

-124.48 - -124.43 (m, 1F, **F-1**)

IR: (cm^{-1})

3409 (N-H, **N-29**, **N-31**), 2977 (C-H), 1721 (C=O, **C-8**, **O-9**), 1657 (C=O, **C-5**, **O-6**),

Melting point: (°C)

160.9-163.0

4.2.1.5 1-cyclopropyl-6-fluoro-4-oxo-7-(4-((phenylcarbamothioyl)glycyl)piperazin-1-yl)-1,4-dihydroquinoline-3-carboxylic acid, 62

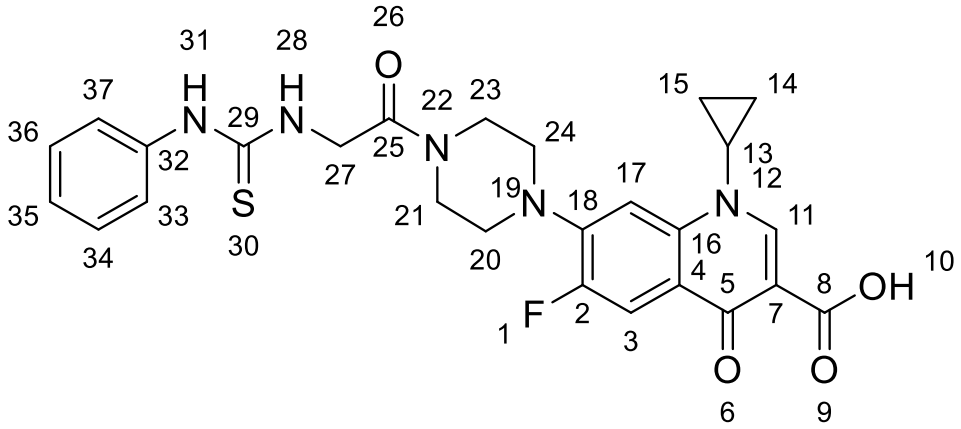

Chemical Formula: $C_{26}H_{26}FN_5O_4S$

Molecular Weight: 523.58

Compound 58 (0.39 2g, 0.727 mmol) was dissolved in DMF (25 mL) and NaOH (0.05 g, 1.25 mmol) was added. The solution was stirred overnight at room temperature. The solvent was removed under reduced pressure and the residue dissolved in water (20 mL) The pH was adjusted to 1 using HCl (6 M, aq, dropwise) and the suspension was filtered to give the title compound as pale yellow crystals.

Yield:

0.198 g, 52 %

m/z (ESI)

524.1772 ($[C_{26}H_{26}FN_5O_4S + H]^+$ calculated mass 524.1762, 1.7 ppm mean error)

^{1}H NMR: (400 MHz, d6-DMSO, δ_H (ppm)):

9.95 (s, 1H, broad, **H-31**, **NH**) 8.87 (s, 1H, **H-11**, **CH**), 7.80 (s, 1H, broad, **H-28**, **NH**), 7.93 (d, $^3J_{F-H}$ = 13.3 Hz, 1H, **H-3**, **CH**), 7.59 (d, $^3J_{H-H}$ = 7.3 Hz, 2H, **H-33**, **H-37**, **CH**), 7.51 (d, $^4J_{F-H}$ = 8.2 Hz, 1H, **H-17**, **CH**), 7.34 (t $^3J_{H-H}$ = 7.3 Hz, **H-**

34, **H-36**, **CH**), 7.12 (t, $^{3}J_{H-H}$ = 7.3 Hz, 1H, **H-35**), 4.46 (d, $^{3}J_{H-H}$ = 4.1 Hz, 2H, **H-27**), 3.82 (s, 1H, **H-13**, **cyclopropane**), 3.74 (s, broad, 2H, **H-21**, **H-23**, **piperazine**), 3.69 (s, broad, 2H, **H-21**, **H-23**, **piperazine**), 3.43 (s, broad, 2H, **H-20**, **H-24**, **piperazine**), 3.38 (s, broad, 2H, **H-20**, **H-24**, **piperazine**), 1.33-1.34 (m, 2H, **H-14**, **H-15**, **cyclopropane**, **CH_2**), 1.19 (m, 2H, **H-14**, **H-15**, **cyclopropane**, **CH_2**)

^{13}C NMR: (100 MHz, d6-DMSO, δ_C (ppm)):

180.00 (s **C-5**), 176.28 (s, **C-30**), 166.62 (s, **C-8**), 165.71 (s, **C-25**), 152.79 (d, $^{1}J_{C-F}$ = 249.2 Hz, **C-2**) 147.89 (s, **C-11**), 144.68 (d, $^{2}J_{C-F}$ = 10.5 Hz, **C-18**), 139.14 (s, **C-7**) 139.04 (s, **C-32**), 128.53 (s, **C-33**, **C-37**), 124.78 (s, **C-35**), 122.78 (s, **C-36**, **C-34**), 118.75 (d, $^{3}J_{C-F}$ = 8.6 Hz, **C-4**), 110.95 (d, $^{2}J_{C-F}$ = 23.0 Hz, **C-3**), 106.76 (s, **C-16**), 106.45 (s, **C-17**), 41.00-49.42 (m, **C-20**, **C-21**, **C-23**, **C-24**), 45.64 (s, **C-27**), 35.73 (s, **C-13**), 7.46 (s, **C-14**, **C-15**)

^{19}F NMR: (376 MHz, d6-DMSO, δ_F (ppm)):

-121.71 - -121.76 (m, **F-1**)

IR: (cm^{-1})

3301 (N-H, **N-29**, **N-31**) 3070, 2830 (C-H) 1713 (C=O, **C-8**, **O-9**), 1651 (C=O, **C-5**, **O-6**),

Melting point: (°C)

Unable to be determined within the range of the instrument

Elemental analysis

Calculated for $C_{26}H_{26}FN_5O_4S$. $0.45H_2O$: %C 58.73 %H 5.10 %N 13.17

Observed for $C_{26}H_{26}FN_5O_4S$. $0.45H_2O$ %C 58.59 %H 4.98 %N 13.08

4.2.1.6 Methyl 7-(4-(((3-chloro-4-fluorophenyl)carbamothioyl)glycyl)piperazin-1-yl)-1-cyclopropyl-6-fluoro-4-oxo-1,4-dihydroquinoline-3-carboxylate, 59

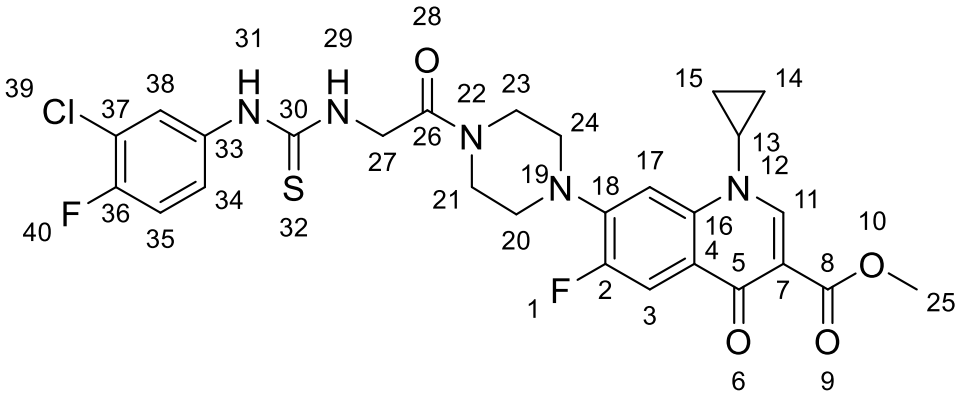

Chemical Formula: $C_{27}H_{26}ClF_2N_5O_4S$

Molecular Weight: 590.04 $gmol^{-1}$

Compound 57 (0.100 g, 0.193 mmol) was dissolved in MeCN (20 mL). Et_3N (0.107 mL, 0.767 mmol) was added followed by 3-chloro-4-fluorophenyl isothiocyanate (0.053 g, 0.282 mmol). The solution was stirred under nitrogen at room temperature for 24 hours. The mixture was cooled in ice and filtered to give the title compound as white crystals.

Yield:

0.097 g, 84 %

m/z (ESI)

590.1442 ($[C_{27}H_{26}{}^{35}ClF_2N_5O_4S + H]^+$ calculated mass 590.1435, 1.0 ppm mean error)

^{1}H NMR: (400 MHz, d6-DMSO, δ_H (ppm)):

10.15 (s, 1H, broad, **H-31**, **NH**) 8.43 (s, 1H, **H-11**, **CH**), 8.01 (s, 1H, broad, **H-29**, **NH**), 7.93 (d, 1H, $^3J_{H-H}$ = 6 Hz, **H-**35), 7.76 (d, $^3J_{F-H}$ = 13.3 Hz, 1H, **H-3**, **CH**), 7.45 (d, $^4J_{F-H}$ = 7.3 Hz, 1H, **H-17**), 7.39-7.37 (m, 2H, **H-38**, **H34**), 4.44 (d, $^3J_{H-H}$ = 3.7 Hz, **H-27**, **CH_2**), 3.73-3.62 (m, 8H, **H-13**, **cyclopropane**, **H-21**, **H-23**, **piperazine H-25**, **CH_3**) 3.29-3.25 (m, 4H, **H-20**, **H-24**, **piperazine**, **CH_2**),

1.27-1.23 (m, 2H, **H-14**, **H-15**, **cyclopropane**, **CH_2**), 1.11-1.10 (m, 2H, **H-14**, **H-15**, **cyclopropane**, **CH_2**)

^{13}C NMR: (100 MHz, d6-DMSO, δ_C (ppm)):

180.3 (s **C-5**), 171.5 (s, **C-30**), 166.5 (s, **C-8**), 164.6 (s, **C-26**), 160.7 (d, $^1J_{F-C}$ = 220.5 Hz, **C-36**), 152.6 (d, $^1J_{C-F}$ = 247.3 Hz, **C-2**) 148.4 (s, **C-11**), 143.5 (d, $^2J_{C-F}$ = 10.5 Hz, **C-18**) 138.0 (s, **C-7**), 124.4 (s, **C-34**), 124.4 (d, $^3J_{F-C}$ = 1.9 Hz, **C-38**), 124.3 (s, **C-33**), 122.7 (d, $^3J_{C-F}$ = 6.7 Hz, **C-4**), 118.8 (d, $^2J_{C-F}$ = 18.2 Hz, **C-37**), 116.7 (d, $^2J_{C-F}$ = 22, **C-35**), 111.6 (d, $^2J_{C-F}$ = 22.0 Hz, **C-3**), 109.0 (s, **C-16**), 106.6 (d, $^3J_{C-F}$ = 1.9 Hz, **C-17**), 51.3 (s, **C-25**), 49.4 (s, **C-20**, **C-21**, **C-23**, **C-24**), 49.4 (s, **C-20**, **C-21**, **C-23**, **C-24**), 45.8 (s, **C-27**), 43.8 (s, **C-20**, **C-21**, **C-23**, **C-24**), 41.2 (s, **C-20**, **C-21**, **C-23**, **C-24**), 34.8 (s, **C-13**), 7.6 (s, **C-14**, **C-15**)

^{19}F NMR: (376 MHz, d6-DMSO, δ_F (ppm)):

-122.0 (d, $^3J_{H-F}$ = 5.8 Hz, **F-40**), -124.4 - -124.47 (m, **F-1**)

IR: (cm^{-1})

3293 (N-H, **N-29**, **N-31**), 3074 (C-H) 1718 (C=O, **C-8**, **O-9**), 1660 (C=O, **C-5**, **O-6**),

Melting point: (°C)

Unable to be determined within the range of the instrument

4.2.1.7 7-(4-(((3-chloro-4-fluorophenyl)carbamothioyl)glycyl)piperazin-1-yl)-1-cyclopropyl-6-fluoro-4-oxo-1,4-dihydroquinoline-3-carboxylic acid, 63

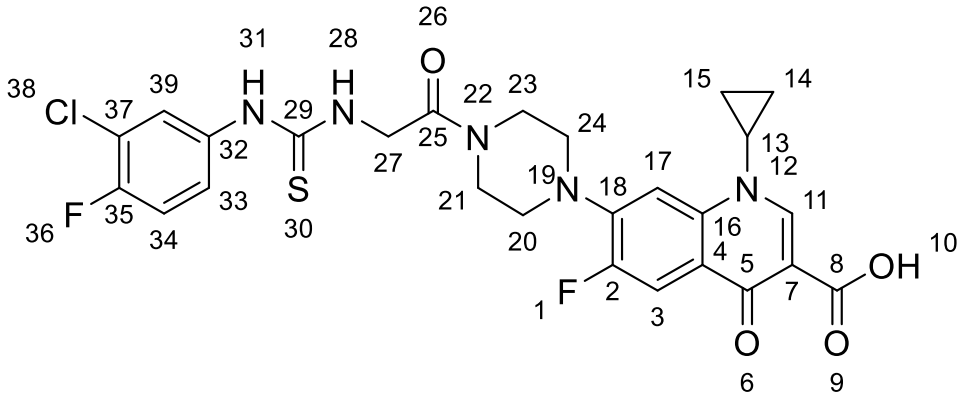

Chemical Formula: $C_{26}H_{24}F_2ClN_5O_4S$

Molecular Weight: 576.02

Compound 59 (0.097 g, 0.164 mmol) was dissolved in DMF (25mL) and NaOH (0.05 g, 1.25 mmol) was added. The solution was stirred overnight at room temperature. The solvent was removed under reduced pressure and the residue dissolved in water (20 mL) The pH was adjusted to 1 using HCl (6 M, aq, dropwise) and the suspension was filtered to give the title compound as pale-yellow crystals.

Yield:

0.046 g, 49 %

m/z (ESI)

576.1280 ($[C_{26}H_{24}{}^{35}Cl\ F_2N_5O_4S + H]^+$ calculated mass 576.1278, 0.5 ppm mean error)

^{1}H NMR: (400 MHz, d6-DMSO, δ_H (ppm)):

10.18 (s, 1H, broad, **H-31**, **NH**) 8.65 (s, 1H, **H-11**, **CH**), 8.04 (s, 1H, broad, **H-28**, **NH**), 7.91 (d, $^3J_{F-H}$ = 13.3 Hz, 1H, **H-3**, **CH**), 7.38 (d, $^4J_{F-H}$ = 8.2 Hz, 1H, **H-17**), 7.94 (s, 1H, **C-39**, **CH_2**), 7.93 (d, 1H, $^3J_{H-H}$ = 6.4 Hz, **H-33**), 7.39-7.37 (m, 1H, **H34**), 4.45 (d, $^3J_{H-H}$ = 2.7 Hz, **H-27**, **CH_2**), 3.82 (s, broad, 1H, **H-13**,

cyclopropane), 3.74 (**H-23**, **H-21**, **piperazine**, **CH_2**) 3.68 (s, broad, **H-23**, **H-21**, **piperazine**, **CH_2**), 3.42 (s, broad, **H-20**, **H-24**, **piperazine**, **CH_2**), 3.34 (s, broad, **H-20**, **H-24**, **piperazine**, **CH_2**), 1.32-1.33 (m, 2H, **H-14**, **H-15**, **cyclopropane**, **CH_2**), 1.19 (s, 2H, **H-14**, **H-15**, **cyclopropane**, **CH_2**)

^{13}C NMR: (100 MHz, d6-DMSO, δ_C (ppm)):

180.3 (s **C-5**), 176.4 (s, **C-29**), 166.6 (s, **C-8**), 164.9 (s, **C-25**), 155.0 (d, $^1J_{C-F}$ = 329.7 Hz, **C-35**), 152.9 (d, $^1J_{F-C}$ = 248.3 Hz, **C-2**), 148.1 (s, **C-11**), 144.8 (d, $^2J_{C-F}$ = 9.6 Hz, **C-18**) 139.1 (s, **C-7**), 124.2 (s, **C-32**), 123.2-123.1 (m, **C-33**, **C-39**), 122.7 (d, $^3J_{C-F}$ = 6.7 Hz, **C-4**), 118.8 (d, $^2J_{C-F}$ = 10.5 Hz, **C-37**), 116.6 (d, $^2J_{C-F}$ = 21.1, **C-34**), 111.2 (d, $^2J_{C-F}$ = 23.0 Hz, **C-3**), 106.8 (s, **C-16**), 106.6 (d, $^3J_{C-F}$ = 2.9 Hz, **C-17**), 49.4-49.1 (m, **C-20**, **C-21**, **C-23**, **C-24**), 45.8 (s, **C-27**), 43.7 (s, **C-20**, **C-21**, **C-23**, **C-24**), 41.2 (s, **C-20**, **C-21**, **C-23**, **C-24**), 35.9 (s, **C-13**), 7.3 (s, **C-14**, **C-15**)

^{19}F NMR: (376 MHz, d6-DMSO, δ_F (ppm)):

-122.0 - -122.01 (d, $^3J_{H-F}$ = 5.8 Hz, **F-40**), -121.66 - -121.61 (m, **F-1**)

IR: (cm^{-1})

3304 (N-H, **N-29**, **N-31**), 3062 (C-H) 1711 (C=O, **C-8**, **O-9**), 1625 (C=O, **C-5**, **O-6**)

Melting point: (°C)

153.5-158.9

Elemental analysis

Calculated for $C_{26}H_{26}FN_5O_4S$. 1.00 H_2O: %C 52.57 %H 4.41 %N 11.79

Observed for $C_{26}H_{26}FN_5O_4S$. 1.00 H_2O %C 52.29 %H 4.11 %N 11.69

4.2.1.8 Methyl 7-(4-(((3-chlorophenyl)carbamothioyl)glycyl)piperazin-1-yl)-1-cyclopropyl-6-fluoro-4-oxo-1,4-dihydroquinoline-3-carboxylate, 60

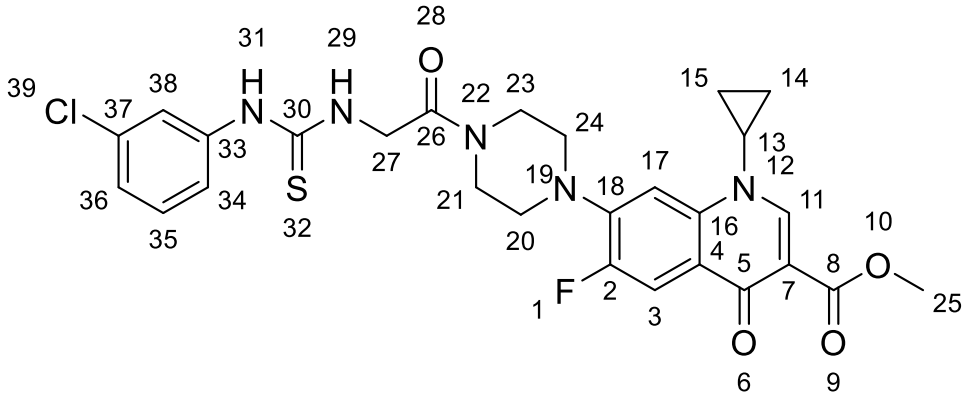

Chemical Formula: $C_{27}H_{27}ClFN_5O_4S$

Molecular Weight: 572.05 $gmol^{-1}$

Compound 57 (0.15 g, 0.291 mmol) was dissolved in MeCN (20 mL). Et_3N (0.162 mL, 1.15 mmol) was added followed by 3-chlorophenyl isothiocyanate (0.076 mL, 0.579 mmol). The solution was stirred under nitrogen at room temperature for 24 hours. The mixture was cooled in ice and filtered to give the title compound as white crystals.

Yield:

0.144 g, 87 %

m/z (ESI)

572.1538 ($[C_{27}H_{27}ClFN_5O_4S + H]^+$ calculated mass 572.1529, 1.7 ppm mean error)

^{1}H NMR: (400 MHz, d6-DMSO, δ_H (ppm)):

10.20 (s, 1H, broad, **H-31**, **NH**) 8.43 (s, 1H, **H-11**, **CH**), 8.05 (s, 1H, broad, **H-29**, **NH**), 7.88 (s, 1H **H-38**), 7.75 (d, $^3J_{F-H}$ = 13.3 Hz, 1H, **H-3**, **CH**), 7.45 (d, $^4J_{F-H}$ = 7.3 Hz, 1H, **H-17**), 7.40-7.32 (m, 2H, **H-34**, **H-35**, **H-36**), 7.14 (d, $^3J_{H-H}$ = 7.3 Hz, **H-34**, **H-35**, **H-36**), 4.45 (d, $^3J_{H-H}$ = 3.7 Hz, **H-27**, **CH_2**), 3.73 (s, 3H, **H-25**, **CH_3**), 3.76-3.60 (m, 5H, **H-13**, **cyclopropane**, **H-23**, **H-21**, **piperazine**), 3.32 (s, broad, 2H, **H-20**, **H-24**, **piperazine**, **CH_2**), 3.25 (s, broad, 2H, **H-20**,

H-24, **piperazine**, **CH_2**), 1.23-1.30 (m, 2H, **H-14**, **H-15**, **cyclopropane**, **CH_2**), 1.11 (s, broad, 2H, **H-14**, **H-15**, **cyclopropane**, **CH_2**)

^{13}C NMR: (100 MHz, d6-DMSO, δ_C (ppm)):

179.9 (s **C-5**), 171.5 (s, **C-30**), 166.5 (s, **C-8**), 164.9 (s, **C-26**), 152.6 (d, $^1J_{C-F}$ = 249.2 Hz, **C-2**) 148.3 (s, **C-11**), 143.5 (d, $^2J_{C-F}$ = 10.5 Hz, **C-18**), 141.1 (s, **C-37**), 138.2 (s, **C-7**), 132.7 (s, **C-33**), 130.0 (s, **C-34**, **C-35**, **C-36**), 123.5 (s, **C-34**, **C-35**, **C-36**), 121.6 (s, **C-38**), 122.7 (d, $^3J_{C-F}$ = 6.7 Hz, **C-4**), 120.6 (s, **C-34**, **C-35**, **C-36**), 111.6 (d, $^2J_{C-F}$ = 23.0 Hz, **C-3**), 108.9 (s, **C-16**), 106.6 (d, $^3J_{C-F}$ = 1.9 Hz, **C-17**), 51.3 (s, **C-25**), 49.6 (s, **C-20**, **C-21**, **C-23**, **C-24**), 49.5 (s, **C-20**, **C-21**, **C-23**, **C-24**), 45.8 (s, **C-27**), 43.8 (s, **C-20**, **C-21**, **C-23**, **C-24**), 41.3 (s, **C-20**, **C-21**, **C-23**, **C-24**), 34.8 (s, **C-13**), 7.6 (s, **C-14**, **C-15**)

^{19}F NMR: (376 MHz, d6-DMSO, δ_F (ppm)):

-124.41 - -124.47 (m, **F-1**)

IR: (cm^{-1})

3281 (N-H, **N-29**, **N-31**), 3055 (C-H) 1725 (C=O, **C-8**, **O-9**), 1655 (C=O, **C-5**, **O-6**),

Melting point: (°C)

Unable to be determined within the range of the instrument

4.2.1.9 7-(4-(((3-Chlorophenyl)carbamothioyl)glycyl)piperazin-1-yl)-1-cyclopropyl-6-fluoro-4-oxo-1,4-dihydroquinoline-3-carboxylic acid, 64

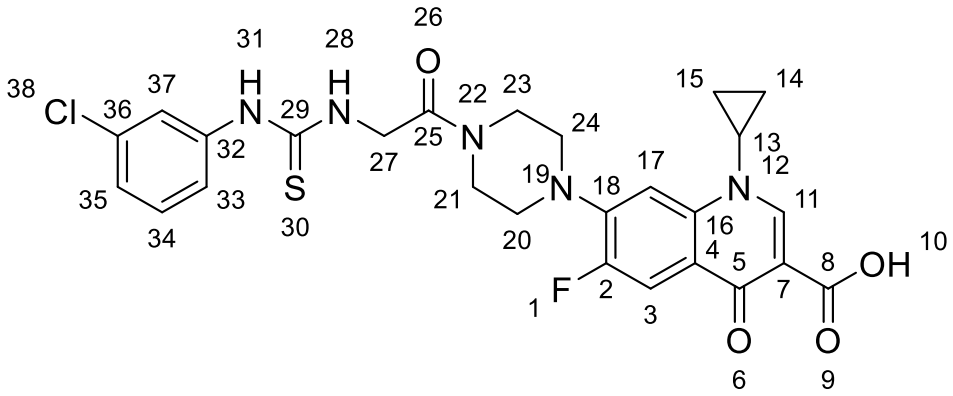

Chemical Formula: $C_{26}H_{25}FClN_5O_4S$

Molecular Weight: 558.03

Compound 60 (0.144 g, 0.251 mmol) was dissolved in DMF (25 mL) and NaOH (0.05 g, 1.25 mmol) was added. The solution was stirred overnight at room temperature. The solvent was removed in vacuo and the residue dissolved in water (20 mL) The pH was adjusted to 1 using HCl (6 M, aq, dropwise) and the suspension was filtered to give the title compound as pale-yellow crystals.

Yield:

0.105 g, 75 %

m/z (ESI)

558.1363 ($[C_{26}H_{25}F^{35}ClN_5O_4S + H]^+$ calculated mass 558.1373, 1.8 ppm mean error)

^{1}H NMR: (400 MHz, d6-DMSO, δ_H (ppm)):

10.28 (s, 1H, broad, **H-30**, **NH**) 8.66 (s, 1H, **H-11**, **CH**), 8.11 (s, 1H, broad, **H-28**, **NH**), 7.88 (s, 1H **H-37**), 7.92 (d, $^3J_{F\text{-}H}$ = 13.3 Hz, 1H, **H-3**, **CH**), 7.58 (s, 1H, **H-34**, **H-35**, **H-36**), 7.40-7.31 (m, 2H, **H-33**, **H-34**, **H-35**), 7.14 (d, $^3J_{H\text{-}H}$ = 7.3 Hz, **H-17**), 4.46 (d, $^3J_{H\text{-}H}$ = 3.7 Hz, **H-27**, **CH_2**), 3.83 (s, broad, 1H, **H-13**, **cyclopropane**, **CH**), 3.75 (s, 2H, **H-21**, **H-23**, **piperazine**), 3.68 (s, 2H, **H-21**,

H-23, **piperazine**), 3.42 (s, broad, 2H, **H-20**, **H-24**, **piperazine**, **CH_2**), 3.35 (under water peak, **H-20**, **H-24**, **piperazine**, **CH_2**), 1.32 (s, broad, 2H, **H-14**, **H-15**, **cyclopropane**, **CH_2**), 1.19 (s, broad, 2H, **H-14**, **H-15**, **cyclopropane**, **CH_2**)

^{13}C NMR: (100 MHz, d6-DMSO, δ_C (ppm)):

179.9 (s **C-5**), 176.4 (s, **C-29**), 166.6 (s, **C-8**), 165. (s, **C-25**), 152.93 (d, $^1J_{C-F}$ = 250.2 Hz, **C-2**) 148.1 (s, **C-11**), 144.9 (d, $^2J_{C-F}$ = 6.7 Hz, **C-18**), 141.1 (s, **C-36**), 139.1 (s, **C-32**) 132.7 (s, **C-7**), 130.2 (s, **C-33**, **C-34**, **C-35**), 123.5 (d, $^3J_{C-F}$ = 2.9 Hz, **C-4**) 121.6 (s, **C-33**, **C-34**, **C-35**), 121.6 (s, **C-37**), 111.0 (d, $^2J_{C-F}$ = 23.0 Hz, **C-3**), 106.8 (s, **C-16**), 106.6 (d, $^3J_{H-H}$ = 1.9 Hz, **C-17**), 49.3 (s, **C-20**, **C-21**, **C-23**, **C-24**), 49.2 (s, **C-20**, **C-21**, **C-23**, **C-24**), 45.7 (s, **C-27**), 43.7 (s, **C-20**, **C-21**, **C-23**, **C-24**), 41.1 (s, **C-20**, **C-21**, **C-23**, **C-24**), 39.9 (s, **C-13**), 7.6 (s, **C-14**, **C-15**)

^{19}F NMR: (376 MHz, d6-DMSO, δ_F (ppm)):

-121.62 -121.68 (m, **F-1**)

IR: (cm^{-1})

3302 (N-H, **N-28**, **N-31**) 3070, 2926 (C-H) 1713 (COOH), 1626 (C=O, **C-5**, **O-6**)

Melting point: (°C)

204.6-207.5

Elemental analysis

Calculated for $C_{26}H_{26}FN_5O_4S$. 0.6HCl . 0.1NaCl: %C 53.31 %H 4.41 %N 11.96

Observed for $C_{26}H_{26}FN_5O_4S$. 0.6HCl . 0.1NaCl %C 53.29 %H 4.35 %N 11.90

4.2.1.10 Methyl 7-(4-(((4-chlorophenyl)carbamothioyl)glycyl)piperazin-1-yl)-1-cyclopropyl-6-fluoro-4-oxo-1,4-dihydroquinoline-3-carboxylate, 61

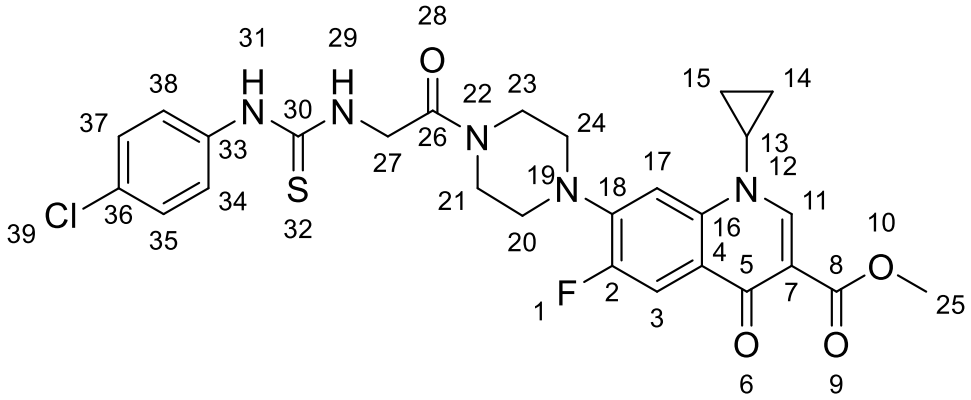

Chemical Formula: $C_{27}H_{27}ClFN_5O_4S$

Molecular Weight: 572.05 $gmol^{-1}$

Compound 57 (0.15 g, 0.291 mmol) was dissolved in MeCN (20 mL). Et_3N (0.162 mL, 1.15 mmol) was added followed by 3-chlorophenyl isothiocyanate (0.076 mL, 0.579 mmol). The solution was stirred under nitrogen at room temperature for 24 hours. The mixture was cooled in ice and filtered to give the title compound as white crystals.

Yield:

0.135 g, 81%

m/z (ESI)

572.1539 ($[C_{27}H_{27}{}^{35}ClFN_5O_4S+H]^+$ calculated mass 572.1529, 1.9 ppm mean error)

^{1}H NMR: (400 MHz, d6-DMSO, δ_H (ppm)):

10.13 (s, 1H, broad, **H-31**, **NH**) 8.43 (s, 1H, **H-11**, **CH**), 7.96 (s, 1H, broad, **H-29**, **NH**), 7.76 (d, $^3J_{F-H}$ = 13.3 Hz, 1H, **H-3**, **CH**), 7.58 (d, $^3J_{H-H}$ = 8.7 Hz, 2H, **H-34**, **H-38**), 7.45 (d, $^4J_{F-H}$ = 7.3 Hz, 1H, **H-17**), 7.37 (d, $^3J_{H-H}$ = 8.7 Hz, 2H, **H-35**, **H-37**), 4.45 (s, **H-27**, **CH_2**), 3.73 (s, 3H, **H-25**, **CH_3**), 3.80-3.65 (m, 5H, **H-13**, **cyclopropane**, **H-23**, **H-21**, **piperazine**), 3.32 (s, broad, 2H, **H-20**, **H-24**, **piperazine**, **CH_2**), 3.25 (s, broad, 2H, **H-20**, **H-24**, **piperazine**, **CH_2**), 1.27-

1.25 (m, 2H, **H-14**, **H-15**, **cyclopropane**, **CH_2**), 1.10 (s, broad, 2H, **H-14**, **H-15**, **cyclopropane**, **CH_2**)

^{13}C NMR: (100 MHz, d6-DMSO, δ_C (ppm)):

180.0 (s **C-5**), 171.5 (s, **C-30**), 166.5 (s, **C-8**), 164.9 (s, **C-26**), 155.3 (d, $^1J_{C-F}$ = 247.3 Hz, **C-2**) 148.4 (s, **C-11**), 143.5 (d, $^2J_{C-F}$ = 10.5 Hz, **C-18**), 138.4 (s, **C-33**) 138.0 (s, **C-7**), 128.4 (s, **C-35**, **C-37**), 127.8 (s, **C-36**), 124.1 (s, **C-38**, **C-34**), 122.1 (d, $^3J_{C-F}$ = 6.7 Hz, **C-4**), 111.6 (d, $^2J_{C-F}$ = 23.0 Hz, **C-3**), 109.0 (s, **C-16**), 106.6 (d, $^3J_{C-F}$ = 2.9 Hz, **C-17**), 51.3 (s, **C-25**), 49.6-49.3 (m, **C-20**, **C-21**, **C-23**, **C-24**), 45.7 (s, **C-27**), 43.8 (s, **C-20**, **C-21**, **C-23**, **C-24**), 41.2 (s, **C-20**, **C-21**, **C-23**, **C-24**), 34.8 (s, **C-13**), 7.6 (s, **C-14**, **C-15**)

^{19}F NMR: (376 MHz, d6-DMSO, δ_F (ppm)):

-124.42 - -124.47 (m, **F-1**)

IR: (cm^{-1})

3279 (N-H, **N-29**, **N-31**), 2981 (C-H), 1724 (COOH), 1656 (C=O, **C-5**, **O-6**)

Melting point: (°C)

Unable to be determined within the range of the instrument

4.2.1.11 7-(4-(((4-Chlorophenyl)carbamothioyl)glycyl)piperazin-1-yl)-1-cyclopropyl-6-fluoro-4-oxo-1,4-dihydroquinoline-3-carboxylic acid, 65

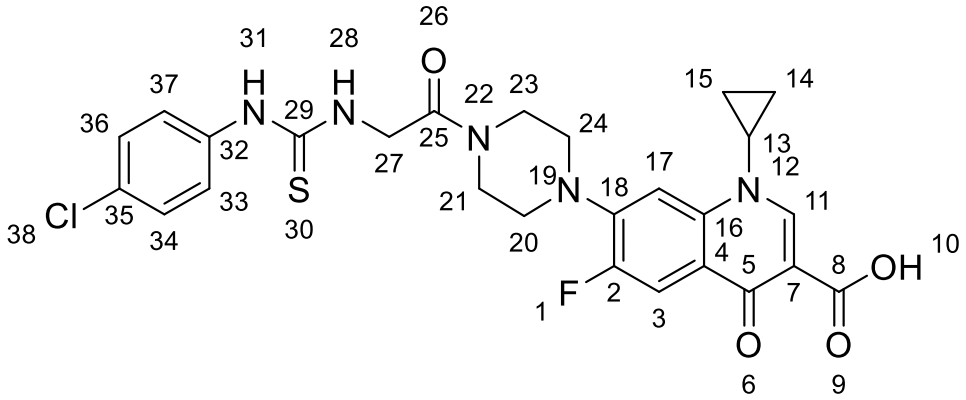

Chemical Formula: $C_{26}H_{25}FClN_5O_4S$

Molecular Weight: 558.03

Compound 61 (0.135 g, 0.236 mmol) was dissolved in DMF (25 mL) and NaOH (0.05 g, 1.25 mmol) was added. The solution was stirred overnight at room temperature. The solvent was removed under reduced pressure and the residue dissolved in water (20 mL) The pH was adjusted to 1 using HCl (6 M, aq, dropwise) and the suspension was filtered to give the title compound as pale yellow crystals.

Yield:

0.053 g, 40 %

m/z (ESI)

558.1381 ($[C_{26}H_{25}{}^{35}ClFN_5O_4S + H]^+$ calculated mass 558.1373, 1.1 ppm mean error)

^{1}H NMR: (500 MHz, d6-DMSO, δ_H (ppm)):

10.17 (s, 1H, broad, **H-31**, **NH**) 8.66 (s, 1H, **H-11**, **CH**), 7.98 (s, 1H, broad, **H-28**, **NH**), 7.93 (d, $^3J_{F-H}$ = 12.8 Hz, 1H, **H-3**, **CH**), 7.58 (d, $^3J_{H-H}$ = 8.7 Hz, 2H, **H-33**, **H-37**), 7.37 (d, $^3J_{H-H}$ = 8.7 Hz, 3H, **H-17**, **H-35**, **H-37**), 4.45 (d, $^3J_{H-H}$ = 4 Hz, **H-27**, **CH_2**), 3.82 (s, broad, 1H, **H-13**, **cyclopropane**), 3.74 (s, 2H, **H-21**, **H-23**, **piperazine**), 3.68 (s, 2H, **H-21**, **H-23**, **piperazine**), 3.42 (s, 2H, **H-20**, **H-**

24, **piperazine**, **CH_2**), 3.34 (s, 2H, **H-20**, **H-24**, **piperazine**, **CH_2**), 1.33-1.32 (m, 2H, **H-14**, **H-15**, **cyclopropane**, **CH_2**), 1.19 (s, broad, 2H, **H-14**, **H-15**, **cyclopropane**, **CH_2**)

^{13}C NMR: (125 MHz, d6-DMSO, δ_C (ppm)):

180.1 (s **C-5**), 176.3 (s, **C-8**), 166.6 (s, **C-29**), 165.8 (s, **C-25**), 152.9 (d, $^1J_{C-F}$ = 246.5 Hz, **C-2**) 148.0 (s, **C-11**), 144.8 (d, $^2J_{C-F}$ = 10.1 Hz, **C-18**), 138.4 (s, **C-32**) 139.1 (s, **C-7**), 128.4 (s, **C-34**, **C-36**), 127.7 (s, **C-36**), 124.0 (s, **C-33**, **C-37**), 118.8 (d, $^3J_{C-F}$ = 7.3 Hz, **C-4**), 111.0 (d, $^2J_{C-F}$ = 22.0 Hz, **C-3**), 106.8 (s, **C-16**), 106.6 (s, **C-17**), 49.3 (s, **C-20**, **C-21**, **C-23**, **C-24**), 49.1 (s, **C-20**, **C-21**, **C-23**, **C-24**), 45.7 (s, **C-27**), 43.7 (s, **C-20**, **C-21**, **C-23**, **C-24**), 41.1 (s, **C-20**, **C-21**, **C-23**, **C-24**), 35.8 (s, **C-13**), 7.6 (s, **C-14**, **C-15**)

^{19}F NMR: (376 MHz, d6-DMSO, δ_F (ppm)):

-124.62 - -124.67 (m, **F-1**)

IR: (cm^{-1})

3299 (N-H, **N-28**, **N-31**) 3095, 2976 (C-H) 1722 (COOH) 1627 (C=O, **C-5**, **O-6**)

Melting point: (°C)

185.4-189.1

Elemental analysis

Calculated for $C_{26}H_{26}FN_5O_4S$. 0.8HCl . 0.1NaCl: %C 52.66 %H 4.39 %N 11.67

Observed for $C_{26}H_{26}FN_5O_4S$. 0.6HCl . 0.1NaCl %C 53.81 %H 4.25 %N 11.67

4.2.2 Synthesis of a Ciprofloxacin Disulfide-linked Dimer

4.2.2.1 7-(4-(*tert*-Butoxycarbonyl)piperazin-1-yl)-1-cyclopropyl-6-fluoro-4-oxo-1,4-dihydroquinoline-3-carboxylic acid, 67

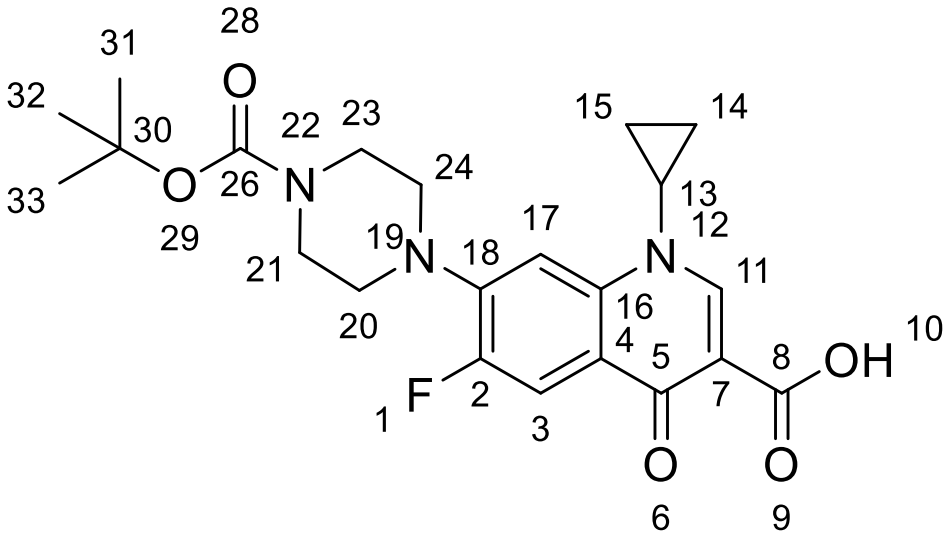

Molecular Formula: $C_{22}H_{26}FN_3O_5$

Molecular weight: 431.46 $gmol^{-1}$

Ciprofloxacin (2.20 g, 6.63 mmol) was dissolved in water (10 mL) and 1,4-dioxane (10 mL). NaOH (1 M, aq, 10 mL) was added and the mixture stirred at RT for 1 hour. Di-tert-butyl dicarbonate (2.08 g, 9.53 mmol) was dissolved in 1,4-dioxane (4 mL) and added. The reaction was stirred at RT for 24 hours. The solvent was reduced to 15% w/v under reduced pressure and acetone (40 mL) was added. The suspension was filtered and washed with cold acetone (3 x 10 mL) to give the title compound as a white solid, **Compound 6**.

Yield:

2.22 g, 99 %

m/z (ESI)

432.1923 $[C_{22}H_{26}FN_3O_5+H]^+$ (calculated 432.1929, 2.3 ppm mean error)

^{1}H NMR: (400 MHz, $CDCl_3$, δ_H (ppm)):

8.73 (s, 1H, **H-11**, **CH**), 7.99 (d, $^{3}J_{F-H}$ = 12.8 Hz, 1H, **H-3**, **CH**), 7.36 (d, $^{4}J_{F-H}$ = 7.3 Hz, **H-17**, **CH**), 3.66-3.38 (m, 4H, **H-21**, **H-23**, **piperazine**, **CH_2**) 3.56-3.53 (m, 1H, **H-13 cyclopropane**, **CH**), 3.31-3.28 (m, 4H, **H-20**, **H-24 piperazine**, **CH_2**), 1.50 (s, 9H, **H-31**, **H-32**, **H-33**, **Boc group**) ,1.42-1.38 (m, 2H, **cyclopropane**, **CH_2**), 1.18-1.23 (m, 2H, **cyclopropane**, **CH_2**)

^{13}C NMR: (100 MHz, $CDCl_3$, δ_C (ppm)):

177.0 (d, $^{4}J_{F-C}$ = 2.9 Hz, **C-5**), 170.4 (s, **C-8**), 166.9 (s, **C-26**), 153.4 (d, $^{1}J_{F-C}$ = 218.5 Hz, **C-2**), 147.5 (s, **C-11**), 145.8 (d, $^{2}J_{F-C}$ = 10.5 Hz, **C-18**), 139.0 (s, **C-7**), 120.0 (d, $^{3}J_{C-F}$ = 7.7 Hz, **C-4**), 112.4 (d, $^{2}J_{F-C}$ = 26.0 Hz, **C-3**), 108.1 (s, **C-16**), 105.0 (d, $^{3}J_{F-C}$ = 2.9 Hz, **C-17**), 80.3 (s, **C-30**), 67.1 (s, **C-20**, **C-22**, **C-23**, **C-24**), 49.7 (s, **C-20**, **C-22**, **C-23**, **C-24**), 49.7 (s, **C-20**, **C-22**, **C-23**, **C-24**), 35.3 (s, **C-13**), 28.4 (s, **C-31**, **C-32**, **C-33**), 8.2 (s, **C-14**, **C-15**)

^{19}F NMR: (376 MHz, $CDCl_3$, δ_F (ppm)):

-120.84 - -120.89 (m, **F-1**)

IR: (cm^{-1})

2969 (C-H) 1731 (COOH) 1688 (C=O, **C-5**, **O-6**)

Melting point: (°C)

Unable to be determined within the range of the instrument

4.2.2.2 Disulfanediylbis(ethane-2,1-diyl) bis(7-(4-(*tert*-butoxycarbonyl)piperazin-1-yl)-1-cyclopropyl-6-fluoro-4-oxo-1,4-dihydroquinoline-3-carboxylate), 68

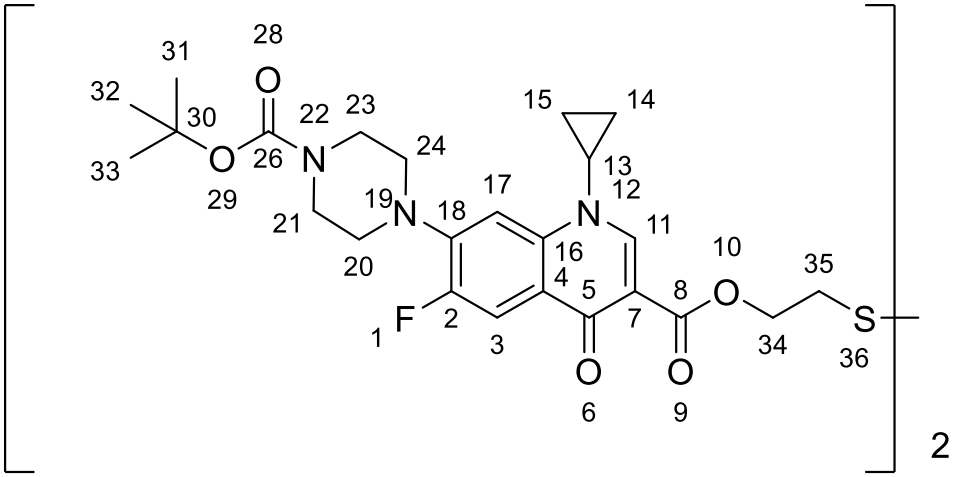

Chemical Formula: $C_{48}H_{58}F_2N_6O_{10}S_2$

Molecular Weight: 981.14 $gmol^{-1}$

Compound 67 (0.32 g, 0.714 mmol), HATU (0.60 g, 1.577 mmol) and DIPEA (0.26 g, 2.01 mmol) were dissolved in $CHCl_3$ (10 mL) and heated to 40 °C for 2 hours. 2,2'-Dithiodiethanol (0.053 g, 0.342 mmol) was dissolved in $CHCl_3$ (10 mL) and added to the mixture. The solution was refluxed at 40 °C for 60 hours. The reaction was diluted with $CHCl_3$ (20 mL) and washed with water (10 mL), sat. $NaHCO_3$ (10 mL), formic acid (0.1 M, 10 mL), sat. brine (10 mL) and water (10 mL). The organic layer was dried on anhydrous $MgSO_4$ and reduced under reduced pressure to give a red crude solid. This solid was purified using HPLC as described in **HPLC Preparatory Method A**, with the compound eluting at 11 minutes to give the title compound as a white solid.

<u>Mass Recovery:</u>

0.018 g, 5.3 % mass recovery

<u>m/z (ESI)</u>

1003.3514 ($[C_{48}H_{58}F_2N_6O_{10}S_2+Na]^+$ calculated mass 1003.3516, 0.2 ppm mean error)

^{1}H NMR: (400 MHz, CD_3OD, δ_H (ppm)):

8.42 (s, 2H, **H-11**, **CH**), 7.53 (d, $^3J_{F-H}$ = 13.3 Hz, 2H, **H-3**, **CH**), 7.14 (d, $^4J_{F-H}$ = 7.3 Hz, 2H, **H-17**, **CH**), 4.55 (t, $^3J_{H-H}$ = 6.0 Hz, 4H, **H-34**, **CH_2**), 3.66-3.64 (m, 8H, **H-21**, **H-23**, **piperazine**, **CH_2**) 3.47-3.41 (m, 2H, **H-13 cyclopropane**, **CH**), 3.20-3.18 (m, 8H, **H-20**, **H-24 piperazine**, **CH_2**), 3.09 (t, $^2J_{H-H}$ = 6.0 Hz, 4H, **H-35**, **CH_2**), 1.50 (s, 18H, **H-31**, **H-32**, **H-33**, **Boc group**) ,1.27-1.22 (m, 8H, **cyclopropane**, **CH_2**)

^{13}C NMR: (100 MHz, CD_3OD, δ_C (ppm)):

172.5 (s, **C-5**), 163.8 (s, **C-8**), 154.6 (s, **C-26**), 152.9 (d, $^1J_{F-C}$ = 248.3 Hz), 148.2 (s, **C-11**), 144.0 (d, $^2J_{F-C}$ = 10.5 Hz, **C-18**), 137.6 (s, **C-7**), 122.20 (d, $^3J_{C-F}$ = 6.7 Hz, **C-4**), 112.3 (d, $^2J_{F-C}$ = 23.0 Hz, **C-3**), 108.8 (d, $^4J_{F-C}$ = 2.9 Hz, **C-17**), 105.3 (s, **C-16**), 80.1 (s, **C-30**), 62.4 (s, **C-34**), 49.8 (s **C-20**, **C-21**, **C-23** **C-24**), 49.7 (s, **C-20**, **C-21**, **C-23**, **C-24**), 37.4 (s, **C-35**), 34.8 (s, **C-13**), 28.4 (s, **C-31**, **C-32**, **C-33**), 8.0 (s, **C-14**, **C-15**)

^{19}F NMR: (376 MHz, CD_3OD, δ_F (ppm)):

-123.60 - -123.55 (m, **F-1**)

IR: (cm^{-1})

2969 (C-H), 1731 (C=O, **C-8**, **O-9**) 1627 (C=O, **C-5**, **O-6**)

4.2.2.3 Disulfanediylbis(ethane-2,1-diyl) bis(1-cyclopropyl-6-fluoro-4-oxo-7-(piperazin-1-yl)-1,4-dihydroquinoline-3-carboxylate) chloride, 66

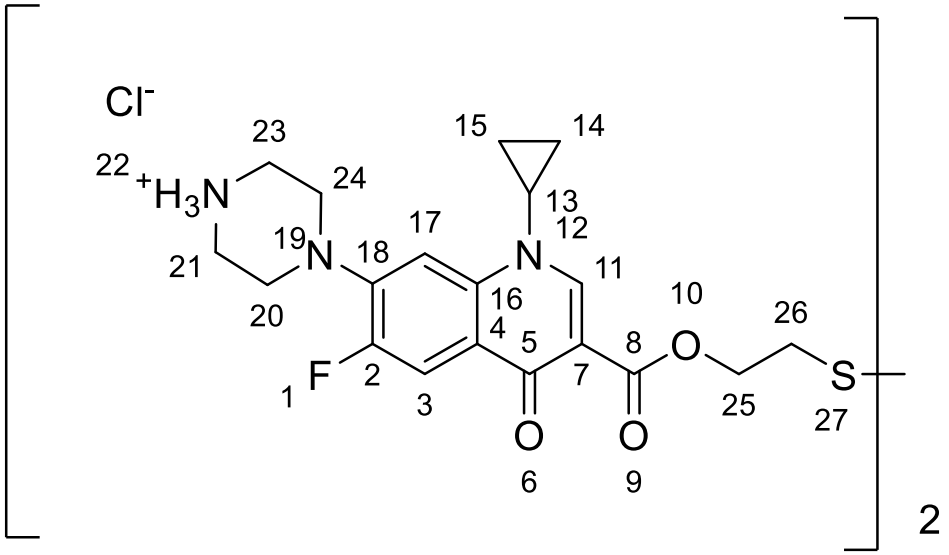

Chemical Formula: $C_{38}H_{46}Cl_2F_2N_6O_6S_2$

Molecular Weight: 855.84

Compound 68 (0.018 g, 0.018 mmol) was dissolved in HCl (3 M, aq, 20 mL) and the solvent was removed under reduced pressure after 2 minutes to give the title compound as sticky yellow oil.

Yield:

0.015 g, 95.6%

m/z (ESI)

781.2662 ($[C_{38}H_{46}F_2N_6O_6S_2+H]^+$ calculated mass 781.2648, 2.4 ppm mean error)

^{1}H NMR: (500 MHz, d6-DMSO, δ_H (ppm)):

9.65 (s, broad, **N-22**), 8.38 (s, 2H, **H-11**, **CH**), 7.46 (d, $^3J_{F-H}$ = 13.2 Hz, 2H, **H-3**, **CH**), 7.33 (d, $^4J_{F-H}$ = 7.3 Hz, 2H, **H-17**, **CH**), 4.41 (t, $^3J_{H-H}$ = 5.9 Hz, 4H, **H-25**, **CH_2**), 3.59 (s, broad, 2H, **H-13 cyclopropane**, **CH**), 3.46 (s, 8H, **H-21**, **H-23**, **piperazine**, **CH_2**) 3.29 (s, 8H, **H-20**, **H-24 piperazine**, **CH_2**), 3.09 (t, $^2J_{H-H}$ =

6.0 Hz, 4H, **H-26**, **CH_2**) ,1.24-1.23 (m, 4H, **cyclopropane**, **CH_2**) 1.14 (s, 4H, **cyclopropane**, **CH_2**)

^{13}C NMR: (125 MHz, d6-DMSO, δ_C (ppm)):

171.3 (s, **C-5**), 163.2 (s, **C-8**), 152.0 (d, $^1J_{F-C}$ = 246.5 Hz), 148.2 (s, **C-11**), 142.5 (d, $^2J_{F-C}$ = 10.1 Hz, **C-18**), 137.6 (s, **C-7**), 122.0 (d, $^3J_{C-F}$ = 6.9 Hz, **C-4**), 111.3 (d, $^2J_{F-C}$ = 23.8 Hz, **C-3**), 108.2 (s, **C-17**), 106.4 (d, $^4J_{F-C}$ = 1.8 Hz, **C-16**), 61.8 (s, **C-25**), 46.4 (s, **C-20**, **C-21**, **C-23 C-24**), 42.5 (s, **C-20**, **C-21**, **C-23**, **C-24**), 36.7 (s, **C-26**), 34.9 (s, **C-13**), 7.4 (s, **C-14**, **C-15**)

^{19}F NMR: (376 MHz, d6-DMSO, δ_F (ppm)):

-124.44 - -124.49 (m, **F-1**)

IR: (cm^{-1})

3353 (N-H), 1493 (C=O)

4.3 Biological Procedures

4.3.1 Bacterial Strains

The bacterial strain used for all studies was wild type *E.coli* BW25113.

4.3.2 Media

All solutions and media were prepared using MilliQ deionised H_2O and sterilised by autoclave prior to use. LB media was prepared using 10 g tryptone, 5 g of yeast extract and 10 g NaCl per litre.

4.3.3 Growth Assays

OD_{650} Measurements

Optical densities were recorded to 3 decimal places using a Biochrom Libra S11 Visible Spectrometer in plastic cuvettes with a 1 cm path length, and are accurate to ±0.0005. These values were used to normalise the OD_{650} of each culture prior to use in each growth assay.

Plate Reader

The plate reader used was an Epoch 2 Microplate Spectrophotometer. The OD650 was measured every 30 minutes for the specified time. The plate was shaken at 200 RPM between each measurement to maintain aerobic bacterial growth. Blank wells were measured for their optical densities

and subtracted from the sample wells to normalise the OD_{650} measurements used for data analysis.

Growth Assay

Cultures of the BW25113 strain were inoculated into 5mL LB growth media and grown overnight at 37°C with shaking to promote aerobic growth. The OD_{650} was normalised to OD_{650} = 2. To a 96 well plate was added 200µl MilliQ deionised water in the external ring of wells, 196µl of LB and 4µl of DMSO in each of the blank wells and in each of the test wells 191µl LB, 4µl of drug stock concentration and 5µl of normalised bacterial culture as shown in **Table 9**. The experiment was placed into the plate reader which ran as described above.

	1	2	3	4	5	6	7	8	9	10	11	12
A	H_2O	H_2O	H_2O	H_2O	H_2O	H_2O	H_2O	H_2O	H_2O	H_2O	H_2O	H_2O
B	H_2O	Drug 1	Drug 1	Drug 1	Drug 2	Drug 2	Drug 2	Drug 3	Drug 3	Drug 3	Blank	H_2O
C	H_2O	Drug 1	Drug 1	Drug 1	Drug 2	Drug 2	Drug 2	Drug 3	Drug 3	Drug 3	Blank	H_2O
D	H_2O	Drug 1	Drug 1	Drug 1	Drug 2	Drug 2	Drug 2	Drug 3	Drug 3	Drug 3	Blank	H_2O
E	H_2O	Drug 1	Drug 1	Drug 1	Drug 2	Drug 2	Drug 2	Drug 3	Drug 3	Drug 3	Variable	H_2O
F	H_2O	Drug 1	Drug 1	Drug 1	Drug 2	Drug 2	Drug 2	Drug 3	Drug 3	Drug 3	Variable	H_2O
G	H_2O	Drug 1	Drug 1	Drug 1	Drug 2	Drug 2	Drug 2	Drug 3	Drug 3	Drug 3	Variable	H_2O
H	H_2O	H_2O	H_2O	H_2O	H_2O	H_2O	H_2O	H_2O	H_2O	H_2O	H_2O	H_2O

Well Conc / µM	Stock Conc / µM
0	0
2	10
4	20
6	30
8	40
10	50

Table 9 General 96 well plate layout used for the growth assays

4.3.4 DNA Gyrase Assay

Agarose Gel Electrophoresis

The gel was run in TAE running buffer which was prepared using 750 mL of H_2O, 48.4 g/L of Tris, 22.8 mL of glacial acetic acid, 200 mL of 29.2 g/L EDTA. The solution was made up to 1 L using H_2O. The solution was diluted by 1 in 10 in H_2O. The agarose gels used were prepared using 1% w/v agarose in 1 x TAE buffer.

Stop Buffer

Once the assay was completed, a combination of 24 : 1 solution of chloroform/isoamyl alcohol and stop buffer were used to stop the reaction. The stop buffer was prepared using 40% w/v sucrose, 12.11 g/L Tris·HCl (pH 7.5), 0.29 g/L EDTA and 0.5 mg/mL of bromophenol blue.

DNA Gyrase Assay Buffer

The assay buffer was used neat from the commercially available Inspiralis DNA Gyrase Assay Kit. The buffer contained 3.92 g/L Tris·HCl (pH 7.5), 1.79 g/L KCl, 0.38 g/L $MgCl_2$, 0.3 g/L dithiothreitol, 0.26 g/L spermidine, 0.5 g/L ATP, 6.5% (w/v) glycerol and 0.1 mg/mL BSA.

DNA Gyrase Assay

Stock solutions of **62** were created in DMSO. The antimicrobial compounds were combined with relaxed pBR322 DNA, DNA gyrase and assay buffer in H_2O at fixed proportions. The solutions were incubated at 37 °C for 30 minutes. The assay was stopped with the addition of 30 µL of 24:1 $CHCl_3$: isoamyl alcohol and 30 µL stop buffer. A portion of 20 µL was

loaded into a 1% agarose gel. The gel was subjected to electrophoresis for 90 minutes at 75 volts. The gel was stained using 0.01% SYBR SAFE in TAE buffer for 50 minutes and photographed using a gel doc.

	Volumes added / µl			
	Positive Control	**Negative Control**	**Test Wells**	**DMSO control**
H_2O	21.5	23.5	20.5	20.5
pBr322	0.5	0.5	0.5	0.5
Assay Buffer	6	6	6	6
Drug Stock	0	0	1	0
DMSO	0	0	0	1
Gyrase Aliquot	2	0	2	2

Stock Drug Conc / µM	**Assay Drug Conc / µM**
0	0
15	0.5
30	1
150	5
300	10
600	20

Table 10 Volumes added to each well of the DNA Gyrase binding assay and the stock drug concentrations used

Abbreviations

AAC	Antibiotic-Antibody Conjugate
ATP	Adenylate TriPhosphate
DNA	Deoxyribose Nucleic Acid
DSB	Disulfide bond forming
DTT	Dithiotreitol
E. coli	*Escherichia coli*
E. faecium	*Enterococcus faecium*
GSSG	Glutathione Disulfide
K. pneumoniae	*Klebsiella pneumoniae*
MATE	Multi Antibiotic and Toxin Extruders
MIC	Minimum Inhibitory Concentration
MRSA	Methicillin-resistant Staphylococcus aureus
NER	Nucleotide Excision Repair
PAF	Mycobacteria proteasome accessory factor
PBP	Penicillin Binding Protein
PEG	Polyethylene Glycol
QRDR	Quinolone Resistance Determining Region
ROS	Reactive Oxygen Species
S. aureus	*Staphylococcus aureus*
S. typhi	*Staphylococcus typhi*
SOD	Superoxide dismutase

Chemistry Terms

α	Alpha
β	Beta
Boc	tert-Butyloxycarbonyl
CD3OD	Deuterated methanol
CDCl3	Deuterated chloroform
CHCl3	Chloroform
Cip	Ciprofloxacin
Conc	Concentration
DCC	N,N'-Dicyclohexylcarbodiimide
DCM	Dichloromethane
DIPEA	N,N'-Diisopropylethylamine
DMAP	4-Dimethylaminopyridine
DMF	Dimethylformamide
EDC	1-Ethyl-3-(3'-dimethylaminopropyl)carbodiimide
EtOAc	Ethyl acetate
FA	Formic Acid
HATU	1-[Bis(dimethylamino)methylene]-1H-1,2,3-triazolo[4,5b]pyridinium 3-oxid hexafluorophosphate
HCl	Hydrochloric acid
HOBt	N-Hydroxybenzotriazolee hydrate
m.p.	Melting point
MeOH	Methanol
MgSO4	Magnesium Sulphate
Na2CO3	Sodium Carbonate
NaHCO3	Sodium Hydrogen Carbonate
NaOH	Sodium Hydroxide
T3P	Propyl phosphonic anhydride

NMR Nuclear Magnetic Resonance Terms

rt	Room Temperature
SOCl2	Thionyl Chloride
TFA	Trifuoroacetic acid
TLC	Thin Layer Chromatography
oC	Degrees Centigrade
µM	Micromolar
cm-1	Wavenumber
g	Grams
g mol-1	Grams per mole
hrs	Hours
Hz	Hertz
mM	millimolar
M	Molar
mol	Moles

Spectroscopy Terms

1H	Proton
13C	Carbon
19F	Fluorine
Calc	Calculated
COSY	Correlation Spectroscopy
δ	Chemical Shift
d	Doublet
ESI	Electronspray Ionisation
M	Multiplet
m/z	Mass to charge ratio
ppm	Parts per million
Rf	Retention factor
s	Singlet
t	Triplet

Bibliography

1 J. Clardy, M. A. Fischbach and C. R. Currie, The natural history of antibiotics, *Curr. Biol.*, 2009, **19**, R437–R441.

2 K. Lewis, Platforms for antibiotic discovery, *Nat. Rev. Drug Discov.*, 2013, **12**, 371–387.

3 J. Davies, Where Have all the Antibiotics Gone?, *Can. J. Infect. Dis. Med. Microbiol.*, 2006, **17**, 287–290.

4 S. Santajit and N. Indrawattana, Mechanisms of Antimicrobial Resistance in ESKAPE Pathogens, *Biomed. Res. Int.*, 2016, **2016**, 1–8.

5 N. E. W. York, U. N. G. Assembly, U. N. G. Assembly, P. Thomson, S. D. Goals, M. States, G. A. Plan and A. Resistance, *Media centre At UN , global leaders commit to act on antimicrobial resistance*, The Hague, 2017.

6 I. Vranakis, I. Goniotakis, A. Psaroulaki, V. Sandalakis, Y. Tselentis, K. Gevaert and G. Tsiotis, Proteome studies of bacterial antibiotic resistance mechanisms, *J. Proteomics*, 2014, **97**, 88–99.

7 Y. Gao, Glycopeptide antibiotics and development of inhibitors to overcome vancomycin resistance, *Nat. Prod. Rep.*, 2002, **19**, 100–107.

8 P. LAMBERT, Bacterial resistance to antibiotics: Modified target sites, *Adv. Drug Deliv. Rev.*, 2005, **57**, 1471–1485.

9 J. Pootoolal, J. Neu and G. D. Wright, Glycopeptide Antibiotic Resistance, *Annu. Rev. Pharmacol. Toxicol.*, 2002, **42**, 381–408.

10 M. A. Cooper, M. T. Fiorini, C. Abell and D. H. Williams, Binding of vancomycin group antibiotics to d -alanine and d -lactate presenting self-assembled monolayers, *Bioorg. Med. Chem.*, 2000, **8**, 2609–2616.

11 E. P. ABRAHAM and E. CHAIN, An Enzyme from Bacteria able to Destroy Penicillin, *Nature*, 1940, **146**, 837–837.

12 K. Bush, Proliferation and significance of clinically relevant β-lactamases, *Ann. N. Y. Acad. Sci.*, 2013, **1277**, 84–90.

13 B. W. Bycroft and R. E. Shute, The Molecular Basis for the Mode of Action of Beta-Lactam Antibiotics and Mechanisms of Resistance, *Pharm. Res.*, 1985, **2**, 3–14.

14 H. Okusu, D. Ma and H. Nikaido, AcrAB efflux pump plays a major role in the antibiotic resistance phenotype of Escherichia coli multiple-antibiotic-resistance (Mar) mutants., *J. Bacteriol.*, 1996, **178**, 306–308.

15 X.-Z. Li, L. Zhang and H. Nikaido, Efflux Pump-Mediated Intrinsic Drug Resistance in Mycobacterium smegmatis, *Antimicrob. Agents Chemother.*, 2004, **48**, 2415–2423.

16 R. HANCOCK, The bacterial outer membrane as a drug barrier, *Trends Microbiol.*, 1997, **5**, 37–42.

17 H. Nikaido and D. G. Thanassi, Penetration of lipophilic agents with multiple protonation sites into bacterial cells: tetracyclines and fluoroquinolones as examples., *Antimicrob. Agents Chemother.*, 1993, **37**, 1393–1399.

18 R. G. Nelson and A. Rosowsky, Dicyclic and Tricyclic Diaminopyrimidine Derivatives as Potent Inhibitors of Cryptosporidium parvum Dihydrofolate Reductase: Structure-Activity and Structure-Selectivity Correlations, *Antimicrob. Agents Chemother.*, 2002, **46**, 940–940.

19 T. Schirmer, General and Specific Porins from Bacterial Outer Membranes, *J. Struct. Biol.*, 1998, **121**, 101–109.

20 H. Nikaido, Porins and specific diffusion channels in bacterial outer

membranes, *J. Biol. Chem.*, 1994, **269**, 3905–3908.

21 K. J. Aldred, R. J. Kerns and N. Osheroff, Mechanism of Quinolone Action and Resistance, *Biochemistry*, 2014, **53**, 1565–1574.

22 M. A. Fischbach, C. T. Walsh and J. Clardy, The evolution of gene collectives: How natural selection drives chemical innovation, *Proc. Natl. Acad. Sci.*, 2008, **105**, 4601–4608.

23 S. M. Drawz and R. A. Bonomo, Three Decades of -Lactamase Inhibitors, *Clin. Microbiol. Rev.*, 2010, **23**, 160–201.

24 K. S. Bora and A. Sharma, The Genus Artemisia : A Comprehensive Review, *Pharm. Biol.*, 2011, **49**, 101–109.

25 M. Gibaldi and M. a Schwartz, Effect of Probenecid on the Distribution and Elimination of Ciprofloxacin in Humans, *Clin. Pharmacol. Ther.*, 1995, **9**, 345–349.

26 E. J. Molinelli, A. Korkut, W. Wang, M. L. Miller, N. P. Gauthier, X. Jing, P. Kaushik, Q. He, G. Mills, D. B. Solit, C. A. Pratilas, M. Weigt, A. Braunstein, A. Pagnani, R. Zecchina and C. Sander, Perturbation Biology: Inferring Signaling Networks in Cellular Systems, *PLoS Comput. Biol.*, 2013, **9**, e1003290.

27 A. Dalhoff, Global Fluoroquinolone Resistance Epidemiology and Implictions for Clinical Use, *Interdiscip. Perspect. Infect. Dis.*, 2012, **2012**, 1–37.

28 P. Ball, Quinolone generations: natural history or natural selection?, *J. Antimicrob. Chemother.*, 2000, **46**, 17–24.

29 L. Mandell and G. Tillotson, Safety of Fluoroquinolones: An Update, *Can. J. Infect. Dis.*, 2002, **13**, 54–61.

30 L. J. Martinez, R. H. Sik and C. F. Chignell, Fluoroquinolone Antimicrobials: Singlet Oxygen, Superoxide and Phototoxicity, *Photochem. Photobiol.*, 1998, **67**, 399–403.

31 M. Peacock, R. Brem, P. Macpherson and P. Karran, DNA repair inhibition by UVA photoactivated fluoroquinolones and vemurafenib, *Nucleic Acids Res.*, 2014, **42**, 13714–13722.

32 N. Hayashi, Y. Nakata and A. Yazaki, New Findings on the Structure-Phototoxicity Relationship and Photostability of Fluoroquinolones with Various Substituents at Position 1, *Antimicrob. Agents Chemother.*, 2004, **48**, 799–803.

33 M. I. Andersson, Development of the quinolones, *J. Antimicrob. Chemother.*, 2003, **51**, 1–11.

34 G. S. Tillotson, Quinolones: structure-activity relationships and future predictions, *J. Med. Microbiol.*, 1996, **44**, 320–324.

35 K. Drlica and X. Zhao, DNA gyrase, topoisomerase IV, and the 4-quinolones., *Microbiol. Mol. Biol. Rev.*, 1997, **61**, 377–392.

36 N. B. Patel, S. D. Patel, J. N. Patel, J. . Patel and Y. . Gorgamwala, Synthesis and Antibacterial Activity of Thioureido Amide of Fluoroquinolone, *Int. J. Biol. Chem.*, 2011, **5**, 37–45.

37 H. Nikaido, Molecular Basis of Bacterial Outer Membrane Permeability Revisited, *Microbiol. Mol. Biol. Rev.*, 2003, **67**, 593–656.

38 F. Collin, S. Karkare and A. Maxwell, Exploiting bacterial DNA gyrase as a drug target: current state and perspectives, *Appl. Microbiol. Biotechnol.*, 2011, **92**, 479–497.

39 A. Gubaev and D. Klostermeier, DNA-induced narrowing of the gyrase N-gate coordinates T-segment capture and strand passage, *Proc. Natl. Acad. Sci.*, 2011, **108**, 14085–14090.

40 J. Kato, H. Suzuki and H. Ikeda, Purification and characterization of DNA topoisomerase IV in Escherichia coli., *J. Biol. Chem.*, 1992, **267**, 25676–25684.

41 L. L. Shen, J. Baranowski and A. G. Pernet, Mechanism of inhibition of DNA gyrase by quinolone antibacterials: specificity and cooperativity of drug binding to DNA, *Biochemistry*, 1989, **28**, 3879–3885.

42 L. L. Shen, L. A. Mitscher, P. N. Sharma, T. J. O'Donnell, D. W. T. Chu, C. S. Cooper, T. Rosen and A. G. Pernet, Mechanism of inhibition of DNA gyrase by quinolone antibacterials: a cooperative drug-DNA binding model, *Biochemistry*, 1989, **28**, 3886–3894.

43 A. Mustaev, M. Malik, X. Zhao, N. Kurepina, G. Luan, L. M. Oppegard, H. Hiasa, K. R. Marks, R. J. Kerns, J. M. Berger and K. Drlica, Fluoroquinolone-Gyrase-DNA Complexes, *J. Biol. Chem.*, 2014, **289**, 12300–12312.

44 K. J. Aldred, S. A. McPherson, C. L. Turnbough, R. J. Kerns and N. Osheroff, Topoisomerase IV-quinolone interactions are mediated through a water-metal ion bridge: mechanistic basis of quinolone resistance, *Nucleic Acids Res.*, 2013, **41**, 4628–4639.

45 S. J. Milner, A. M. Snelling, K. G. Kerr, A. Abd-El-Aziz, G. H. Thomas, R. E. Hubbard, A. Routledge and A.-K. Duhme-Klair, Probing linker design in citric acid–ciprofloxacin conjugates, *Bioorg. Med. Chem.*, 2014, **22**, 4499–4505.

46 M. Malik, X. Zhao and K. Drlica, Lethal fragmentation of bacterial chromosomes mediated by DNA gyrase and quinolones, *Mol. Microbiol.*, 2006, **61**, 810–825.

47 F. Krasin and F. Hutchinson, Repair of DNA double-strand breaks in Escherichia coli, which requires recA function and the presence of a duplicate genome, *J. Mol. Biol.*, 1977, **116**, 81–98.

48 X. Wang, X. Zhao, M. Malik and K. Drlica, Contribution of reactive oxygen species to pathways of quinolone-mediated bacterial cell death, *J. Antimicrob. Chemother.*, 2010, **65**, 520–524.

49 X. Wang and X. Zhao, Contribution of Oxidative Damage to Antimicrobial Lethality, *Antimicrob. Agents Chemother.*, 2009, **53**, 1395–1402.

50 Q. Li, L. Xie, Q. Long, J. Mao, H. Li, M. Zhou and J. Xie, Proteasome Accessory Factor C (pafC) Is a novel gene Involved in Mycobacterium Intrinsic Resistance to broad-spectrum antibiotics - Fluoroquinolones, *Sci. Rep.*, 2015, **5**, 11910.

51 K. R. Marks, Investigating the fluoroquinolone-topoisomerase interaction by use of novel fluoroquinolone and quinazoline analogs, PhD Thesis, University of Iowa, 2011.

52 H. Yoshida, M. Bogaki, M. Nakamura and S. Nakamura, Quinolone resistance-determining region in the DNA gyrase gyrA gene of Escherichia coli., *Antimicrob. Agents Chemother.*, 1990, **34**, 1271–1272.

53 D. C. Hooper, Mechanisms of fluoroquinolone resistance, *Drug Resist. Updat.*, 1999, **2**, 38–55.

54 X. Xiong, E. H. C. Bromley, P. Oelschlaeger, D. N. Woolfson and J. Spencer, Structural insights into quinolone antibiotic resistance mediated by pentapeptide repeat proteins: conserved surface loops direct the activity of a Qnr protein from a Gram-negative bacterium, *Nucleic Acids Res.*, 2011, **39**, 3917–3927.

55 D. Hooper, Emerging Mechanisms of Fluoroquinolone Resistance, *Emerg. Infect. Dis.*, 2001, **7**, 337–341.

56 P. Klahn and M. Brönstrup, Bifunctional antimicrobial conjugates and hybrid antimicrobials, *Nat. Prod. Rep.*, 2017, **34**, 832–885.

57 Y. Fu, Y. Zhang, S. Zhou, Y. Liu, J. Wang, Y. Wang, C. Lu and C. Li, Effects of Substitution of Carboxyl with Hydrazide Group on Position 3 of Ciprofloxacin on its Antimicrobial and Antitumor Activity, *Int. J. Pharmacol.*, 2013, **9**, 416–429.

58 S. Wang, X.-D. Jia, M.-L. Liu, Y. Lu and H.-Y. Guo, Synthesis, antimycobacterial and antibacterial activity of ciprofloxacin derivatives containing a N-substituted benzyl moiety, *Bioorg. Med. Chem. Lett.*, 2012, **22**, 5971–5975.

59 P. C. Sharma, A. Jain, S. Jain, R. Pahwa and M. S. Yar, Ciprofloxacin: review on developments in synthetic, analytical, and medicinal aspects, *J. Enzyme Inhib. Med. Chem.*, 2010, **25**, 577–589.

60 B. Bozdogan and P. C. Appelbaum, Oxazolidinones: activity, mode of action, and mechanism of resistance, *Int. J. Antimicrob. Agents*, 2004, **23**, 113–119.

61 S. Mariathasan and M.-W. Tan, Antibody–Antibiotic Conjugates: A Novel Therapeutic Platform against Bacterial Infections, *Trends Mol. Med.*, 2017, **23**, 135–149.

62 A. G. Ross, B. M. Benton, D. Chin, G. De Pascale, J. Fuller, J. A. Leeds, F. Reck, D. L. Richie, J. Vo and M. J. LaMarche, Synthesis of ciprofloxacin dimers for evaluation of bacterial permeability in atypical chemical space, *Bioorg. Med. Chem. Lett.*, 2015, **25**, 3468–3475.

63 R. J. Kerns, M. J. Rybak and C. M. Cheung, Susceptibility studies of piperazinyl–cross-linked fluoroquinolone dimers against test strains of Gram-positive and Gram-negative bacteria, *Diagn. Microbiol. Infect. Dis.*, 2006, **54**, 305–310.

64 G. Pintér, P. Horváth, S. Bujdosó, F. Sztaricskai, S. Kéki, M. Zsuga, S. Kardos, F. Rozgonyi and P. Herczegh, Synthesis and antimicrobial activity of ciprofloxacin and norfloxacin permanently bonded to polyethylene glycol by a thiourea linker, *J. Antibiot. (Tokyo).*, 2009, **62**, 113–116.

65 T. J. Sanderson, Exploring Design Concepts for Trojan Horse Antimicrobials, PhD Thesis, University of York, 2016.

66 B. Sithole, Peptide-Antiobiotic Conjugates as Novel Developments for Increased Antimicrobial Transport and Efficiency, MSc Thesis, University of York, 2015.

67 A. K. Jain, M. G. Gund, D. C. Desai, N. Borhade, S. P. Senthilkumar, M. Dhiman, N. K. Mangu, S. V. Mali, N. P. Dubash, S. Halder and A. Satyam, Mutual prodrugs containing bio-cleavable and drug releasable disulfide linkers, *Bioorg. Chem.*, 2013, **49**, 40–48.

68 Allergen Inc, Patent, World Intellectual Property Organisation, 138350 A1, 2014.

69 A. Thakur, R. S. Kadam and U. B. Kompella, Influence of Drug Solubility and Lipophilicity on Transscleral Retinal Delivery of Six Corticosteroids, *Drug Metab. Dispos.*, 2011, **39**, 771–781.

70 M. Trivedi, J. Laurence and T. Siahaan, The Role of Thiols and Disulfides on Protein Stability, *Curr. Protein Pept. Sci.*, 2009, **10**, 614–625.

71 A. Pompella, A. Visvikis, A. Paolicchi, V. De Tata and A. F. Casini, The changing faces of glutathione, a cellular protagonist, *Biochem. Pharmacol.*, 2003, **66**, 1499–1503.

72 M. H. Lee, Z. Yang, C. W. Lim, Y. H. Lee, S. Dongbang, C. Kang and J. S. Kim, Disulfide-Cleavage-Triggered Chemosensors and Their Biological Applications, *Chem. Rev.*, 2013, **113**, 5071–5109.

73 L. R. Jones, E. A. Goun, R. Shinde, J. B. Rothbard, C. H. Contag and P. A. Wender, Releasable Luciferin−Transporter Conjugates: Tools for the Real-Time Analysis of Cellular Uptake and Release, *J. Am. Chem. Soc.*, 2006, **128**, 6526–6527.

74 P. E. Thorpe, P. M. Wallace, P. P. Knowles, M. G. Relf, A. N. Brown, G. J. Watson, D. C. Blakey and D. R. Newell, Improved Antitumor Effects of Immunotoxins Prepared with Deglycosylated Ricin A-Chain and Hindered Disulfide Linkages, *Cancer Res.*, 1988, **48**,

6396–6403.

75 S. C. Alley, D. R. Benjamin, S. C. Jeffrey, N. M. Okeley, D. L. Meyer, R. J. Sanderson and P. D. Senter, Contribution of Linker Stability to the Activities of Anticancer Immunoconjugates, *Bioconjug. Chem.*, 2008, **19**, 759–765.

76 G. D. Lewis Phillips, G. Li, D. L. Dugger, L. M. Crocker, K. L. Parsons, E. Mai, W. A. Blattler, J. M. Lambert, R. V. J. Chari, R. J. Lutz, W. L. T. Wong, F. S. Jacobson, H. Koeppen, R. H. Schwall, S. R. Kenkare-Mitra, S. D. Spencer and M. X. Sliwkowski, Targeting HER2-Positive Breast Cancer with Trastuzumab-DM1, an Antibody-Cytotoxic Drug Conjugate, *Cancer Res.*, 2008, **68**, 9280–9290.

77 G. Saito, J. A. Swanson and K.-D. Lee, Drug delivery strategy utilizing conjugation via reversible disulfide linkages: role and site of cellular reducing activities, *Adv. Drug Deliv. Rev.*, 2003, **55**, 199–215.

78 H. Nakamoto and J. C. A. Bardwell, Catalysis of disulfide bond formation and isomerization in the Escherichia coli periplasm, *Biochim. Biophys. Acta - Mol. Cell Res.*, 2004, **1694**, 111–119.

79 M. Sela and S. Lifson, On the reformation of disulfide bridges in proteins, *Biochim. Biophys. Acta*, 1959, **36**, 471–478.

80 M. Gund, P. Gaikwad, N. Borhade, A. Burhan, D. C. Desai, A. Sharma, M. Dhiman, M. Patil, J. Sheikh, G. Thakre, S. G. Tipparam, S. Sharma, K. V. S. Nemmani and A. Satyam, Gastric-sparing nitric oxide-releasable 'true' prodrugs of aspirin and naproxen, *Bioorg. Med. Chem. Lett.*, 2014, **24**, 5587–5592.

81 C. Baigent, N. Bhala, J. Emberson, A. Merhi, S. Abramson, N. Arber, J. A. Baron, C. Bombardier, C. Cannon, M. E. Farkouh, G. A. FitzGerald, P. Goss, H. Halls, E. Hawk, C. Hawkey, C. Hennekens, M. Hochberg, L. E. Holland, P. M. Kearney, L. Laine, A. Lanas, P. Lance, A. Laupacis, J. Oates, C. Patrono, T. J. Schnitzer, S. Solomon, P.

Tugwell, K. Wilson, J. Wittes, O. Adelowo, P. Aisen, A. Al-Quorain, R. Altman, G. Bakris, H. Baumgartner, C. Bresee, M. Carducci, D. M. Chang, C. T. Chou, D. Clegg, M. Cudkowicz, L. Doody, Y. El Miedany, C. Falandry, J. Farley, L. Ford, M. Garcia-Losa, M. Gonzalez-Ortiz, M. Haghighi, M. Hala, T. Iwama, Z. Jajic, D. Kerr, H. S. Kim, C. Kohne, B. K. Koo, B. Martin, C. Meinert, N. Muller, G. Myklebust, D. Neustadt, R. Omdal, S. Ozgocmen, A. Papas, P. Patrignani, F. Pelliccia, V. Roy, I. Schlegelmilch, A. Umar, O. Wahlstrom, F. Wollheim, S. Yocum, X. Y. Zhang, E. Hall, P. McGettigan, R. Midgley, R. A. Moore, R. Philipson, S. Curtis, A. Reicin, J. Bond, A. Moore, M. Essex, J. Fabule, B. Morrison, L. Tive, N. Bhala, K. Davies, J. Emberson, H. Halls, L. E. Holland, P. M. Kearney, A. Merhi, C. Patrono, K. Wilson and F. Yau, Vascular and upper gastrointestinal effects of non-steroidal anti-inflammatory drugs: meta-analyses of individual participant data from randomised trials, *Lancet*, 2013, **382**, 769–779.

82 M. H. Lee, J. H. Han, P.-S. Kwon, S. Bhuniya, J. Y. Kim, J. L. Sessler, C. Kang and J. S. Kim, Hepatocyte-Targeting Single Galactose-Appended Naphthalimide: A Tool for Intracellular Thiol Imaging in Vivo, *J. Am. Chem. Soc.*, 2012, **134**, 1316–1322.

83 S. Reuter, S. C. Gupta, M. M. Chaturvedi and B. B. Aggarwal, Oxidative stress, inflammation, and cancer: how are they linked?, *Free Radic. Biol. Med.*, 2010, **49**, 1603–16.

84 T. H. Pillow, J. D. Sadowsky, D. Zhang, S.-F. Yu, G. Del Rosario, K. Xu, J. He, S. Bhakta, R. Ohri, K. R. Kozak, E. Ha, J. R. Junutula and J. A. Flygare, Decoupling stability and release in disulfide bonds with antibody-small molecule conjugates, *Chem. Sci.*, 2017, **8**, 366–370.

85 J. R. McCombs and S. C. Owen, Antibody Drug Conjugates: Design and Selection of Linker, Payload and Conjugation Chemistry, *AAPS J.*, 2015, **17**, 339–351.

86 M. Danial and A. Postma, Disulfide conjugation chemistry: a mixed

blessing for therapeutic drug delivery?, *Ther. Deliv.*, 2017, **8**, 359–362.

87 G. P. Suresha, R. Suhas, W. Kapfo and D. Channe Gowda, Urea/thiourea derivatives of quinazolinone–lysine conjugates: Synthesis and structure–activity relationships of a new series of antimicrobials, *Eur. J. Med. Chem.*, 2011, **46**, 2530–2540.

88 P. Umadevi, K. Deepti and I. Srinath, Synthesis and In-Vitro Antibacterial Activity of Some New Urea, Thiourae and Thiosemicarbazide Derivatives, *Int. J. Pharm. Pharm. Sci.*, 2012, **4**, 3–7.

89 P. Çikla, Synthesis and evaluation of antiviral, antitubercular and anticancer activities of some novel thioureas derived from 4-aminobenzohydrazide hydrazones, *MARMARA Pharm. J.*, 2010, **1**, 13–20.

90 A. Bielenica, J. Stefańska, K. Stępień, A. Napiórkowska, E. Augustynowicz-Kopeć, G. Sanna, S. Madeddu, S. Boi, G. Giliberti, M. Wrzosek and M. Struga, Synthesis, cytotoxicity and antimicrobial activity of thiourea derivatives incorporating 3-(trifluoromethyl)phenyl moiety, *Eur. J. Med. Chem.*, 2015, **101**, 111–125.

91 B. Medapi, J. Renuka, S. Saxena, J. P. Sridevi, R. Medishetti, P. Kulkarni, P. Yogeeswari and D. Sriram, Design and synthesis of novel quinoline–aminopiperidine hybrid analogues as Mycobacterium tuberculosis DNA gyraseB inhibitors, *Bioorg. Med. Chem.*, 2015, **23**, 2062–2078.

92 M. Wasil, B. Halliwell, M. Grootveld, C. P. Moorhouse, D. C. S. Hutchison and H. Baum, The specificity of thiourea, dimethylthiourea, and dimethyl sulfoxide as scavengers of OH radicals. Their protection of alpha-antiproteinase against

inactivation by HOCl., *Biochem.J.*, 1987, **243**, 867–870.

93 A. K. Prasad and P. C. Mishra, Scavenging of superoxide radical anion and hydroxyl radical by urea, thiourea, selenourea and their derivatives without any catalyst: A theoretical study, *Chem. Phys. Lett.*, 2017, **684**, 197–204.

94 J. Kelner and J. Welchl, Thioureas Compound React with Superoxide Radicals to Yield a Sulfhydryl Compound, *J. Biol. Chem.*, 1990, **265**, 1306–1311.

95 M. Hoffmann and J. O. Edwards, Kinetics and mechanism of the oxidation of thiourea and N,N'-dialkylthioureas by hydrogen peroxide, *Inorg. Chem.*, 1977, **16**, 3333–3338.

96 I. A. J. M. Bakker-Woudenberg, M. T. ten Kate, L. Guo, P. Working and J. W. Mouton, Improved Efficacy of Ciprofloxacin Administered in Polyethylene Glycol-Coated Liposomes for Treatment of Klebsiella pneumoniae Pneumonia in Rats, *Antimicrob. Agents Chemother.*, 2001, **45**, 1487–1492.

97 S. S. Panda, O. S. Detistov, A. S. Girgis, P. P. Mohapatra, A. Samir and A. R. Katritzky, Synthesis and molecular modeling of antimicrobial active fluoroquinolone–pyrazine conjugates with amino acid linkers, *Bioorg. Med. Chem. Lett.*, 2016, **26**, 2198–2205.

98 C. Ji and M. J. Miller, Siderophore–fluoroquinolone conjugates containing potential reduction-triggered linkers for drug release: synthesis and antibacterial activity, *BioMetals*, 2015, **28**, 541–551.

99 P. M. S. D. Cal, M. J. Matos and G. J. L. Bernardes, Trends in therapeutic drug conjugates for bacterial diseases: a patent review, *Expert Opin. Ther. Pat.*, 2017, **27**, 179–189.

100 J. Stefanska, G. Nowicka, M. Struga, D. Szulczyk, A. E. Koziol, E. Augustynowicz-Kopec, A. Napiorkowska, A. Bielenica, W. Filipowski, A. Filipowska, A. Drzewiecka, G. Giliberti, S. Madeddu, S. Boi, P. La

Colla and G. Sanna, Antimicrobial and Anti-biofilm Activity of Thiourea Derivatives Incorporating a 2-Aminothiazole Scaffold, *Chem. Pharm. Bull. (Tokyo).*, 2015, **63**, 225–236.

101 Z. Liu, N. Yasuda, M. Simeone and R. A. Reamer, N -Boc Deprotection and Isolation Method for Water-Soluble Zwitterionic Compounds, *J. Org. Chem.*, 2014, **79**, 11792–11796.

102 A. I. Caço, F. Varanda, M. J. Pratas de Melo, A. M. A. Dias, R. Dohrn and I. M. Marrucho, Solubility of Antibiotics in Different Solvents. Part II. Non-Hydrochloride Forms of Tetracycline and Ciprofloxacin, *Ind. Eng. Chem. Res.*, 2008, **47**, 8083–8089.

103 K. Jarowicki and P. Kocienski, Protecting groups, *J. Chem. Soc. Perkin Trans. 1*, 2000, 2495–2527.

104 A. Maxwell, N. P. Burton and N. O'Hagan, High-throughput assays for DNA gyrase and other topoisomerases, *Nucleic Acids Res.*, 2006, **34**, e104–e104.

105 N. Nakajima and Y. Ikada, Mechanism of Amide Formation by Carbodiimide for Bioconjugation in Aqueous Media, *Bioconjug. Chem.*, 1995, **6**, 123–130.

106 A. A. Waghmare, R. M. Hindupur and H. N. Pati, Propylphosphonic anhydride (T3P®): An expedient reagent for organic synthesis, *Rev. J. Chem.*, 2014, **4**, 53–131.

107 J. Cornish, K. E. Callon, C. Q. Lin, C. L. Xiao, T. B. Mulvey, G. J. Cooper and I. R. Reid, Trifluoroacetate, a contaminant in purified proteins, inhibits proliferation of osteoblasts and chondrocytes., *Am. J. Physiol.*, 1999, **277**, E779–E783.

108 J.-A. Richard, Y. Meyer, V. Jolivel, M. Massonneau, R. Dumeunier, D. Vaudry, H. Vaudry, P.-Y. Renard and A. Romieu, Latent Fluorophores Based on a Self-Immolative Linker Strategy and Suitable for Protease Sensing †, *Bioconjug. Chem.*, 2008, **19**, 1707–

1718.

109 K. Neumann, S. Jain, A. Gambardella, S. E. Walker, E. Valero, A. Lilienkampf and M. Bradley, Tetrazine-Responsive Self-immolative Linkers, *ChemBioChem*, 2017, **18**, 91–95.